



<https://theses.gla.ac.uk/>

Theses Digitisation:

<https://www.gla.ac.uk/myglasgow/research/enlighten/theses/digitisation/>

This is a digitised version of the original print thesis.

Copyright and moral rights for this work are retained by the author

A copy can be downloaded for personal non-commercial research or study,
without prior permission or charge

This work cannot be reproduced or quoted extensively from without first
obtaining permission in writing from the author

The content must not be changed in any way or sold commercially in any
format or medium without the formal permission of the author

When referring to this work, full bibliographic details including the author,
title, awarding institution and date of the thesis must be given

Enlighten: Theses

<https://theses.gla.ac.uk/>
research-enlighten@glasgow.ac.uk

SUMMARY.

The effect of temperature on the micellar properties, in aqueous solution, of three non-ionic detergents has been studied. The materials used were synthetic materials of the general formula $\text{CH}_3(\text{CH}_2)_{15}(\text{OCH}_2\text{CH}_2)_n\text{OH}$ where $n = 7, 8, \text{ and } 9$; the detergents were abbreviated to Hn_7 , Hn_8 and Hn_9 . The thesis was divided into three parts.

Part I: Introduction.

A brief review of the general physico-chemical properties of non-ionic detergents in aqueous solution was given, dealing with micellar structure, critical micellar concentration and solubilisation together with a more detailed account of the effect of temperature on non-ionic detergents in solution.

In the second section of the introduction the theory of light-scattering was reviewed, together with the interpretation of viscosity results and second virial coefficients.

Part II: Materials and Experimental Methods.

The purification of hexadecyl bromide and the purification and preparation of octaoxyethylene glycol (n_8) and the detergent Hn_8 were described.

ProQuest Number: 10647871

All rights reserved

INFORMATION TO ALL USERS

The quality of this reproduction is dependent upon the quality of the copy submitted.

In the unlikely event that the author did not send a complete manuscript and there are missing pages, these will be noted. Also, if material had to be removed, a note will indicate the deletion.



ProQuest 10647871

Published by ProQuest LLC (2017). Copyright of the Dissertation is held by the Author.

All rights reserved.

This work is protected against unauthorized copying under Title 17, United States Code
Microform Edition © ProQuest LLC.

ProQuest LLC.
789 East Eisenhower Parkway
P.O. Box 1346
Ann Arbor, MI 48106 – 1346

The light-scattering apparatus and vapour pressure apparatus were described, and their use outlined, together with the measurement of specific refractive index increment, viscosity, densities and cloud points.

Part III: Results and Discussion.

Micellar weights were determined at 15°C and 17.5°C for Hn₇, between 15° - 45°C for Hn₈ and between 45° - 57.5°C for Hn₉. Measurements of viscosities at suitable temperatures were made, and also measurements of vapour pressure over concentrated detergent solutions. The vapour pressure measurements were used to give an idea of micellar hydration. Generally, it was found that micellar weights, hydrations and intrinsic viscosities increased with temperature.

Above a particular temperature, designated T_h, which differed for each detergent, the micellar weights as measured from light-scattering increased exponentially with temperature. T_h was found to be 22°C for Hn₇, 36.3°C for Hn₈ and 48°C for Hn₉. Also at these temperatures the micelles of the three detergents were found to have the same number of monomers within experimental error.

Below T_h the micelles appeared to be spherical and the micellar weight increased gradually with temperature. Above T_h the micelles became asymmetric in shape and fitted the oblate ellipsoid model.

The structure of the micelles was discussed below T_h , at T_h , and above T_h . A qualitative discussion of the interpretation of second virial coefficients obtained from light-scattering was given.

A STUDY OF THE EFFECT OF TEMPERATURE
ON THE MICELLAR PROPERTIES OF A SERIES
OF NON-IONIC DETERGENTS IN AQUEOUS SOLUTION.

A Thesis presented

by

Charles McDonald

in fulfilment of the requirements

of the degree of

MASTER OF SCIENCE

of the

UNIVERSITY OF GLASGOW

Department of Pharmacy,
The Royal College of
Science and Technology,

October, 1963.

Glasgow.

Acknowledgments.

I should like to thank Dr. P. H. Elworthy for his help and guidance and also Professor J. B. Stenlake for his interest.

CONTENTS.

PART 1.	Page No.
INTRODUCTION.	
<u>Introduction</u>	1
<u>Synthetic Methods of Preparing Non-Ionic Detergents.</u>	3
<u>Micellar Structure of Non-Ionic Detergents.</u>	8
<u>Critical Micellar Concentration and Surface Activity.</u>	17
<u>Solubilisation.</u>	25
<u>Effect of Temperature on Non-Ionic Detergents in Solution.</u>	27
a). Effect of temperature on cmc.	27
b). The cloud point.	30
c). Effect of temperature on micellar weight	32
d). Effect of temperature on viscosity	36
<u>Theory of Light-Scattering</u>	38
1. <u>Small Particles.</u>	39
a). Rayleigh treatment for small particles	39
b). Light-Scattering by transparent crystals	45
c). Light-Scattering by pure liquids	46
d). Theory of fluctuations applied to macromolecular solutions.	47
e). Optical anisotropy of scattering particles.	54

2. <u>Large Particles.</u>	55
<u>Interpretation of Second Virial Coefficients</u>	57
<u>Interpretation of Viscosity Results</u>	60

PART II.

MATERIALS AND EXPERIMENTAL METHODS

<u>Materials and Synthesis of Hng-</u>	64
<u>Experimental Methods</u>	68
<u>Light-Scattering</u>	68
a). Description of Light Scatterer	68
b). Description of Light-Scattering Solution Cell	70
c). Measurement of Turbidity	71
d). Measurement of dn/dc	73
<u>Measurement of Vapour Pressure</u>	74
<u>Viscosity</u>	77
<u>Densities</u>	77
<u>Cloud Points</u>	78

PART III.

RESULTS AND DISCUSSION.

<u>Results.</u>	79
<u>Discussion.</u>	91
<u>Structure of Micelles below T_h.</u>	91
<u>Structure of Micelles at T_h.</u>	94
<u>Structure of Micelles above T_h.</u>	99
<u>Other Considerations.</u>	102
<u>REFERENCES.</u>	at end.

PART I

INTRODUCTION

INTRODUCTION.

In spite of the large number of published papers on the colloid chemical properties of non-ionic detergents, few studies have been made on the effect of temperature on micellisation. Most work has been done on commercial detergents, which are prepared by polymerising ethylene oxide in the presence of, say, a long chain alcohol, and thus contain a range of ethylene oxide chain lengths attached to the hydrophobic group. These materials are not chemical entities, and their properties can be expected to be average ones, depending on the distribution of polyoxyethylene chain length in the sample. Only a few papers^{9,16} have been published on temperature effects of pure (synthetic) detergents in solution. No studies on how temperature might effect the properties of detergents in a homologous series have been made.

In an attempt to obtain more information on these temperature effects, work on the micellar size and shape of three synthetic detergents, all based on hexadecyl alcohol, but containing seven, eight, and nine ethylene oxide units has been undertaken eg. using $\text{CH}_3(\text{CH}_2)_{15}(\text{OCH}_2\text{CH}_2)_n\text{OH}$ where $n = 7, 8, \text{ and } 9$. (These compounds will be abbreviated to $\text{Hn}_7, \text{Hn}_8, \text{ and } \text{Hn}_9$ where n denotes the number of ethylene oxide units in the chain.)

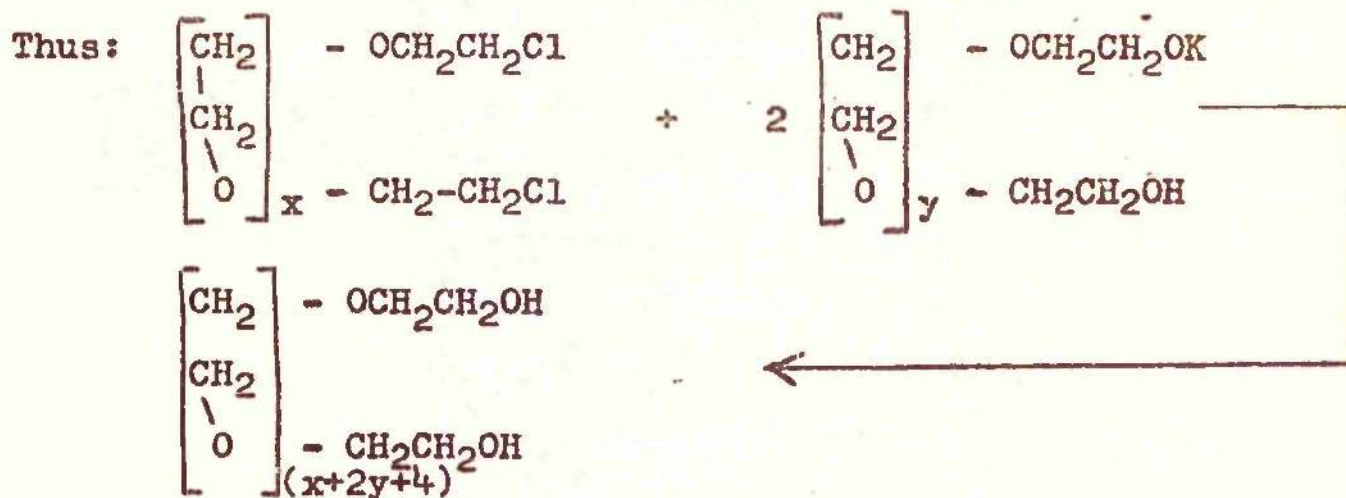
As an extensive review of the preparation and properties of non-ionic detergents has been undertaken by

Macfarlane¹, only a brief review of physical chemistry is given here in order to indicate the general effects of detergent structure on micellar properties, together with fuller accounts of synthetic methods and temperature effects relevant to this thesis.

SYNTHETIC METHODS OF PREPARING NON-IONIC DETERGENTS.

Synthetic methods of preparing polyoxyethylene ethers have been aimed at eliminating the heterogeneity which may occur in commercial materials. The normal approach has been to prepare the polyoxyethylene glycols by means of Williamson ether syntheses and to link these glycols to the hydrocarbon parts of the molecules.

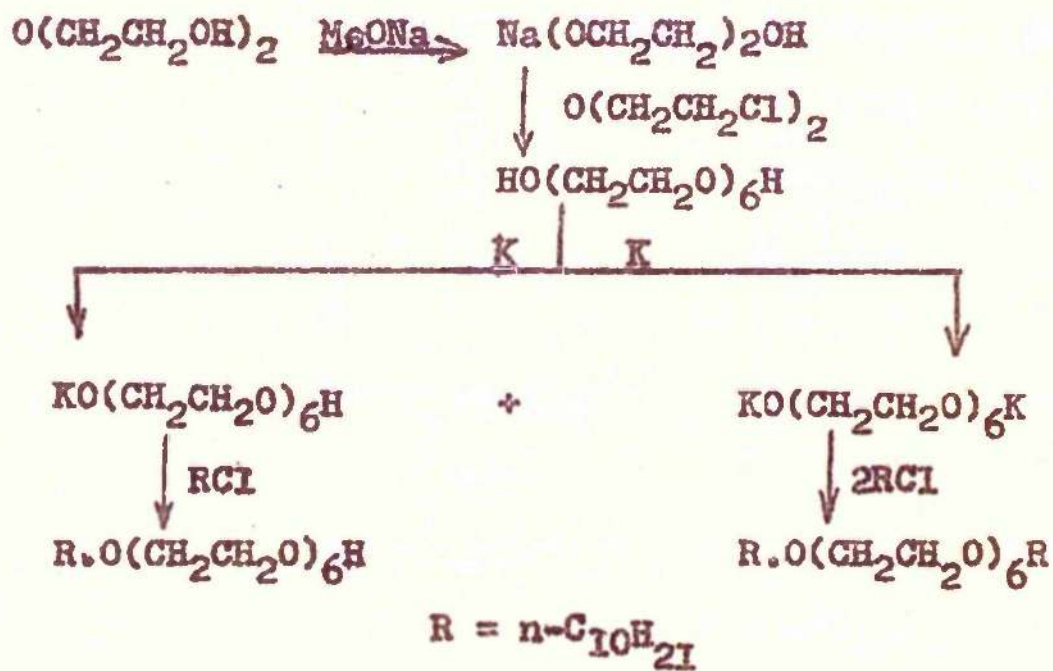
The first direct synthesis of higher polyoxyethylene glycols was that described by Perry and Hibbert² who reacted the dichloride of a polyoxyethylene glycol with the monometallic salt of a polyoxyethylene glycol.



The monometallic salt was used to prevent the polymerisation which was likely to occur with a dimetallic salt.

A modification of this method was used³ to prepare hexaoxyethylene glycol, $\text{HO}(\text{CH}_2\text{CH}_2\text{O})_6\text{H}$, octadeca-oxyethylene glycol, $\text{HO}(\text{CH}_2\text{CH}_2\text{O})_{18}\text{H}$ and dotetracontaoxyethylene glycol, $\text{HO}(\text{CH}_2\text{CH}_2\text{O})_{42}\text{H}$.

Hexaoxyethylene glycol was made by reacting diethylene glycol monosodium salt with 2,2 -dichlorodiethyl ether and subsequent distillation. Octadecaoxyethylene glycol was prepared by reacting the monopotassium salt of hexaoxyethylene glycol with hexaoxyethylene glycol dichloride. Similarly the dotetracontaoxyethylene glycol was prepared by reacting octadecaoxyethylene glycol with hexaoxyethylene dichloride. Purification of the compounds was effected by repeated high vacuum distillation, and by crystallisation for the higher members of the series. Methods similar to the above have been used to prepare polyoxyethylene glycol monoethers of the type $R.O(CH_2CH_2O)_6H$ where $R = n-C_{10}H_{21}$, $n-C_{12}H_{25}$, $n-C_{14}H_{29}$ and $p\text{-iso-}C_8H_{17}C_6H_4O-CH_2CH_2-$ and di-ethers of the type $R.O(CH_2CH_2O)_6R$ where $R = n-C_{10}H_{21}$, and $n-C_{14}H_{29}$. The scheme of reactions may be represented as follows:



After completion of the reaction the residue remaining after distillation was separated by chromatography on a silica gel column into the hexaoxyethylene glycol monodecyl ether and the hexaoxyethylene glycol didecyl ether.

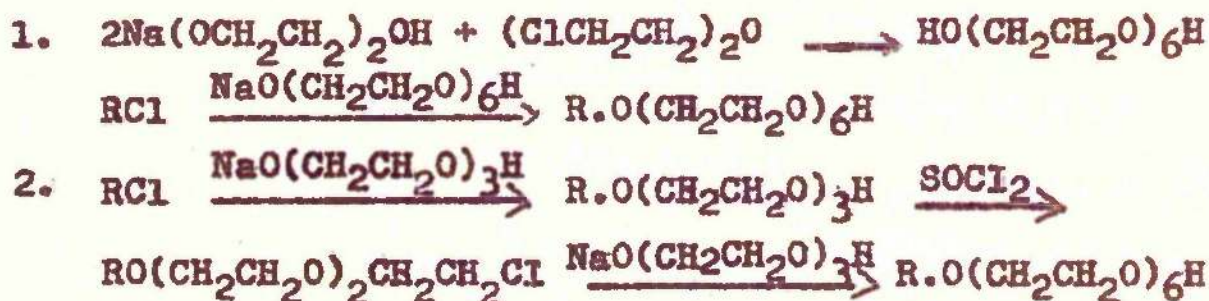
Similarly, the same authors⁴ have reported the preparation of n-octylhexaoxyethylene glycol ether, $C_8H_{17}O(CH_2CH_2O)_6H$, and hexaoxyethylene glycol monohexadecyl ether, $C_{16}H_{33}O(CH_2CH_2O)_6H$, and hexaoxyethylene glycol dihexadecyl ether, $C_{16}H_{33}O(CH_2CH_2O)_6C_{16}H_{33}$.

Monohexyl ethers linked with two to six ethylene oxide units have been prepared⁵ using eight equivalents of the glycol to minimise the formation of dialkyl ethers. These compounds were purified by extraction of the reaction mixture with petroleum ether, removal of this solvent and distillation.

Using Williamson ether syntheses these authors⁶ have also prepared polyoxyethylene glycol monodecyl ether, polyoxyethylene glycol monododecyl ether and polyoxyethylene glycol monohexadecyl ether with the polyoxyethylene units ranging from 2 - 6.

Low yields were obtained and recrystallisation failed to resolve a difference in melting points from those quoted by Gingras and Bayley⁴ for hexaoxyethylene glycol monodecyl ether and hexaoxyethylene glycol dodecyl ether.

n-Butyl, n-octyl, n-dodecyl and n-hexadecyl monoethers have been prepared ⁷ by two methods described by Corkill et al.



The n-octyl and n-hexadecyl ethers were prepared by method one, but the yields were small due to a large quantity of unsaturated hydrocarbon being produced by dehydrohalogenation of the alkyl chloride. Difficulty was also experienced in separating the n-octyl monoether compound from the unreacted glycol by distillation. The second method gave better results and was used to prepare the n-butyl, n-octyl and n-dodecyl compounds.

Monohexadecyl ethers have been prepared ^{8,9} containing six, seven, nine, twelve, fifteen and twenty-one ethylene oxide units. Nonaoxyethylene and dodecaoxyethylene glycols were synthesised by a Williamson ether synthesis and, in excess, were reacted with hexadecyl bromide. The reaction mixture was extracted with ether and the residue obtained after evaporation of the solvent, was re-extracted with petroleum ether, 60°-80°, and the residue after evaporation of the petroleum ether was recrystallised

from ether. The recrystallised material was then chromatographed on alumina and this treatment appears to give pure compounds of $\text{CH}_3(\text{CH}_2)_{15}(\text{CH}_2\text{CH}_2\text{O})_9$ or 12^{OH} . ie. Hn_9 and Hn_{12} . Chlorination of the terminal $-\text{OH}$ of Hn_9 , followed by condensation with the monosodium salt of hexaoxyethylene or nonaoxyethylene glycols yielded Hn_{15} , and Hn_{21} . The two smallest members of the series were prepared in the usual manner from hexaoxyethylene and septaoxyethylene glycols.

MICELLAR STRUCTURE OF NON-IONIC DETERGENTS.

The elucidation of the micellar structure of non-ionic detergents is an extremely difficult problem. It has been complicated by the fact that most studies have been made on detergents containing a range of ethylene oxide chain length. For example Kushner, Hubbard and Doane¹⁵ fractionated a sample of Triton X 100, a polyoxyethylene iso-octyl phenol ether, by molecular distillation to give three fractions whose molecular weights in water were 208,000, 90,000, and 54,000 (the fractions having $n = 8, 10,$ and 12 respectively). Stauff and Rasper¹⁴ fractionated a polyoxyethylene dodecyl ether, and found a similar decrease in micellar weight with increasing ethylene oxide content. Presumably the properties of these commercial materials are average ones. The behaviour of this type of detergent in solution will be discussed to give a general picture of the effects of monomer structure on the micelles.

A number of authors^{9,10,13} have studied the effect of increasing the polyoxyethylene chain length for the same hydrophobic group, which gives a decrease in micellar size. The aggregation number m , number of monomers per micelle, was shown¹³ to be related to the molar ratio of ethylene oxide to hydrophobic part of the condensate R , by

$$m = \frac{1025}{R} - 5.1 \quad \text{for lauryl alcohol derivatives}$$

and by $m = \frac{1215}{R} - 22.5$ for nonyl phenol derivatives.

Similar results were reported for polyoxyethylene condensates of n-octadecanol, n-dodecanol, nonyl phenol¹⁰, and decanol, and iso-octyl phenols,¹⁵ methoxy polyoxyethylene decanoates and dodecanoates^{64,65}. Increase of the hydrocarbon chain length increased the micellar weight.

The general structure of the micelles in water is one in which the hydrocarbon chains are in the interior, and the polyoxyethylene parts in an external layer. The stability of the micelles is thought to be due to a heavy hydration of the polyoxyethylene part. Kushner¹¹ and Hubbard found an intrinsic viscosity of 0.055 dl/g for Triton X 100 in solution. Using their observed molecular weight of 90,000, they calculated intrinsic viscosities of 0.029 dl/g for a disk shaped micelle, and 0.038 dl/g for a rod shaped one, neither figures fitting the observed intrinsic viscosity. They attributed the deviation of $[\eta]$ from the Einstein value to be due to hydration, and on this basis calculated that 43 water molecules were kinetically bound to each detergent monomer in the micelle. This value was thought to be high, but it was suggested that two water molecules were bound to each ether linkage, accounting for twenty, and the remainder were trapped in the hydrophilic "tentacles" of polyoxyethylene chains. On this basis the radius of the

micelle was found to be equal to the length of the nearly completely extended monomer.

A large amount of hydration (1.9 gwater/g. detergent) was found¹² for Cetomacragol 1000, a commercially produced detergent of structure $\text{CH}_3(\text{CH}_2)_{15}(\text{OCH}_2\text{CH}_2)_{22}\text{OH}$, which has a micellar weight of 101,000 from light scattering, and 96,000 from diffusion and viscosity measurements. Large hydrations have also been found for methoxy polyoxyethylene decanoates and dodecanoates^{64,65}.

The configuration of the polyoxyethylene chain in the outer layer of the micelles is not certain, and coiled and random arrangements have been suggested^{9,10}.

Normally, having obtained the molecular weight of the micelle, an attempt is made to fit the experimental results to some particular geometric shape. It has been suggested¹⁰ that micelles of molecular weight 45,000 - 100,000 are spherical in shape and that micelles with higher molecular weights are either disk or rod shaped, but it is possible that these limits are too narrow. The difficulty in assessing shape is that hydration must be known in order to calculate the total micellar volume, and to interpret viscosity results in terms of shape. Calculations of micellar shape of polyoxyethylene lauryl and nonyl phenol ethers have been made¹³, but in view of the uncertainty of the micellar hydration, it is not felt that their reliability is high.

Less work has been done on the micellar structure of synthetic compounds. The micellar weights, chemical structure, and critical micelle concentrations are listed in Table 1.

TABLE 1.

Micellar Properties of Synthetic Non-Ionic Detergents.

Structure.	$M \times 10^{-5}$	Temp. °C	cmc. moles/l	Ref.
$\text{CH}_3(\text{CH}_2)_{15}(\text{OCH}_2\text{CH}_2)_6 \text{OH}$	12.3	25	1.6×10^{-6}	9
$\text{CH}_3(\text{CH}_2)_{15}(\text{OCH}_2\text{CH}_2)_7 \text{OH}$	1.37	20		"
$\text{CH}_3(\text{CH}_2)_{15}(\text{OCH}_2\text{CH}_2)_7 \text{OH}$	3.2	25	1.7×10^{-6}	"
$\text{CH}_3(\text{CH}_2)_{15}(\text{OCH}_2\text{CH}_2)_9 \text{OH}$	1.4	25	2.0×10^{-6}	"
$\text{CH}_3(\text{CH}_2)_{15}(\text{OCH}_2\text{CH}_2)_{12} \text{OH}$	1.17	25	2.34×10^{-6}	"
$\text{CH}_3(\text{CH}_2)_{15}(\text{OCH}_2\text{CH}_2)_{15} \text{OH}$		25	3.09×10^{-6}	"
$\text{CH}_3(\text{CH}_2)_{15}(\text{OCH}_2\text{CH}_2)_{21} \text{OH}$	0.82	25	3.89×10^{-6}	"
$\text{CH}_3(\text{CH}_2)_7 (\text{OCH}_2\text{CH}_2)_6 \text{OH a.}$	0.1245	25	$9.8 \times 10^{-3} \text{L}$	7
			$7.6 \times 10^{-3} \text{F}$	"
$\text{CH}_3(\text{CH}_2)_7 (\text{OCH}_2\text{CH}_2)_6 \text{OH b.}$		25	$9.3 \times 10^{-3} \text{L}$	"
			$16.8 \times 10^{-3} \text{F}$	"
$\text{CH}_3(\text{CH}_2)_{11}(\text{OCH}_2\text{CH}_2)_6 \text{OH}$				"
Sample c	0.846			"
" d	0.714			"
" e		15	$10.8 \times 10^{-5} \text{L}$	"
" e	0.715	25	$8.7 \times 10^{-5} \text{L}$	"
" e		35	$7.2 \times 10^{-5} \text{L}$	"
" e	0.84			"
Sample f (in 0.1MNaCl)	0.60			

Structure.	$M \times 10^{-5}$	Temp. °C.	cmc. moles/l 1.0×10^{-6}	Ref.
$CH_3(CH_2)_{15}(CH_2CH_2O)_6OH$				7
$CH_3(CH_2)_{11}(OCH_2CH_2)_6OH$	0.63	15		16
"	0.84	18		"
"	1.8	25		"
"	3.2	30		"
"	6.3	35		"
"	10.0	42		"
"	18.0	45		"
$C_{6H_{13}}(OCH_2CH_2)_nOH$ $n = 3, 4, 5 \text{ or } 6.$			Probably in range 0.05 - 0.1M	74

Ref 7 * cmc from light-scattering.

L cmc from surface tension at indicated temperature.

a, c, d, e, and f were freshly prepared samples.

b, sample stored for six months.

A series of synthetic detergents, based on hexadecyl alcohol, and containing from six to twenty-one ethylene oxide units per molecule have been studied by light scattering and viscosity methods^{8,9}. A decrease in aggregation number was found as the series was ascended, in line with work on commercial materials. As the c/T against c graphs obtained from light scattering showed negative gradients at low concentrations, it was considered that as concentration increased, small micelles aggregated to form larger ones. A similar effect has been reported by Balmbra¹⁶ et al, who designated this second association concentration c_1 ; it is much greater than the cmc. Usually turbidities are too small to be measured in the region between c_1 and cmc, but in the case of Hn_6 and Hn_7 at 25° , it was found that c_1 was sufficiently large and the micellar sizes great enough for the measurements to be made. The aggregated species had micellar weights of 6.3×10^6 and 1.17×10^6 for Hn_6 and Hn_7 respectively. A somewhat similar result was reported earlier by Kushner, Hubbard, and Doane¹⁵ who found that the micellar size of molecularly distilled fractions of Triton X 100 was concentration dependent. However, as they were unable to find a well defined cmc it may be that their material had not been sufficiently purified.

As the series of detergents was ascended micellar asymmetry became less, while micellar hydration appeared to increase. The same authors¹⁷ have developed an empirical method for determining micellar hydration, consisting of determining the concentration of a solution of detergent which has the same vapour pressure as water, within experimental error, water being progressively added to the solid detergent. The hydration obtained from this method agreed well with that calculated from intrinsic viscosity for spherical micelles.

The results shown in Table 1, reference 7, follow the general trend i.e. the micellar weight increases with increasing hydrophobicity of the hydrocarbon chain.

The theory of formation of micelles and micelle size has not been fully developed for non-ionic detergents. It has been suggested that in the course of aggregation with increasing concentration there is a temporary inflection of the free energy of the total system, which halts the formation of a new phase at a given micellar size¹⁰, but this does not fully explain the phenomena. Other factors which resist the fall in particle-solvent contact, and the resulting dehydration and entropy changes are also thought to be of importance.

The entropy and energy changes taking place during micelle formation of non-ionic detergents in aqueous

solutions have been studied¹⁸. The calculations were based on a simple model of coalescence of a hydrocarbon chain to a liquid droplet and the fitting of ethylene oxide units over the surface. It was calculated that:-

1. Micellar formation of non-ionic detergents in aqueous solution occurs at a distinct cmc.
2. Cmc decreases with an increase in the hydrophobic part of the molecule.
3. For a given hydrophobic group the cmc increases with an increase in the ethylene oxide units present.

These three theoretical conclusions are generally in agreement with experimental work.

An attempt to apply statistical mechanics to the theory of micelle formation and shape has been made¹⁹. It was accepted that the reason for micelle formation is a decrease in the free energy of the system when the hydrocarbon portion of the detergent molecules aggregate leaving hydrophilic groups in the aqueous phase. It was assumed that geometrical restrictions in micelles are such that the micelle should have a fixed density and a limited hydrocarbon length. Bearing in mind these restrictions it was suggested that two shapes could be proposed for very large micelles viz. rod-like, with a circular cross-section, or plate-like.

Recent work ²⁰ has attempted by means of statistical mechanics to study the meaning of temperature variation of cmc, the effect of interaction of micelles upon the distribution of micellar sizes, the meaning of ideality, the nature of the spread of micellar sizes about the average value and whether or not a single micellar size can be used as the basis for the theoretical treatment of micelles.

CRITICAL MICELLE CONCENTRATION AND SURFACE ACTIVITY.

The postulate of colloidal aggregates was first put forward by McBain²¹ to account for the combination of low osmotic activity with high electrical conductivity found in higher fatty acid soaps. These aggregates still retained considerable conductivity due to their high electrical charges, but behaved osmotically as single particles. McBain called these aggregates ionic micelles and the concentration at which these molecules formed micelles he called the critical micelle concentration (cmc).

The cmc can be measured readily, as it appears that if almost any physical property of aqueous solutions of detergents is plotted against the concentration of the solution a break occurs at the cmc.

Initially, difficulty was experienced in deciding if non-ionic detergents exhibited pronounced cmc's. For example in an early paper²², a cmc, determined by depression of freezing point, was reported for Triton X 100. In a later paper¹¹ it was stated that a well defined cmc for Triton X 100 could not be obtained by light-scattering techniques.

15

The same workers have been unable to establish a well defined cmc on molecularly distilled fractions of Triton X 100.

However, the presence of a cmc in aqueous solutions of non-ionic detergents seems to have been established by other workers^{23,24,25}, and later work assumes the existence of cmc's and they have been reported widely for many different compounds. It has been noticed that cmc values obtained from different techniques for the same compound may differ considerably and it may be that a sharp value for the cmc is only an approximation, as has been suggested²⁶. The situation may also be complicated by the spread of chain lengths in the commercial detergents.

The values of cmc's of non-ionics have been found to be much lower than those of ionic detergents. This is to be expected as the non-ionic materials have hydrophilic groups which are about the same length as the hydrocarbon chain, and micellisation is not hindered by electrical forces^{23,25,7,63}. For example the cmc of sodium dodecyl sulphate has been found⁶³ to be 0.0081 mole/litre (no temperature quoted), whereas that of n-dodecyl hexaoxyethylene glycol varies from 0.000108 mole/litre at 15° to 0.000072 mole/litre at 35°⁷.

Also the value of the cmc has been found to depend on the hydrophilicity of the molecule. Generally it has been accepted that an increase in cmc is brought about by an increase in hydrophilicity.

For example it has been shown by Lorenz²³ for a series

of commercial non-ionic detergents based on a nonyl phenol hydrophobic portion and various chain lengths of ethylene oxide, that the increase in cmc with increasing ethylene oxide units is approximately given by $\ln(\text{cmc}) = 0.056R + 3.87$ where R represents the mole ratio of ethylene oxide to phenol. An increase in the positive value of R, i.e. in the hydrophilic part of the molecule, is thought to increase the total hydration, and thus the cmc, as hydrophilic properties of the molecule are increased. It was also noted by Lorenz and other workers²⁷ that a decrease in the hydrophobic part of the molecule also increases the cmc. Conversely, an increase in the hydrophobic part of the molecule has been shown²⁸ to lead to a decrease in the cmc as aggregation of the hydrophobic parts of the molecules is brought about by the cohesive forces acting between them. These forces would increase on lengthening the hydrocarbon chain.

The measurement of the lowering of the interfacial tension at the air / water surface, i.e. surface tension provides a suitable method for the cmc. A plot of log concentration v. surface tension (dynes cm^{-1}) gives an inflection at what is thought to be the cmc. A plot of almost any physical property against concentration gives a similar inflection, but the measurement of the

decrease in surface tension appears to be among the most sensitive and also enables the measurement to be made without the addition of any other material

This lowering of the surface tension is a general property of surface active agents. The phenomenon of surface activity is essentially one of adsorption and this may lead to several distinct effects ^{61,62}.

1. There may be a lowering of one or more of the boundary tensions prevailing at the interfaces of the system.
2. There may be stabilisation of one or more of the interfaces by the formation of adsorbed layers which may oppose any tendency for these interfaces to be diminished in area or destroyed.
3. There may be formation of micelles i.e. molecular aggregates above a certain concentration known as the critical micelle concentration.
4. There may be solubilisation of water insoluble substances into the micelles.

From surface tension measurements it is possible to calculate the area per molecule by an application of a simplified Gibbs equation relating surface excess, Γ , to surface tension γ .

Several authors have published results of area per molecule measurements for a wide range of non-ionic detergents ^{75,76,13,23}.

Generally it seems established that the area per molecule increases with increasing chain length and that at the air / surface interface the molecules are orientated with the hydrocarbon chain directed out of the surface of the solution and the polyoxyethylene chain coiled in the solution.

For example Macfarlane and Elworthy⁷⁵ have shown that the area per molecule for a series of synthetic polyoxyethylene monohexadecyl ethers increases with increasing ethylene oxide units varying from 38 \AA^2 for the ether with a hexaoxyethylene glycol hydrophilic group to 120 \AA^2 for the ether with a heneicosanoxyethylene glycol hydrophilic group. They also found that the area per ethylene oxide unit decreased with increasing chain length. As the areas per molecule were all larger than the cross-sectional area of the hydrocarbon chain it was thought that the polyoxyethylene chain determined the area per molecule.

Work on molecularly distilled commercial ethylene oxide condensates of aliphatic alcohols and alkyl phenols⁷⁶ agrees with the above results in all respects. This work is of particular interest in that the areas per molecule were determined at 25°C and 55°C . It was noted that the areas found at 55°C tended to be smaller than those found at 25°C . An example of this change in area is shown below.

Hydrophobic portion.	Number of Ethylene oxide units.	Area per molecule in adsorbed o ₂ surface film Å	
		25°C	55°C
Nonyl Phenol	10	64	62
	30	80	74
	50	120	115

It can be seen that there is a small difference in the areas measured at the different temperatures. It is thought that this is due to a variation in the mode of packing of the molecules due to hydration changes as the temperature rises.

Becher¹³ has quoted values for area per molecule at the air / solution interface and in the micelle for polyoxyethylene lauryl alcohol ethers and polyoxyethylene nonyl phenol ethers with 8 to 27 and 10 to 20 ethylene oxide units respectively. For the lauryl alcohol series the area per molecule at the solution surface ranges from 46 Å² to 74 Å² (ascending the series), and in the micelle the increase was from 49 Å² to 58 Å². For the nonyl phenol series the increase in area was found to range from 60 Å² to 107 Å² at the surface but for the areas measured in the micelles the areas per molecule were found to be 60 Å² (10 Ethylene Oxide Units), 64 Å² (15 Ethylene Oxide Units), 62 Å² (20 Ethylene Oxide Units). However as the hydrations of the micelles were assumed, some doubt is thrown on the areas per molecule calculated for the monomers of the micelles in the solution.

The areas per molecule of a series of commercial polyoxyethylene nonyl phenol ethers have been measured²³. For hydrophilic chain lengths varying from 9.5 to 100 ethylene oxide units, areas per molecule were found to vary from 55 \AA^2 to 173 \AA^2 . It is interesting to compare the values for area per molecule obtained by the above authors for polyoxyethylene nonyl phenol ethers as far as they are comparable (Table 2).

TABLE 2.

Areas / Molecule of Some Non-Ionic Detergents.

Number of Ethylene Oxide Units.	Area per Molecule \AA^2	Reference
10	60	13
10	64	65
10.5	60	23
15.0	72	13
15.0	72	23
20	107	13
20	82	23
30	80	65
30	101	23

Solubility may also be conveniently* mentioned here.

The solubility of polyoxyethylene type non-ionic detergents is believed to be due to hydrogen bonding between the oxygen atoms of the ethylene oxide chain and water molecules.

*conveniently

Increased solubility results from an increase in the
number of ethylene oxide units in the detergent ^{23,28,29,49}.

SOLUBILISATION.

It has been shown that materials which are not normally soluble in water may be solubilised in solutions of non-ionic detergents. Although it is thought that below the cmc solubilisate may in some way become attached to molecules of detergent it is not always possible to detect this and solubilisation studies are carried out above the cmc normally.

It is generally believed³⁰ that non-polar hydrocarbons are solubilised into the interior of the micelle, partly ionic compounds are adsorbed into the micellar surface with the non-polar group inside the micelle and the polar group outside. Water soluble polar compounds such as glycerol are taken up on the exterior of the micelle and may act as peptising agents.

Another method of incorporating partly polar compounds such as phenol into non-ionic micelles with polyoxyethylene chains has been suggested.³¹ It is thought to be more accurate to consider that these compounds are included in the polyoxyethylene chain layer of the micelle rather than to consider that they are adsorbed onto the micellar surface. For example the hydroxyl group of phenol is thought to form hydrogen bonding with the ether oxygens of the ethylene oxide groups.

The formation of complex phenolic substances with polyoxyethylene groups has been reported^{50, 51} and it has also

been observed⁵² that many phenolic substances are readily dissolved in concentrated solutions of polyoxyethylene glycols and solubilised in aqueous solutions of polyoxyethylene type non-ionic detergents.

It has been shown,³² using methoxyoctaoxyethylene decyl ether, $C_{10}H_{21}O(CH_2CH_2O)_8CH_3$, and methoxyundecaoxyethylene decyl ether, $C_{10}H_{21}O(CH_2CH_2O)_{11}CH_3$, solutions, and n-decane and n-decanol as solubilisates, that cmc decreases and micellar size increases with the addition of the water insoluble materials. The effect of added n-decane on the micellar weight of methoxydodecaoxyethylene decyl ether, $C_{10}H_{21}O(CH_2CH_2O)_{12}CH_3$, has been observed at $50^\circ C$ ⁵³, by light-scattering. Again the cmc decreased and the micellar weight increased.

An interesting use to which the solubilising properties of non-ionic detergents have been put is in the estimation of cmc.

Of particular interest is a method developed by Ross and Olivier⁵⁵ using the absorption maxima of a coloured iodine-micelle complex to give a measure of the cmc. A plot of percentage transmission against concentration gives a break at the cmc. This method has been used⁵⁶ to measure the cmc's of solutions of commercial polyoxyethylene lauryl, stearyl, oleyl and tridecyl alcohols as well as commercial polyoxyethylene sorbitan monolaurate.

EFFECT OF TEMPERATURE ON NON-IONIC DETERGENTS IN SOLUTION.

Most of the work on temperature changes in solutions of non-ionic detergents has been concerned with the effect of temperature on cmc, micellar size, cloud-point changes associated with solubilisation, and on viscosity, and these topics will be separately considered.

a). Effect of Temperature on C.M.C.

In contrast to solutions of ionic detergents where an increase in temperature brings about an increase in cmc³⁴, the cmc of solutions of non-ionic detergents appears to be decreased by a rise in temperature.

The cmc's of methoxypolyoxyethylene octanoate, $C_7H_{15}COO(CH_2CH_2O)_{7.6}CH_3$, have been measured over the temperature range of $10^\circ - 43^\circ C$, and have been found to decrease with increase in temperature³⁵. The cmc's were measured by the spectral colour change of pinacyanol chloride and by the solubilisation of Sudan III. Agreement between the results from the two methods was not good, but both showed the same general trend.

Light-scattering estimations of the cmc of a methoxypolyoxyethylene decyl ether, $C_{10}H_{21}(OCH_2CH_2)_{12}OCH_3$, MPd12, over a range of temperatures, were carried out by the same workers³⁶ and again a decrease in cmc with increase in temperature was found. Concurrent experiments

on the cmc of sodium dodecyl sulphate were carried out and an increase in cmc was obtained with increasing temperature as was expected with an ionic detergent. The micellar heats of formation for the above non-ionic compounds were found to be positive. Later measurements on the variation of cmc with temperature have been made by Kuriyama³⁷ on MPd 12. It was suggested by him that the decrease in cmc found by increasing the temperature is due to a decrease in the hydrophilicity of the ethylene oxide chain as the temperature rises. The cohesive force between the hydrophobic parts of the molecules which counterbalance the hydrophilic ethylene oxide would thus become predominant and the cmc would be lowered.

Broadly similar results have been obtained⁷ from the measurement of the variation of cmc with temperature using n-dodecyl hexaoxyethylene glycol ether, $C_{12}m_6$. Again a decrease in cmc was obtained with increasing temperature.

Positive values of 5.9 kT for ΔH_m , molar heat of micelle formation, between 15° and 35°C and 5.9 cal mole⁻¹ deg⁻¹ for ΔS , entropy of micelle formation, were obtained from solutions of $C_{12}m_6$. It was not thought likely that a gain in entropy was caused by the molecules being less restricted in micelles than in water, and it was suggested by the magnitude of ΔS , that the energetics of micellisation of non-ionic detergents is governed by partial dehydration

of the monomer as it enters the micelle. An increase in temperature, it was explained, would lead to a decreased hydration and as was stated previously³⁷ to a decrease in cmc. This gain in entropy was thought to be the result of a change in the orientation of some or all of the water molecules in the vicinity of a monomer of detergent when the monomer became incorporated into a micelle.

The formation of micelles of n-dodecyl hexaoxyethylene glycol in solutions of sodium dodecyl sulphate (SDS) an ionic detergent, was also studied. Very little change in micellar weight was found, as compared to water, in 10^{-4} M SDS, but in 10^{-3} M SDS as a plot of H_c/T gave a higher intercept than that found in water, so either a decrease in micellar weight or an increase in micellar charge had occurred. It was thought that this change was due to a change in micellar charge i.e. a 'mixed' micelle of some type had been formed.

Mixed micelles containing ionic and non-ionic²⁸ detergents have also been reported by Kuriyama .et al . These micelles have been shown to have properties which depend on the relative proportions of ionic to non-ionic species. With respect to the effect of temperature on cmc of these micelles it was shown that in solutions containing various concentrations of sodium dodecyl

sulphate, and constant concentrations of methoxypolyoxyethylene dodecyl ether, $C_{12}H_{25}(OCH_2CH_2)_{12}OCH_3$, MP 1-12, the cmc's decrease with increasing temperature until the ratio of SDS to MP 1-12 reaches 1:4 whereupon ionic behaviour is exhibited by the micelles and the cmc rises with temperature.

b). The Cloud Point.

When solutions of non-ionic detergents are heated, at a certain temperature precipitation of the detergent and phase separation occurs. The temperature at which this occurs is known as the cloud point. The cloud point is affected by materials solubilised into the micelles in the solution and also by electrolytes.

It has been shown ²⁹ that the decrease in the cloud point of Triton X 100 solutions obtained by addition of electrolytes is a linear function of the ionic strengths of the added electrolytes. The addition of nonpolar organic compounds and anionic detergents to Triton X 100 solutions was found to increase the cloud point. If the polarity of the organic solubilisate was increased by the introduction of more polar groups the increase in cloud point was found to be less pronounced. The cloud point of Triton X 100 was greatly decreased by the addition of polar aliphatic compounds and also by the addition of polar aromatic compounds, a fact which had been previously

reported³⁸. The increase of micellar weight of Triton X 100 with temperature has been stated to be the dominant factor for cloud point formation and phase separation³⁹. A marked depression in the cloud point of polyoxyethylene iso-octyl phenol ether has also been observed⁵⁴ on the addition of various polar phenolic compounds.

The cloud point of a methoxypolyoxyethylene decyl ether, $C_{10}H_{21}(OCH_2CH_2)_{10}OCH_3$ ⁴⁰, was found to rise on the addition of n-octane, decane and dodecane, which are non-polar substances. As the concentration of the solubilisate was raised, the cloud point was also raised until at a particular concentration of solubilisate, emulsion drops of the added compound were formed, indicating that a saturation concentration had been reached. Conversely, it was shown that the cloud point was decreased by the addition of n-octanol, decanol, and dodecanol which are more polar compounds. By increasing the concentration of the solubilisate it was found possible to decrease the cloud point to room temperature.

H_m , calculated from $H_m = RT^2 \left(\frac{\lambda \ln C_s}{\delta T} \right)_p$ where H_m is the

heat of mixing of a solubilisate in a surfactant and C_s the saturation amount of solubilisation, was found to be positive for hydrocarbon solubilisation and to be almost zero for

alcohols.

Phase separation above the cloud point was explained by the fact that the micelles in solution grew so large that they separate to form a distinct layer which may consist of large micelles solely, or of a complex mass composed of surface active agent, solubilisate and water molecules randomly mixed or regularly arranged.

A similar explanation of cloud point formation in solutions of a methoxypolyoxyethylene decyl ether, $C_{10}H_{21}(OCH_2CH_2)_{12}OCH_3$, MPd 12, has been given by Kuriyama³⁷. According to him the micellar weight increases with temperature and at the cloud point opalescence occurs and the micelle floats or sinks as the bouyancy of the micelle overwhelms the Browian movement and two layers are formed.

c). Effect of Temperature on Micellar Weight.

It has been mentioned that the micellar weights of non-ionic detergents increase with increasing temperature. Several papers have been published in which this effect has been studied.

The micellar weight variation of a methoxypolyoxyethylene octanoate, $C_7H_{15}COO(CH_2CH_2O)_{7.6}CH_3$, has been observed³⁵ between 10 - 43°C. Assuming a hydrated spherical molecule the molecular weights were calculated from diffusion - viscosity measurements. The length of the monomer in the

elongated state was found to be 38.9 Å, of which the hydrophobic portion contributed 11.5 Å and the hydrophilic portion 27.4 Å. However, the micelle radius at 43°C, from diffusion measurements, was found to be considerably larger than this showing that the assumption of a spherical molecule was wrong. The effective volume per g. surface active agent was found to decrease from 10° - 38°C and this was explained as a progressive dehydration of the hydrophilic part of the monomer with a rise in temperature. An apparent increase in effective volume was obtained from viscosity measurements at 43°C. These conclusions are somewhat uncertain as the micelles were assumed to be spherical over the whole temperature range.

The effect of temperature on solutions of methoxypolyoxyethylene decyl ether, $C_{10}H_{21}(OCH_2CH_2)_{12}OCH_3$, MPd 12, has also been noted³⁶. The micellar weight was found to increase with temperature particularly near the cloud point and the second virial coefficient was found to decrease with increase in temperature.

These results for MPd 12 have been substantiated³⁷. The decrease in second virial coefficient which was obtained has been attributed to a decrease in hydration as the temperature is raised.

Similarly the micellar weights of solutions of a

polyoxyethylene dodecyl ether, MP 1-12, have been observed to increase with temperature while the hydration was thought to decrease with increasing temperature.

Results have been obtained³⁹ for the effect of temperature on the micellar weights of a methoxypolyoxyethylene dodecyl ether, MP 1-12, and Triton X 100 in water (20 - 76°C), 0.3M sodium chloride (30 - 70°C), 1 M sodium chloride (30 - 60°C), 0.5M calcium chloride (30 - 64°C) and 1 M calcium chloride (30 - 60°C). At fixed temperatures the micellar weights of those compounds have been shown to increase on the addition of salts and the effect of the salts has been shown to be greater at higher temperatures. Also at a fixed salt concentration the micellar weight has been observed to increase with temperature. Light -scattering, solubilisation and viscosity measurements have been used at different temperatures to estimate the change in micellar weight of aqueous solutions of n-dodecyl hexaoxyethylene glycol monoether¹⁶ ($C_{12}n_6$). The micellar weight was found to increase with temperature. A plot of log. Micellar Weight v Temperature gave a straight line. However for the light-scattering results it was necessary to consider critical opalescence as a factor affecting micellar weight as this phenomenon may occur as far as 30° from a phase

boundary. The critical opalescence is dependent upon the scattering angle and this effect was considered to be small as unit dissymmetries were obtained. It was suggested that the increase in micellar size with temperature is an entropy effect associated with a temperature dependent dehydration of single molecules. Also as the ratios of solubilities of Orange OT in micellar solution and in pure liquid detergents were found to be independent of temperature, it was considered that the increase in micellar size is not accompanied by any radical change in micellar shape.

From the light-scattering results the micelles are not thought to be spherical above 25°C, but if the micelles were considered to be rod-like shapes, the rod length would be below that necessary to produce any dissymmetry of scattered light.

The molecular weight of heptaoxyethylene glycol monohexadecyl ether, Hn7, has been shown to increase with temperature from 20 - 25°C. Micellar asymmetry is thought to develop as the temperature is raised, although very little change was noted in the dissymmetry ($Z_{45^\circ} 20^\circ 1.00$, $Z_{45^\circ} 25^\circ 1.02$).

d). Effect of Temperature on Viscosity.

The effect of temperature on the viscosity of concentrated solutions has been studied ^{33.} The materials used were

p-t-t-octylphenyl polyoxyethylene ethanols, OPE_n, where n is the weight average moles of ethylene oxide condensed per mole of octyl phenol. OPE 7.5, OPE 9.7 and OPE 12.3 were used. An iso-octyl methyl phenol OMPE_n, where n = 9.7 was also used. Gelling or high viscosities were obtained in the concentration range 50-70% detergent, this phenomena decreasing with increasing temperature. The formation of gels at high concentrations of detergent was prevented by the addition of salts and the viscosities of more dilute solutions were increased by the addition of salts.

The effect of salts at higher concentrations was stated to be due to a decrease in the hydration of the ether links, thus giving more aqueous phase and making the deformation of the micelles formed easier

This dehydration was considered to be responsible for both the positive temperature coefficient of viscosity observed for all compounds but OPE 7.5, and the increased viscosity brought about in more dilute solutions by salts.

The effect of temperature on the viscosity of solutions of hepta⁹oxyethylene glycol monohexadecyl ether, Hn₇, has been described. Values for $\left(\frac{\eta_{sp}}{\phi}\right)_{\phi=0}$ were found to be 2.8 (20°C), 9.5 (25°C), and 29.4 (30°C). These viscosity results were interpreted as being due to a large micellar

asymmetry developing with increase in temperature, but the dissymmetry measurements obtained from light-scattering at 20° and 25°C did not vary appreciably from unity.

Some preliminary viscosity studies¹⁶ on n-dodecyl hexaoxyethylene glycol monoether, C₁₂n₆, have shown that the intrinsic viscosity was increased by increasing the temperature. As it was assumed that this increase in temperature brought about a decreased hydration, the viscosity results were thought to be consistent with an increase in asymmetry as molecular weight increased with temperature.

THEORY OF LIGHT-SCATTERING.

If a beam of light falls on matter, the electrical field associated with the light induces periodic oscillations of the electrons in the material. The material will then serve as a secondary source of light whose radiation will be scattered with a wave length equal to that of the incident light. The intensity, angular distribution and polarization of the scattered radiation are determined by the size, shape, optical constants and interactions of the molecules present in the material.

The earlier theories of light-scattering were mainly concerned with small independent particles such as would be found in gases. Later theories have been applied to interacting systems such as solutions in which the particles cannot be considered to be independent.

Two methods of calculating the intensity of scatter have been developed.

The Rayleigh method ⁴¹ may be used to calculate the intensity of scatter from dilute gases. Debye ⁴² showed it could also be applied to dilute non-interacting solutions.

The Fluctuation theory was developed by Einstein ⁴³ and Schmoluchowski ⁴⁴.

This method is applicable to solutions and may be applied to pure liquids.

Small Particles.

- a) Rayleigh Treatment for Particles which are small compared with the Wavelength of Light.

When the particles of an ideal gas are subjected to an electric field of force E , a dipole moment p is set up, as the electrons of the particles are subjected to a force in one direction, while the nuclei of the particles are subject to a force in the opposite direction.

If the particles are optically isotropic the direction of the dipole is parallel to that of the electric field.

The dipole induced in any particle is proportional to E or $p = \alpha E$ (1)

where α is the polarisability of the particle.

If the particle is considered to be in the path of a plane polarised beam of light the general equation for the electric field of the light wave is

$$E = E_0 \cos 2\pi(vt - x/\lambda) \quad (2)$$

where E_0 is the maximum amplitude, t the time, λ the wavelength, v the frequency and x the position along the line of the light beam.

Combining (1) and (2) gives.

$$p = \alpha E_0 \cos 2\pi(vt - x/\lambda) \quad (3)$$

Equation (3) gives the magnitude of the oscillating dipole induced by the incident electric field. An oscillating dipole can be shown to be a source of electromagnetic radiation which, in this case, is the scattered radiation. The field strength of this scattered radiation, E_s , is proportional to d^2p/dt^2 .

At a distance r , where r is a great distance from the dipole, the field strength is proportional to $\sin \theta_1$, where θ is the angle between the axes of the dipole and the line joining the point of observation to the dipole.

It can be shown, also, that E_s^2 is proportional to the intensity, I , where I is the energy flowing per cm^2 . From the law of conservation of energy, I varies as $1/r^2$. Therefore E_s varies as $1/r$.

Differentiating equation (3) to get d^2p/dt^2 gives

$$\frac{d^2p}{dt^2} = 4\pi^2 v^2 d E_0 \cos 2\pi(vt - x/\lambda)$$

Substituting E_s for d^2p/dt^2 , introducing $\sin \theta_1/r$, and dividing by the square of the velocity of light (c^2), to make the dimensions correct gives

$$E_s = \frac{4\pi^2 v^2 d E_0 \sin \theta_1 \cos 2\pi(vt - x/\lambda)}{c^2 r} \quad (4)$$

The normal quantity measured experimentally is the

intensity of the light, which is proportional to the square of the amplitude, or field strength, measured over one vibrational period.

The ratio of the intensity of the scattered light, i_s , to that of the incident light, I_0 , can be obtained from equations (2) and (4), this ratio is

$$\frac{i_s}{I_0} = \frac{16\pi^4 \alpha^2 \sin^2 \theta_1}{\lambda^4 r^2} \quad (5)$$

The wavelength, λ , is substituted for \bar{c}/v .

Equation (5) is Rayleigh's equation.

An evaluation of α^2 is necessary for experimental purposes. It can be shown that the polarisability of a medium can be related to its dielectric constant. If the molecules are in a vacuum

$$\epsilon - 1 = 4\pi N \alpha \quad 66 \quad (6)$$

where ϵ is the dielectric constant and N is the number of particles per cc.

Also $\epsilon = n^2$, where n is the refractive index

$$\therefore n^2 - 1 = 4\pi N \alpha \quad (7)$$

As n is close to unity

$$n^2 - 1 = 2(n - 1)$$

$$2(n - 1) = 4\pi N \alpha$$

$$\text{so } n - 1 = 2\pi N \alpha$$

Dividing by c ,

$$\frac{n - 1}{c} = \frac{2\pi N \alpha}{c}$$

where c is the concentration in g/ml.

$$\frac{n - 1}{c} = \frac{dn}{dc}$$

ie. the change in refractive index with addition of gas molecules.

$$\therefore \frac{dn}{dc} = \frac{2\pi N \alpha}{c}$$

$$\text{or, } \alpha = \frac{c \cdot \frac{dn}{dc}}{2\pi N} \quad (8)$$

Equation (5) was derived for one particle. Multiplying by N , where N is the number of particles, and substituting for α^2 gives

$$\frac{I_s}{I_o} = \frac{4\pi^2 c^2 (dn/dc)^2 \sin^2 \theta_1}{\lambda^4 N r^2} \quad (9)$$

If M is the molecular weight of the particles and N_a is Avogadro's Number, $\frac{M}{N_a} = \frac{c}{N}$, $\therefore N = \frac{c N_a}{M}$

Substituting for N in (9) gives

$$\frac{I_s}{I_o} = \frac{4\pi^2 (dn/dc)^2 M c \sin^2 \theta_1}{\lambda^4 N_a r^2} \quad (10)$$

The term $\sin^2 \theta_1$ gives the angular dependence of the scattered light. From Fig. 1, page 43A, it can be seen that the incident light wave is polarised in the ZX plane. At O the oscillating dipole radiates a secondary wave the intensity of which varies as the square of the sine of the angle between the observer and the Z axis. In Fig. 1 page 43A, the lengths of the arrows are proportional to the intensity in any given direction. The intensity tends towards a maximum in the YX plane and towards zero along the Z axis. The scatter is symmetrical about the Z axis.

Unpolarised light may be considered to be a superposition of two plane-polarised beams with their planes of polarisation perpendicular to one another. Fig. 1A page 43A, shows the distribution of scattered light in this case. Here, the vertical ZX wave behaves as in Fig. 1 page 43A. The horizontal XY plane sets up a secondary wave, the intensity of which goes to a maximum in the ZX plane, to zero on the Y axis and is symmetrical about the Y axis.

Therefore i_o , the intensity of scatter of the unpolarised light represents the sum of two terms in equation 1D.

ANGULAR DEPENDENCE OF SCATTERED LIGHT.

FIGURE I.

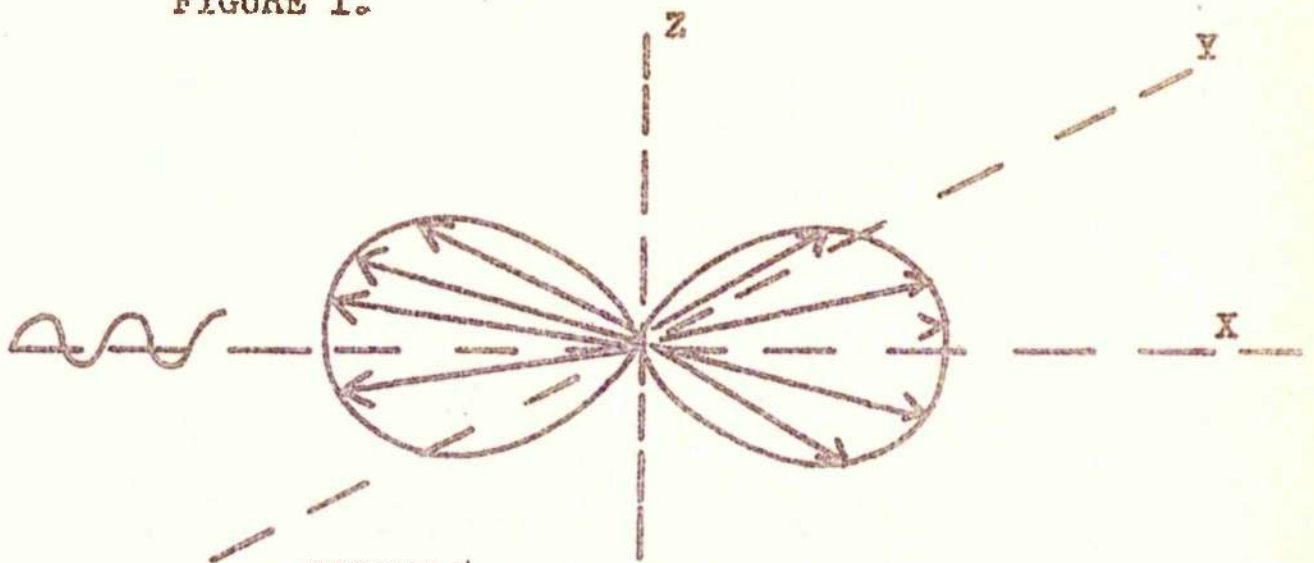
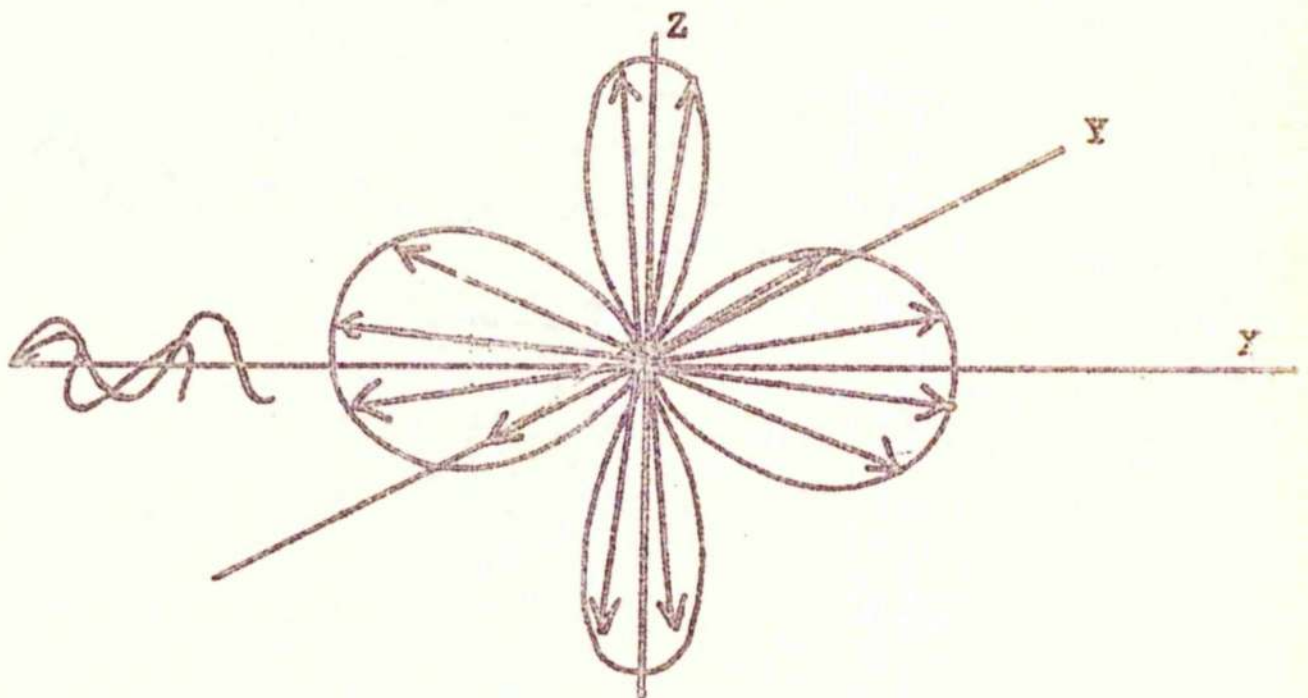


FIGURE Ia.



Each term represents the scattering from half the incident intensity. The left hand side of equation (10) will be $\frac{i_s}{\frac{1}{2}I_0}$ for each of these terms. The terms will be identical except that the angular distribution term will differ. One term will contain $\sin^2 \theta_1$, and the other $\sin^2 \theta_2$, where if the direction of the incident beam is designated as the x-axis of a rectangular coordinate system, θ_1 and θ_2 represent the angles made by the line from the point of observation with the y and z axes respectively.

Therefore, for unpolarised light, equation (10) becomes

$$\frac{i_e}{I_0} = \frac{2\pi^2 (dn/dc)^2 Mc}{\lambda^4 N_a r^2} (\sin^2 \theta_1 + \sin^2 \theta_2) \quad (11)$$

$\sin^2 \theta_1 + \sin^2 \theta_2$ may be replaced by $1 + \cos^2 \theta$, where θ is the angle between the line of observation and the x axis.

$$\therefore \frac{i_e}{I_0} = \frac{2\pi^2 (1 + \cos^2 \theta) (dn/dc)^2 Mc}{\lambda^4 N_a r^2} \quad (12)$$

If this equation is applied to dilute solutions α^2 must be redetermined.

Equation (7) becomes

$$n^2 - n_0^2 = 4\pi N \alpha \quad (13)$$

where n_0 is the refractive index of the solvent.

If n is close to n_0

$$2n_0(n - n_0) = 4\pi N \alpha$$

$$n_0(n - n_0) = 2\pi N \alpha$$

$$n_0(n - n_0)/c = 2\pi N \alpha / c$$

ie. $n_0 dn/dc = 2\pi N \alpha / c$

$$\therefore \alpha^2 = \frac{n_0^2 (dn/dc)^2 c^2}{4\pi^2 N^2} \quad (14)$$

Insertion of this new value of α^2 into equation (5)

leads to

$$\frac{I_\theta}{I_0} = \frac{2\pi^2(1 + \cos^2 \theta)n_0^2 (dn/dc)^2 Mc}{\lambda^4 N_a r^2} \quad (15)$$

This equation applies to very dilute solutions only, and is only strictly true at infinite dilution.

b) Light-Scattering by Transparent Crystals.

Whereas, in the treatment given before for gases, the scattering points were considered to be independent, for transparent solids this is not so.

In the latter case the scattering points are fixed rigidly in space. For any volume element A, another, B, can be found, with the same number of scattering points, which destructively interferes with the scatter from A and cancels out any radiation. This occurs where the

wavelength of light is much greater than the distance between the particles and when the light paths from A and B to an observer viewing at any angle θ are different by one half wavelength.

c) Light-Scattering by Pure Liquids.

Pure liquids may be considered to be intermediate between gases and transparent crystals. Order is present, but not complete order.

Two equal volume elements can be considered with dimensions $\ll \lambda$, separated by such a distance that the light paths to an observer differ by half a wavelength. However, in a liquid the scattering points in any volume element do not remain constant because of the partially random movement of the particles. Therefore, no two volume elements can be considered to have the same number of scattering particles at any particular time. The difference in the number of scattering particles gives rise to fluctuations in the density or refractive index of the liquid. There is therefore an excess of scattering from one, of any two pairs of volume elements, which is not cancelled out.

So pure liquids give a small scattering of light.

d). The Theory of Fluctuations as Applied to
Macromolecular Solutions.

Let the solution be made up of small elements of volume Ψ , whose dimensions are very much less than the wavelength of light so that each element can be considered as a single source of scattering, but such that each element contains a large number of solvent molecules and a few solute molecules.

If the concentration of the solute is considered to be variable, and if the average value of this in g/ml. throughout the solution is considered to be \bar{c} , the fluctuation concentration in Ψ will equal $c = \bar{c} + \delta c$, where δc is the concentration fluctuation.

Also, due to the fluctuation in concentration, there will be fluctuation in the polarisability of the solution. If \mathcal{L}' is the average polarisability $\mathcal{L} = \mathcal{L}' + \delta \mathcal{L}$, $\delta \mathcal{L}$ being due to δc .

Therefore equation (5) becomes

$$\frac{I_s}{I_0} = \frac{16\pi^4 (\mathcal{L}' + \delta \mathcal{L})^2 \sin^2 \theta_1}{\lambda^4 r^2} \quad (16)$$

The expansion of $(\mathcal{L}' + \delta \mathcal{L})^2$ is $\mathcal{L}'^2 + 2\mathcal{L}'\delta \mathcal{L} + (\delta \mathcal{L})^2$
The \mathcal{L}'^2 term is zero as this term for any element is the same. Therefore a similar phenomenon takes place as

occurs in transparent crystals which give no scattering. Any term in $\delta\alpha$ has an equal chance of being positive or negative and therefore this term disappears. As all terms in $(\delta\alpha)^2$ will be positive this term remains and is written $(\overline{\delta\alpha})^2$ to signify the average value of a large number of elements.

If there are N volume elements/mol., N is equal to $1/\psi$, where ψ is the volume of each element.

$$\therefore \frac{i_s}{i_0} = \frac{16\pi^4 (\overline{\delta\alpha})^2 \sin^2 \theta_1}{\lambda^4 r^2 \psi} \quad (17)$$

Temperature, pressure and solute concentration will all affect the polarisability of a volume element.

$$\therefore \delta\alpha = \left(\frac{\partial \alpha}{\partial P} \right)_{T,c} \delta P + \left(\frac{\partial \alpha}{\partial T} \right)_{P,c} \delta T + \left(\frac{\partial \alpha}{\partial c} \right)_{T,P} \delta c \quad (18)$$

As the scatter from pure solvent will be subtracted from that of the solution, the first two terms in (18) can be ignored, in dilute solutions, as similar terms are present in the corresponding equation for scatter by solvent.

Putting:

$$n_0 \left(\frac{\partial n}{\partial c} \right)_{T,P} = 2\pi N \left(\frac{\partial \alpha}{\partial c} \right)_{T,P}$$

Substituting $N = 1/\psi$

$$\left(\frac{\partial \alpha}{\partial c}\right)_{T,P} = \frac{\psi n_0}{2\pi} \left(\frac{\partial n}{\partial c}\right)_{T,P} \quad (19)$$

From equation (18)

$$\overline{(\delta \alpha)} = \left(\frac{\partial \alpha}{\partial c}\right)_{T,P} \delta c$$

Squaring this and introducing the value for $\overline{(\delta \alpha)}^2$ into equation (17) gives

$$\frac{I_s}{I_0} = \frac{16\pi^4 \sin^2 \theta_1 \left(\frac{\partial \alpha}{\partial c}\right)_{T,P}^2 (\delta c)^2}{\lambda^4 r^2 \psi}$$

Introducing into this equation the value of $\left(\frac{\partial \alpha}{\partial c}\right)_{T,P}^2$ obtained by squaring the right-hand side of equation (19) gives

$$\frac{I_s}{I_0} = \frac{4\pi^2 \psi n_0^2 \left(\frac{\partial n}{\partial c}\right)^2 \sin^2 \theta_1 \overline{(\delta c)^2}}{\lambda^4 r^2} \quad (20)$$

where $\overline{(\delta c)^2}$ is the average $(\delta c)^2$.

For unpolarised light equation (20) becomes

$$\frac{I_\theta}{I_0} = \frac{2\pi^2 \psi n_0^2 \left(\frac{\partial n}{\partial c}\right)^2 (1 + \cos^2 \theta) \overline{(\delta c)^2}}{\lambda^4 r^2} \quad (21)$$

It is necessary to evaluate $\overline{(\delta c)^2}$. This quantity depends on the variation of free energy of the macromolecular solution with concentration. The probability of a given

fluctuation δc may be calculated by considering all volume elements with a given value of δc as individual chemical species. The quantity of elements of a particular kind, relative to elements with the average concentration \bar{c} , has the form of an equilibrium constant equal to $e^{(-\Delta G^0/kT)}$, where ΔG^0 is difference in the free energy per element. If the standard state chosen is the state of unit mole fraction ΔG^0 , which can be designated ΔG , becomes the difference of free energy between solutions of concentrations $c + \bar{c}$ and \bar{c} .

The probability of a given value of δc becomes proportional to $e^{(-\Delta G/kT)}$.

As neither large concentration fluctuations nor large ΔG values will occur, ΔG may be expanded as a Taylor series in which only the first two terms are retained.

$$\text{i.e. } \Delta G = \left(\frac{\partial G}{\partial c} \right)_{T,P} \delta c + \frac{1}{2!} \left(\frac{\partial^2 G}{\partial c^2} \right)_{T,P} (\delta c)^2$$

The average concentration about which fluctuations occur may be taken as the equilibrium concentration at constant pressure. Therefore $(\partial G / \partial c) = 0$.
Substituting the value got for δG in $e^{-\delta G/kT}$ gives

$$e^{-\delta G/kT} = e^{-(\partial^2 G / \partial c^2)(\delta c)^2 / 2kT} \quad (22)$$

The average value of $(\delta c)^2$ from equation (22) can be shown to be $kT/(\partial^2 G/\partial c^2)_{T,P}$.

Substitution of this value for $(\delta c)^2$ in equation (21) gives

$$\frac{i_{\theta}}{i_0} = \frac{2\pi^2 \psi n_0^2 (dn/dc)^2 (1 + \cos^2 \theta)}{\lambda^4 r^2} \left[\frac{kT}{(\partial^2 G/\partial c^2)_{T,P}} \right] \quad (23)$$

As free energy has now been incorporated in this equation it can be related to the colligative properties of the solution.

If n_1 and n_2 are the number of moles of solvent and solute respectively, in a volume element of the solution

$$n_1 \bar{V}_1 + n_2 \bar{V}_2 = \psi \quad (24)$$

where \bar{V}_1 and \bar{V}_2 are the partial molar volumes of solvent and solute respectively in a volume element

$$\therefore dn_1 = (-\bar{V}_2/\bar{V}_1) dn_2 \quad (25)$$

The free energy change accompanying any change in concentration at constant pressure and temperature can be shown to be

$$dG = \mu_1 dn_1 + \mu_2 dn_2 \quad (25a)$$

where μ_1 and μ_2 are the chemical potentials of solvent and solute respectively.

$$\therefore dG = dn_2 (\mu_2 - (\bar{V}_2/\bar{V}_1) \mu_1) \quad (26)$$

The number of moles of solute per ml. = $n_2/V_1 = c/M$

$$\therefore dn_2 = (\psi/M)dc$$

$$\therefore \left(\frac{\partial G}{\partial c} \right)_{T,P} = \frac{\psi}{M} \left(n_2 - \frac{\bar{V}_2}{\bar{V}_1} n_1 \right) \quad (27)$$

Differentiating with respect to c gives

$$\left(\frac{\partial^2 G}{\partial c^2} \right)_{T,P} = \frac{\psi}{M} \left[\left(\frac{\partial n_2}{\partial c} \right)_{T,P} - \frac{\bar{V}_2}{\bar{V}_1} \left(\frac{\partial n_1}{\partial c} \right)_{T,P} \right] \quad (28)$$

From Gibbs-Duhem equation

$$n_1 du_1 + n_2 du_2 = 0$$

Equation (28) becomes

$$\left(\frac{\partial^2 G}{\partial c^2} \right)_{T,P} = \frac{\psi}{M} \left[\frac{n_1 \bar{V}_1 + n_2 \bar{V}_2}{n_2 \bar{V}_1} \right] \left(\frac{\partial n_1}{\partial c} \right)_{T,P} \quad (29)$$

As $n_2 M / (n_1 \bar{V}_1 + n_2 \bar{V}_2) = c$

So equation (29) becomes

$$\left(\frac{\partial^2 G}{\partial c^2} \right)_{T,P} = \frac{\psi}{c \bar{V}_1} \left(\frac{\partial n_1}{\partial c} \right)_{T,P} \quad (30)$$

Insertion of Equation (30) into equation (23) gives

$$\frac{i_e}{I_o} = \frac{2W^2 n_o^2 (dn/dc)^2 (1 + \cos^2 \theta) c}{\lambda^4 r^2 \cdot \left[(1/\bar{V}_1 kT) \cdot \left(\frac{\partial n_1}{\partial c} \right)_{T,P} \right]} \quad (31)$$

The dependence of chemical potential of the solvent on the concentration of the solute is related by the following equation.

$$\left(\frac{\partial \mu_1}{\partial c}\right)_{T,P} = -RT\bar{V}_1\left(\frac{1}{M} + 2Bc + 3Cc^2\right)$$

where M is the molecular weight of solute of concentration c and B and C are the second and third virial coefficients respectively. As $k = R/N_a$

$$-\frac{1}{\bar{V}_1 kT} \left(\frac{\partial \mu_1}{\partial c}\right)_{T,P} = N_a \left(\frac{1}{M} + 2Bc + 3Cc^2 + \dots\right) \quad (32)$$

Insertion of the right-hand side of equation (32) into equation (31) gives

$$\frac{i_\theta}{I_0} = \frac{2\pi^2 n_0^2 (dn/dc)^2 (1 + \cos^2 \theta) c}{N_a \lambda^4 r^2 (1/M + 2Bc + 3Cc^2)} \quad (33)$$

In very dilute solutions equation (33) reduces to equation (15).

Equation (33) is often written as

$$R_\theta = r^2 \frac{i_\theta}{I_0} \quad (34)$$

or as $R_\theta = \frac{r^2 i_\theta}{I_0 (1 + \cos^2 \theta)}$, which is independent of

the scattering angle, where $R_\theta = \frac{Kc}{1/M + 2Bc + 3Cc^2 + \dots}$

$$\text{where } K = \frac{2\pi^2 n_0^2 (\frac{dn}{dc})^2}{N_a \lambda^4}$$

$$\therefore \frac{Kc}{R_\theta} = \frac{1}{M} + 2Bc + 3Cc^2 + \dots \quad (35)$$

It can be shown that the turbidity, T , equals $\frac{16\pi R_\theta}{3}$

Substitution of this value into equation (35) gives

$$\frac{Hc}{T} = \frac{1}{M} + 2Bc + 3Cc^2 + \dots \quad (36)$$

$$\text{where } H = \frac{32\pi^3 n_0^2 (\frac{dn}{dc})^2}{3N_a \lambda^4}$$

The molecular weight obtained is the weight average molecular weight.

e). Optical Anisotropy of Scattering Particles.

If the particles considered are anisotropic, a correction must be made for the possibility of increased scattering due to the fluctuations in the orientations.

In an isotropic particle the ratio of horizontally to vertically polarised light will be zero at $\theta = 90^\circ$, because the induced dipole is parallel to the electric vector of the incident light. However, if the particle is not isotropic the induced dipole is not parallel to the electric vector. Consequently, the ratio of horizontally

polarised to vertically polarised light, ρu , is not zero. This ratio has been shown by Cabannes⁶⁷ to be related to the excess scattering due to anisotropy. The Cabannes factor is $(6 - 7\rho u)/(6 + 6\rho u)$.

This correction factor must be applied to R_θ or T , if an accuracy of 1% is wanted in molecular weight calculations.

Large Particles.

Light Scattering from Large Particles.

When the particle has a dimension which exceeds $\lambda/20$, interference will occur between light waves scattered from different parts of the particle; the interference is greater at larger values of θ than for small ones. There is thus a reduction of the light scattered other than at $\theta = 0$. The function $P(\theta)$ is defined:

$$P(\theta) \equiv \frac{\text{scattered intensity for large particle}}{\text{scattered intensity without interference}} \quad (37)$$

$P(\theta)$ can be related to molecular shape, and is also used to correct measured intensities for the effect of internal interferences. If the particle is divided into δ scattering points.

$$P(\theta) = \frac{1}{6^2} \sum_{i=1}^6 \sum_{j=1}^6 \frac{\sin \mu r_{ij}}{\mu r_{ij}} \quad (38)$$

where r_{ij} is the distance from the i th to the j th scattering point, and $\mu = \frac{4\pi}{\lambda_1} \sin \theta/2$

It can be shown that $P(\theta)$ has a limiting form, which is related to the radius of gyration of the particle:

$$\frac{1}{P(\theta)} = 1 + \frac{16\pi^2}{3\lambda_1^2} R_G^2 \sin^2 \frac{\theta}{2} \quad (39)$$

where λ_1 is the wavelength of the light in the medium.

Using equations (36), (37), and (39) gives

$$\lim_{c \rightarrow 0} \left(\frac{Hc}{T} \right) = \frac{1}{M P(\theta)} = \frac{1}{M} \left(1 + \frac{16\pi^2}{3\lambda_1^2} R_G^2 \sin^2 \frac{\theta}{2} \right) \quad (40)$$

If the values of Hc/T are extrapolated to zero concentration at various values of θ , and the limiting values plotted against $\sin^2 \theta/2$, then the molecular weight and radius of gyration can be obtained. This is the basis of the Zimm⁶⁸ method for treating the angular distribution of scattered light.

A second method of treating data is the dissymmetry method. It is possible to evaluate $P(\theta)$ in terms of molecular properties for certain models⁶⁹ eg. for flexible coils

$$P(\theta) = (2/W^2) (e^{-W} + W - 1) \quad (41)$$

where $W = \mu^2 R_G^2$

expressions for rods⁶⁹ and spheres⁷⁰ are also available. $P(\theta)$ can thus be calculated as a function of the characteristic dimension for particular models (eg. diameter of a sphere, length of a rod, end to end distance of a coil), and tables are available of these functions⁷¹. The measured dissymmetry ($Z_{45} = I_{45}/I_{135}$) can be used to calculate the characteristic dimension, and also the correction to be made to the 90° scattering to correct it for the effect of internal interference in the calculation of molecular weight. Equation (36) becomes

$$\frac{Kc}{T} = \frac{1}{MP(\theta)} + 2Bc \quad (42)$$

In the dissymmetry method a choice of model for the particle had to be made, while in the Zimm method the radius of gyration is obtained without having to assign a model to the particle.

Interpretation of the Second Virial Coefficient B.

It has been shown⁶⁰ that the chemical potential of a non-electrolyte in solution for a non-ideal case can be expanded as a power series of the type.

$$\mu_1 - \mu_1^0 = -RTV_1^0 c_2 (1/M_2 + Bc_2 + Cc_2^2 + \dots) \quad (43)$$

where V_1^0 is the molar volume of the solvent and c_2 is the solute concentration in moles per litre. The deviation from ideality is attributed to the virial coefficients B and C which are interpreted as molecular properties.

The chemical potential may also be expressed as

$$\mu_1 - \mu_1^0 = -RTV_1^0 c_2 \left(\frac{1}{M_2} + \frac{N_a u c_2}{2M_2^2} \right) \quad (44)$$

where u is the excluded volume of the solute.

∴ From equations (43) and (44) it can be seen that

$$B = \frac{N_a u}{2M_2^2} \quad (45)$$

For spherical molecules the excluded volume can be shown to be $(32/3)\pi r^3$ or $8M_2 v_2 / N_a$, where v_2 is the specific volume of the solute.

Hence

$$B = \frac{N_a 8M_2 v_2}{2M_2^2 N_a} = \frac{4v_2}{M_2} \quad (46)$$

B is therefore related to the volume of the solute molecule.

For rods $u = 2M_2 v_2 L / N_a d$, where L is the length of the rod.

So

$$B = \frac{Lv_2}{M_2 d} \quad (47)$$

Again B is related to the volume of the solute molecule.

For flexible polymers the calculations are more complex, but the result obtained is that

$$u = (32/3)\pi\gamma^3 R_G^3 \quad (48)$$

where γ is a proportionality factor and R_G is the radius of gyration of the polymer.

As B is determinable from light-scattering measurements an idea of the shape of the molecule may be obtained.

INTERPRETATION OF VISCOSITY RESULTS.

Experimentally viscosity is conveniently calculated as the specific viscosity η_{sp} where

$$\eta_{sp} = \frac{\eta' - \eta}{\eta} \quad \text{or} \quad \frac{\eta'}{\eta} - 1$$

η' is the macroscopic viscosity of the solution and η is the viscosity of the solvent. η_{sp}/c , where c is the concentration, is independent of concentration at the limit of zero concentration. This value η_{sp}/c is called the intrinsic viscosity $[\eta]$

$$[\eta] = \lim_{c \rightarrow 0} \frac{\eta_{sp}}{c} = \lim_{c \rightarrow 0} \frac{\eta' - \eta}{\eta c} \quad (49)$$

It was shown by Einstein⁵⁷ for any number of suspended particles, that the macroscopic viscosity, η' , of the suspension is

$$\eta' = \eta(1 + 2.5\phi) \quad (50)$$

where η = solvent viscosity, and ϕ is the volume fraction of the particles in the total volume of the solution.

This equation is only valid for spherical particles.

An extension of Einstein's treatment to ellipsoids of revolution has been made by Simha⁵⁸ who obtained the result

$\eta^i = \eta (1 + \nu\beta)$, where ν is the shape factor. For spheres ν is 2.5, and it is invariably larger for ellipsoids, and is a function of the axial ratio.

The volume fraction, β , cannot be readily determined practically (for a particle as it exists in solution) and is replaced by the concentration, c . If V_h is the hydrodynamic volume of the dissolved macromolecules and c is the concentration in g/cc, then $N_a c/M$ is the number of particles/cc. Therefore $\beta = N_a c V_h / M$. The combination of equations (49) and (50) gives

$$[\eta] = \frac{\nu N_a V_h}{M} \quad (51)$$

It has been shown by Oncley⁵⁹ that

$$V_h = \frac{M}{N_a} (\bar{v}_2 + W \bar{v}_1^0) \quad (52)$$

where M is the molecular weight of the solute, N_a is Avogadro's Number, \bar{v}_2 is the average specific volume of solute particles, W is the amount of water associated with the solute particles i.e. the hydration, and \bar{v}_1^0 is the average specific volume of water.

Introduction of equation (52) into (51) gives

$$[\eta] = \nu (\bar{v}_2 + W \bar{v}_1^0) \quad (53)$$

Equation (53) can be used to find the amount of hydration for solutes where it can be assumed that the particles are spherical and ν has the theoretical value

of 2.5. Unless the hydration can be independently determined, intrinsic viscosities can only be interpreted in terms of alternative axial ratios and hydrations. The approach outlined above is only applicable to rigid macromolecules.

It can be considered that flexible polymers behave like spheres with a radius related to the radius of gyration of the polymer by $r_g = \xi R_G$, where ξ is a proportionality constant and r_g is the radius of a spheroid hydrodynamically equivalent to the polymer molecule.

Thus $V_h = 4\pi \xi^3 R_G^3 / 3$ and substituting in equation (51) gives

$$[\eta] = \frac{10\pi N_A \xi^3 R_G^3}{3M} \quad (54)$$

The radius of gyration can be expressed in terms of the molecular weight of the monomer unit M_0 , the effective bond length β , and the expansion factor of the polymer coil α i.e. $R_G^2 = \alpha^2 \beta^2 M / 6M_0$

Inserting into equation (54);-

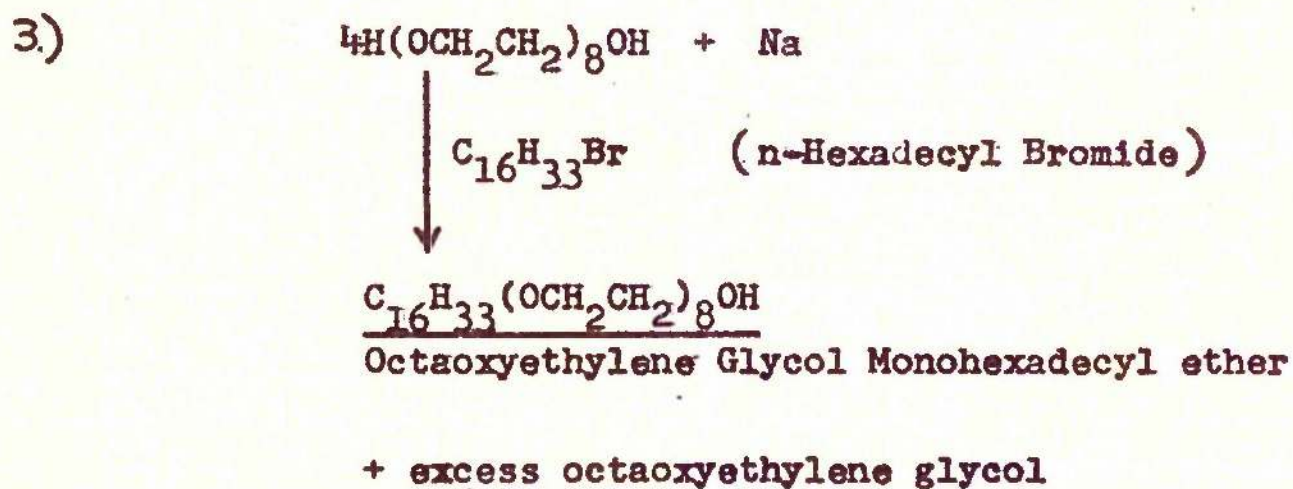
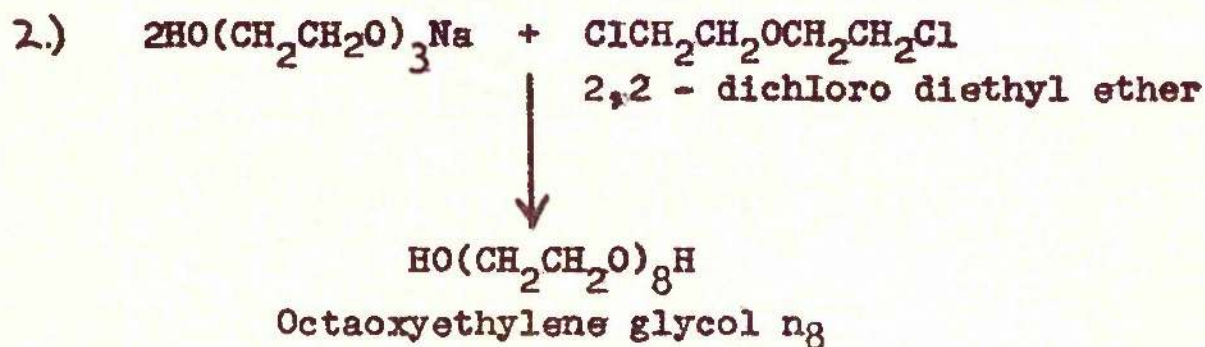
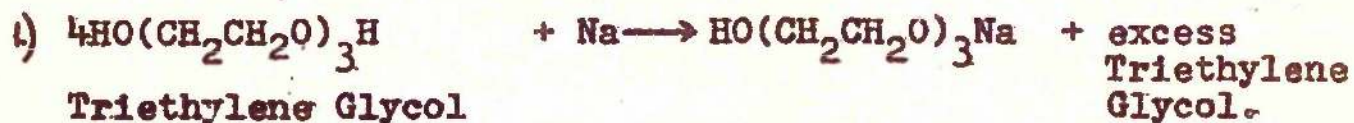
$$[\eta] = \frac{10\pi N_A \alpha^3 \beta^3 \xi^3 M^{\frac{1}{2}}}{3(6M_0)^{\frac{3}{2}}} \quad (55)$$

α has the value of one in an ideal solvent, and is

proportional to $M^{0 - 0.1}$ in good solvent. Hence, from equation (55), $[\eta]$ is proportional to $M^{0.5 - 0.8}$ depending on solvent.

PART 11.

MATERIALS AND EXPERIMENTAL METHODS.

MATERIALS.Reaction Scheme.

Purification of Hexadecyl Bromide.

Two samples of commercial hexadecyl bromide were used, viz. B.D.H. and Eastmann - Kodak.

Both batches were vacuum distilled twice at 125°C 0.25mm Hg., and the following physical constants were obtained.

	n_D^{20}	F.Pt.	d_{20}^0
B.D.H.	1.4628	16.3°	
Eastmann - Kodak	1.4630	16.3°	1.0049
Heilbron and Bunbury ⁷³	1.4620	15.0°	1.0000

The Eastmann - Kodak preparation was used in the subsequent preparation.

3,6,9,12,15,18,21-Heptaooxatricosane-1-23-diol

(octaoxyethylene glycol n₈).

The starting material was triethylene glycol (Trigol, B.D.H.). This material was vacuum distilled at 165°C 0.25mm Hg., (n_D^{20} 1.4550). To the redistilled triethylene glycol (1500 g.), at 70°C, sodium (57.5 g.) was added piece by piece until completely dissolved. The temperature was raised to approximately 120°C to ensure complete solution of the sodium. Four times the equivalent quantity of triethylene glycol was used to ensure that the monosodium

salt of triethylene glycol was formed.

The temperature of the reaction was allowed to fall to below 100°C and 2,2 -dichloro diethyl ether (179 g.) was added slowly with stirring. The temperature of the reaction mixture was raised to $130 - 140^{\circ}\text{C}$ and the reaction was continued until sodium chloride was precipitated and the mixture was neutral. It was filtered hot and the filtrate was vacuum distilled in small batches to remove excess triethylene glycol. If sodium chloride was precipitated in any of these small batches they were filtered hot and redistilled. The residues from the individual distillations were bulked and vacuum distilled at approximately 220°C (0.01mm Hg.) Pure octagol (160 g.) was distilled (n_D^{20} 1.4661, d_{20}^0 1.1237, b.pt. 216° (0.01mm Hg)) Found: C, 51.8; H, 9.2; $\text{CH}_2\text{CH}_2\text{O}$, 95.0%. $\text{C}_{16}\text{H}_{34}\text{O}_9$ requires C, 51.9; H, 9.3; $\text{CH}_2\text{CH}_2\text{O}$, 95.1%.

3,6,9,12,15,18,21,24-Octaoxatetracontane-1-ol

(octaoxyethylene glycol monohexadecyl ether Hg).

Octaoxyethylene glycol (75 g.), in excess, was heated to $100 - 120^{\circ}\text{C}$ and sodium (1.18 g.) was added and dissolved. Hexadecyl bromide (16.3 g.) was added and the reaction was allowed to continue for four hours at 120°C . On completion of the reaction, the mixture was shaken with three portions

of hot petroleum ether.

The petroleum ether extracts were bulked and evaporated to dryness leaving an oily liquid (36.4g.) which solidified on cooling. This solid was recrystallised from ether (16.4g.) and then from acetone, giving 10.0 g. crude Hn_8 . 4.3 g. of the crude material were dissolved in dry benzene and put on a column of dried alumina (75 g.). The column was washed with 250mls 1:9 Acetone: Benzene solution. 1.66 g. (37.8%) impurity were washed off by this process.

The column was then eluted with 800mls acetone: methanol: benzene (25: 1: 24). Evaporation of the solvent and subsequent recrystallisation of the residue from ether gave 1.98 g. (46%) of pure Hn_8 , m.pt. 41.5°C .

(Found: C, 64.23; H, 11.13; $\text{CH}_2\text{CH}_2\text{O}$, 59.12%.

$\text{C}_{32}\text{H}_{66}\text{O}_9$ requires C, 64.6; H, 11.11;

$\text{CH}_2\text{CH}_2\text{O}$; 59.24%).

Septaoxyethylene glycol monohexadecyl ether (Hn_7) and nonaoxyethylene glycol monohexadecyl ether (Hn_9) were gifts from Mr. C. B. Macfarlane, and had the physical constants already reported^{8,9}.

Water was twice distilled from permanganate in an all glass still.

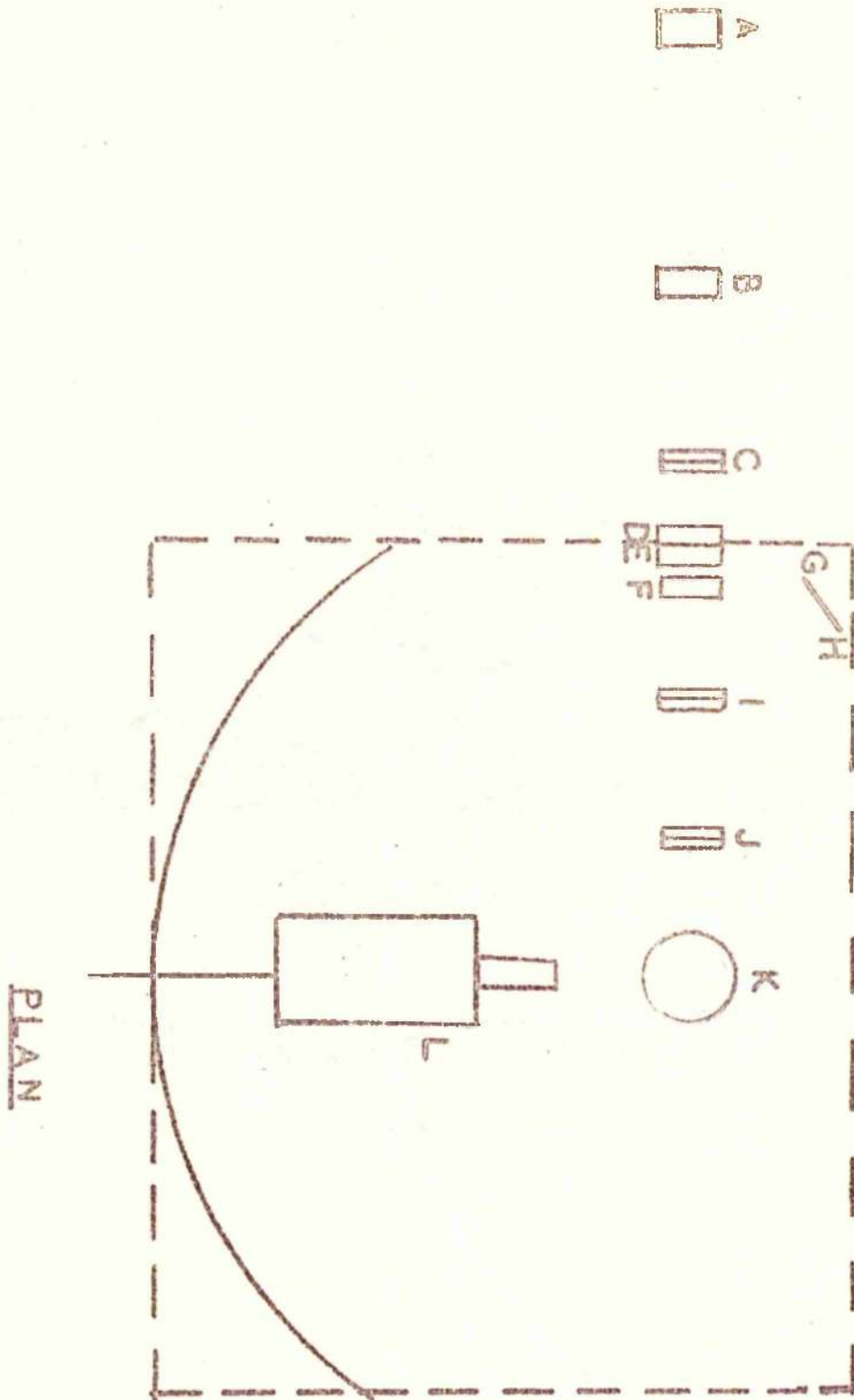
EXPERIMENTAL METHODS.1. Light-Scattering.a). Description of Light-Scatterer.

The light-scatterer used was that described previously by Elworthy and McIntosh⁴⁵. A diagram of the apparatus is shown in Figure 2. page 68a.

The light source, A, is a G.E.C. 250W Mercury Vapour lamp, type ME/D. The voltage supply to the lamp was stabilised to 1% by an Advance Constant Voltage Transformer (250 W, type CVN). The light is passed through a 5cm focal length lens, B, and brought into focus on a narrow slit, C, to give a secondary source of light. Lens D is placed at its focal length from C to give a parallel beam of light through the slits. A Barr and Stroud interference filter, E, which transmits the 5461 Å green line was used. To eliminate the last traces of yellow light the beam passes through a neodymium glass, F. Part of the beam is reflected by a polished brass plate^G to an E.M.I. type 25110 photocell^H, which monitors instant beam intensity. Final collimation of the beam is brought about by passing it through two slits (I and J).

The cell-holder, K, contains seating for allowing the cell to be firmly fixed in place and also a plastic wedge

Diagram of Light-Scatterer.



for keeping the perspex standard block, used in turbidity measurements, in place.

The light from the cell is scattered to an EMI 6097 B eleven stage photomultiplier, L. The signal from the photomultiplier goes to a Cambridge D'arsonval spot galvanometer which has a sensitivity of 0.1μ amps for full scale deflection.

The surface of the photomultiplier is coated with an aluminium paint, held at cathode potential, and supported, inside a metal container, by layers of Parafilm. In this way any stray fluctuations over the envelope of the tube are evened out. The photomultiplier is mounted on a flat tufnol arm resting on a tufnol plate and can move smoothly around the cell. The power for the photomultiplier is supplied by two Siemens Ediswan R 1184 power packs in series, each of which is capable of providing 300 - 1100 v. D.C.

Components D to L are enclosed in a light-proof box shown as a dotted line in Fig. 2. The floor of the box contains studs, every 10° , between 50° and 130° and also at 45° and 135° with respect to the line of incident light onto the solution cell. A metal rod fitted to the end of the photomultiplier allows it to be brought to the required angle.

The electrical circuit for the photomultiplier is shown in Figure 3, page 70a.

b). Description of Light-Scattering Solution Cell.

The cell is similar to that described by Elworthy and McIntosh⁴⁵. It is made of brass and consists of a brass shell of internal diameter 31mm, and height 59mm. It is circular except for two flattened portions (A) Figure 4, page 70b, I, to which the end windows are fixed. Two holes drilled horizontally at D and D₁ (Fig. 4, page 70b, I) connect with vertically drilled inter connecting holes at C and allow water to be circulated through the wall of the cell; a piece of brass is fixed over C with Araldite after the holes are drilled. The end windows are made from microscope slide glass and are stuck to the cell with Araldite. The light passes through the end windows and thence through a slit in the cell wall 33mm. high and 5mm. wide (Fig. page 70 b, II). The front window is made from pyrex glass tubing, examined visually for any flaws, cut to a suitable size and again fixed in place with Araldite. The inside of the cell is blackened by the Relanol process to cut down stray light.

FIGURE 3.

Electronic Circuit of Light-Scatterer.

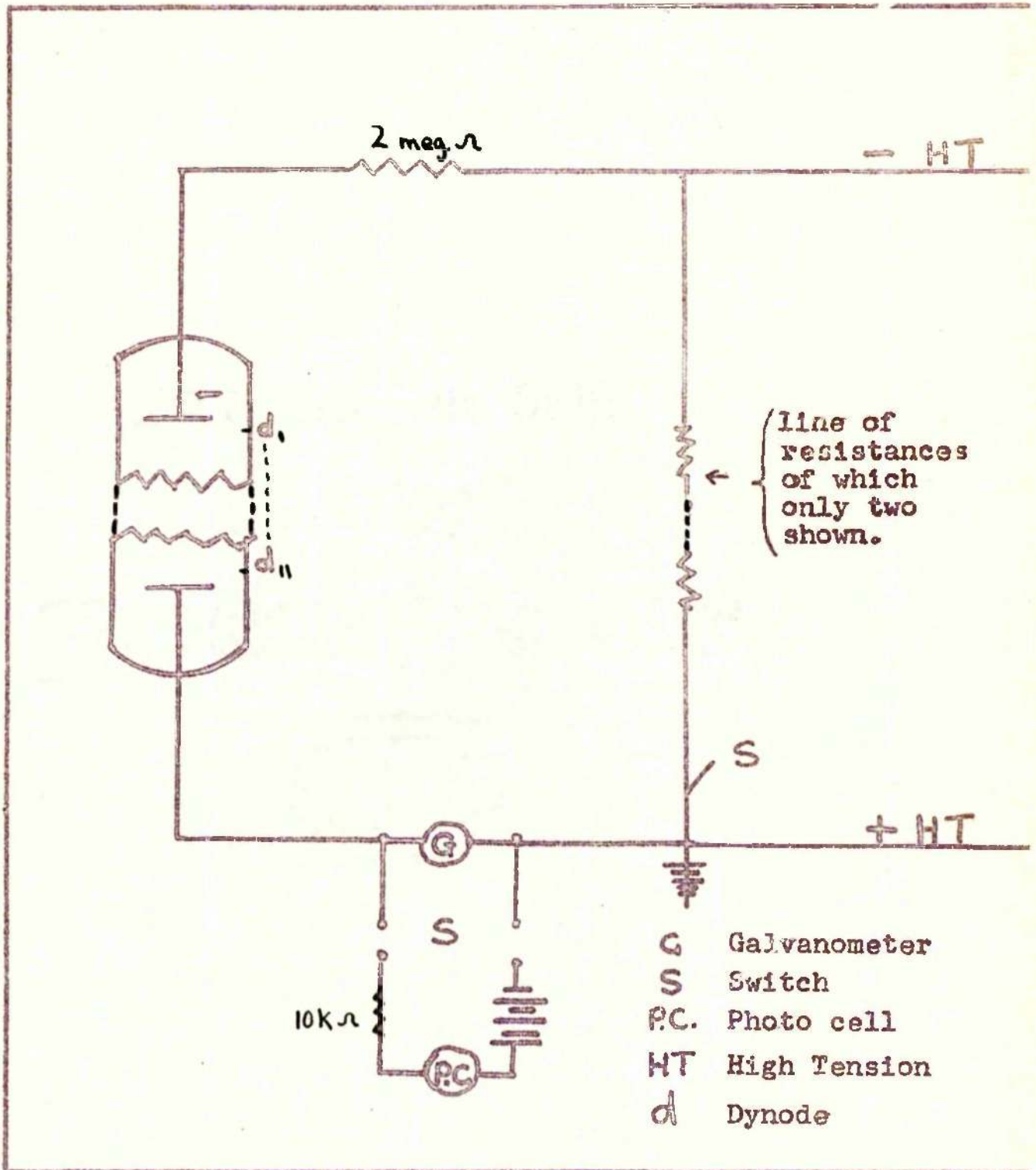
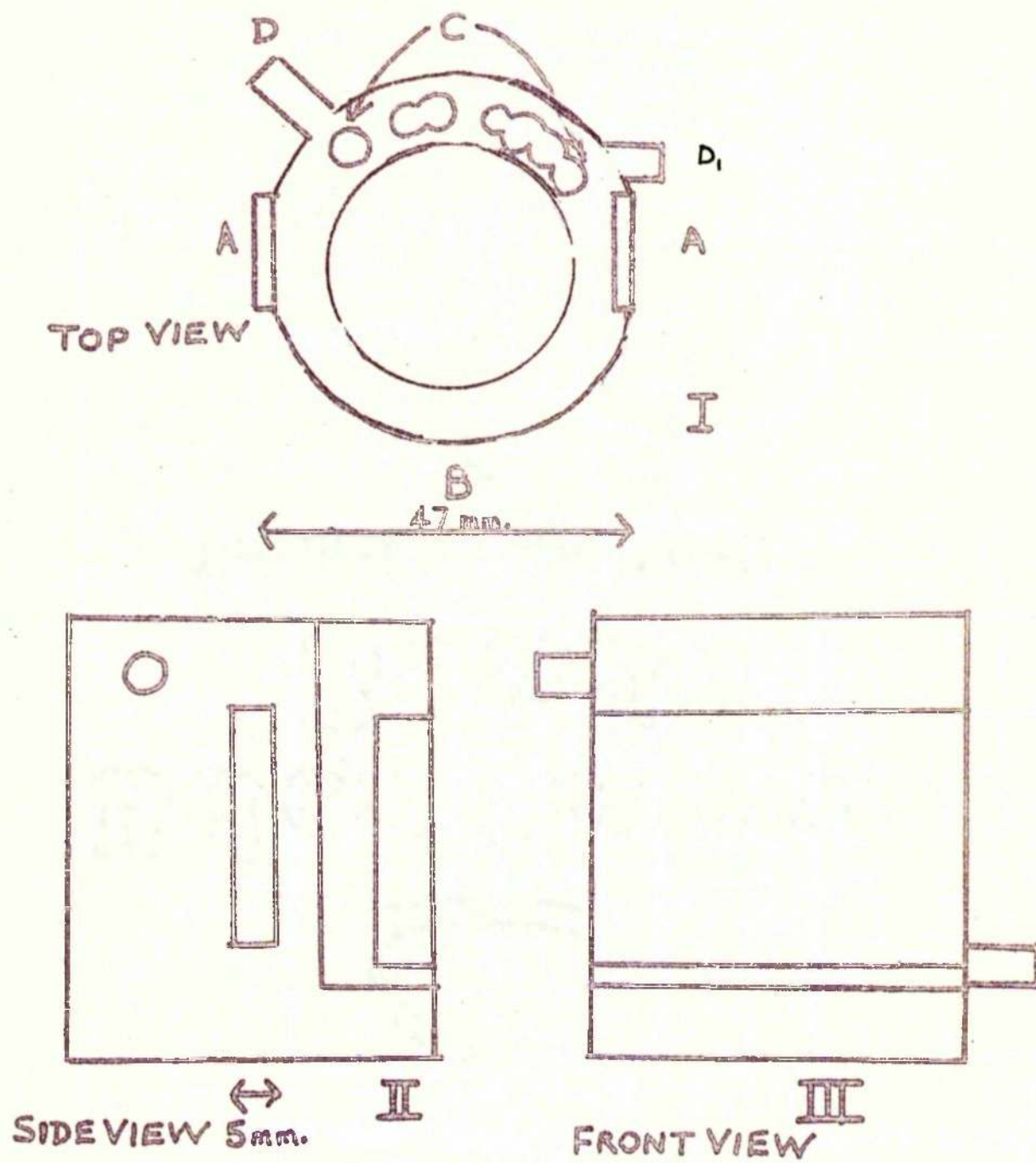


FIGURE 4.

Description of Light-Scattering Cell.



c). Measurement of Turbidity.

All glassware used was cleaned with chromic acid, washed well with water, and finally with acetone vapour. The light-scattering solution cell was cleaned with teepol, washed with water, and then with acetone vapour.

Solutions for measurement were made up with filtered distilled water. The solutions were filtered through a millipore membrane filter, mean pore size 0.45μ , to remove extraneous matter. Normally the solutions were filtered twice into a suitable glass container protected from the atmosphere, and then directly into the cell which was covered with a brass lid. Visual inspection in the light beam was found to be an efficient way of testing for dust particles after filtration.

A polished perspex block, $84\text{mm.} \times 15\text{mm.} \times 54\text{mm.}$, was used as a light-scattering standard. This block was calibrated from Ludox solutions by Macfarlane⁸ and McIntosh⁴⁵ and gave a standard turbidity of $2.71 \times 10^{-4} \text{cm}^{-1}$. As a check on the calibration, the turbidity of benzene was determined, giving $27.3 \pm 0.3 \times 10^{-5} \text{cm}^{-1}$, mean of four measurements, which agrees well with a literature value⁴⁶ of $27.5 \times 10^{-5} \text{cm}^{-1}$. and with the figure obtained after the

initial Ludox calibration ($27.2 \pm 0.4 \times 10^{-5} \text{ cm.}^{-1}$).

The block was fitted into the cell-holder, the galvanometer was switched into the circuit, and a reading of the scattering from the block taken. The block was removed and the cell was inserted into the holder. The thermostat attachment, which consisted of rubber tubes from and to a thermostat bath, was fixed to the cell and the cell was lined up to ensure that the light beam passed directly through the side windows of the cell. Readings were taken every 5 minutes, with the photomultiplier at right angles to the path of light entering the cell, until a constant value for the ratio, S_{90}° , of the reading for solution to that for the block was obtained. Cell and block were interchanged to give a reading from each in obtaining S_{90}° values. It was found that 30 minutes was sufficient time to allow equilibrium to be reached even at the higher temperatures, there being no further change of turbidity after this time. Dissymmetry was measured by taking a reading at 45° and 135° for the solution and calculating the ratio $Z_{45^{\circ}/135^{\circ}}$. Depolarisation was measured by inserting a polaroid square between the solution and the photomultiplier, in positions to transmit the horizontal and vertical components of the scattered light.

Concentrations of solutions after filtration were measured interferometrically and dilutions were made by adding known quantities of water to the solution in a beaker.

2. Measurement of dn/dc .

Measurements of dn/dc were made in a Hilger Rayleigh interferometer, type M 154, using the method of Bauer⁴⁷ et al.

With pure water in both halves of the interferometer cell, the zero drum reading, r_0 , was determined for green light. The water in one of the compartments was replaced by solution, and after allowing time for temperature equilibrium to be reached, the bands were brought into coincidence and the drum reading r , was noted. The balance points were located using white light, and the final reading was taken with the interference filter in place, i.e. for the 5461 \AA wavelength.

The drum was then rotated slowly towards r_0 , the number of bands, N , passed being counted until coincidence of bands was obtained at, r' , the nearest drum reading above r_0 .

Invariably a fractional part of a band, f , is obtained by this method. This band fraction is calculated as follows.

One band is equivalent to a band distance $\frac{r - r'}{N} = P$

∴ the fractional part of a band is $\frac{r' - r_0}{P} = f$

The total number of bands is therefore $N + f$.

If d is the path - length of light through the cell the refractive index change $n - n_0$ at wavelength λ is given by

$$\begin{aligned} (n - n_0) &= (\lambda/d)(N + f) \\ \text{i.e.} \quad dn &= (\lambda/d)(N + f) \\ \therefore \quad \frac{dn}{dc} &= \frac{\lambda(N + f)}{d \cdot c} \quad 56 \end{aligned}$$

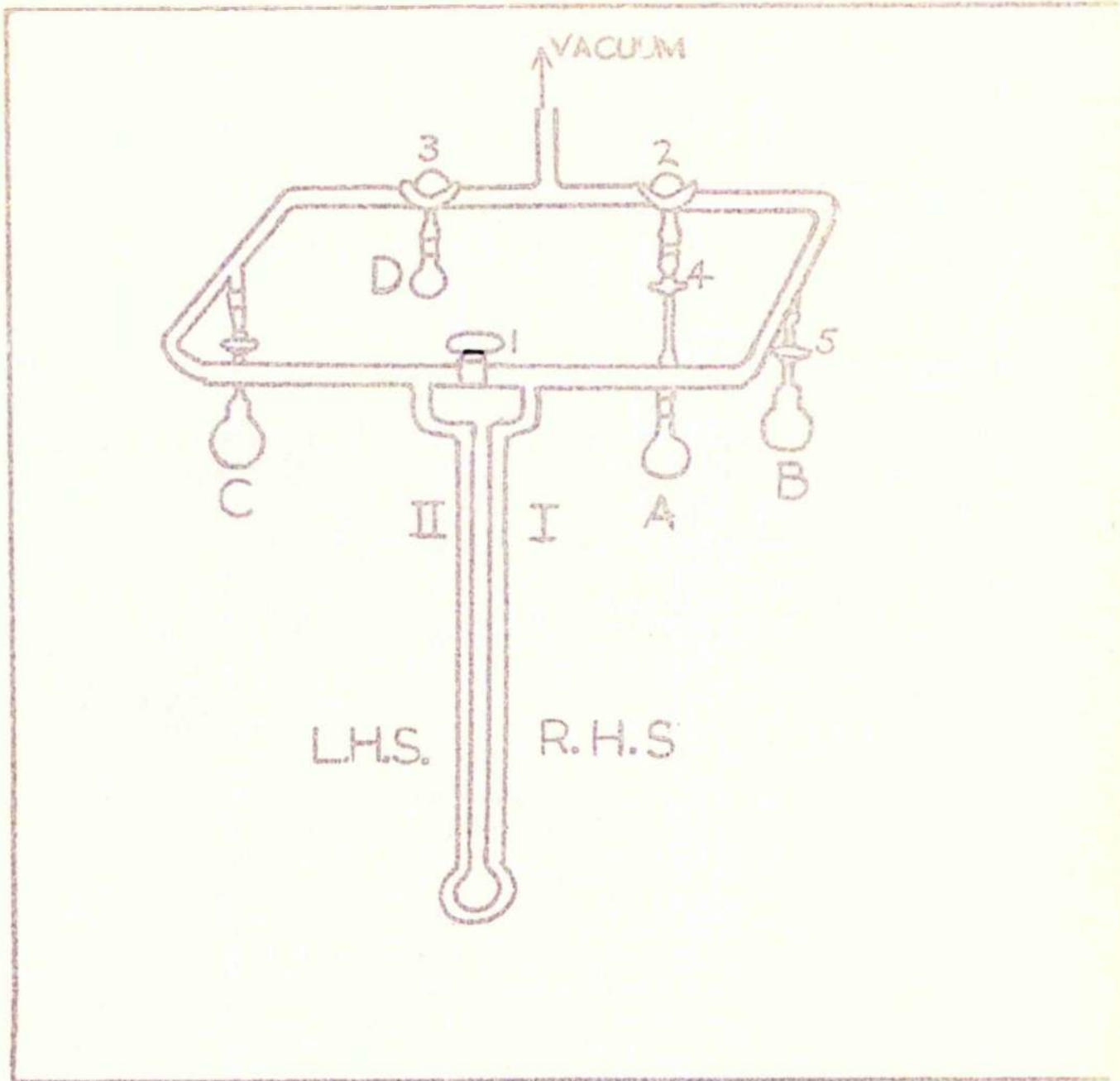
where c is the concentration of solute in solution in g./ml.

In measuring dn/dc for any particular system three solutions of varying concentrations were made up accurately and the measurements were taken as above. Also a plot of $(r - r_0)$ v. concentration was made which was used for finding the concentration of solutions which have been filtered prior to light-scattering and which may have lost some solute on the filter.

3. Measurements of Vapour Pressure.

The apparatus used is shown in Figure 5, page 74a, being based on the design of Gibson and Adams⁴⁸, and

Vapour Pressure Apparatus.



described by Elworthy and Macfarlane¹⁷. The flasks used were ground to fit their particular joints, and seals obtained using high vacuum grease.

Gels were prepared by warming approximately measured amounts of detergent and water together in flask A, which contained a magnetic follower, until a homogenous mixture was obtained. The mixture was first outgassed on a water pump, the flask attached to the apparatus, and outgassed for at least 30 minutes at 0.01 mm.Hg. Flasks B, C, and D contained water, and were outgassed by pumping. The whole apparatus was immersed in a thermostatically controlled water bath, and allowed to come to temperature equilibrium.

To measure the vapour pressure of water tap 3 was adjusted to cut the left hand side of the apparatus off from the vacuum line, and tap 1 closed. The right hand side of the apparatus was evacuated. Water vapour from flask C was allowed to enter the system, the tap to this flask then being closed, and tap 3 opened to allow water vapour from flask D to enter the apparatus. This procedure of injecting most of the required vapour from a subsidiary flask, prevents too much cooling by evaporation of the sample flask, and the consequent slow approach to

equilibrium. The difference between levels 1 and 11 of the manometer was read to 0.01 cm from a mirror scale fitted behind it. Readings were taken for some time to ensure equilibrium had been reached. (Most solutions equilibrated within 2 hours, see Macfarlane¹). Tests for leaks of the apparatus were also carried out with no water vapour in the system, pumping out from each side in turn, and observing the manometer; any leaks were stopped by cleaning and regreasing taps and joints. The values for the vapour pressure of water agreed reasonably with those in the literature⁷².

Temperature.	15°C	25°C	35°C	45°C
Literature Value.	1.2782	2.3753	4.2180	7.190 cm.Hg.
Found.	1.25	2.40	4.20	7.15 cm.Hg.

To read the vapour pressure of the solution, the left hand side of the apparatus was evacuated, tap 2 shut off from the vacuum line, tap 1 closed, vapour admitted from the auxiliary flask B to bring the manometer reading to roughly the value for the solution (which was roughly predetermined). Tap 5 was shut, and tap 4 opened, connecting the solution flask to the manometer, and readings taken over a 2-4 hour period.

Tap 4 was closed, tap 1 opened, and the apparatus

removed from the bath, and a sample of the gel removed from the flask A to a tared beaker, and weighed.

The weights of water and detergent in the sample were determined by drying to constant weight in a vacuum oven over P_2O_5 . Water was added to the remaining gel in flask A, the mixture warmed and stirred as before, and the procedure repeated to obtain a further result. A set of results of vapour pressure and concentration was built up in this way.

Because of difficulty in manipulating the apparatus it was not found possible to measure the vapour pressures at temperatures above $50^{\circ}C$.

4. Viscosity.

Viscosities were measured in a suspended level viscometer. Solutions were filtered through a No 3 sintered glass filter prior to use. The viscometer was immersed in a thermostatically controlled water bath ($\pm 0.05^{\circ}$).

5. Densities.

Densities of glycols were determined in a 10 ml pycnometer. The densities of Hn_8 and Hn_9 were measured in a 1 ml. pycnometer above their melting points, but otherwise were determined from the known densities of

glycols and hexadecane, calculating the molar volume of detergent, and neglecting molar volume of hydrogen.

The experimentally determined densities agreed well with those calculated.

6). Cloud Points.

Cloud points were measured by heating aqueous solutions of known concentrations of detergents gently in a test-tube immersed in a beaker of water. The solutions were stirred continuously and the temperature of clouding was read from a thermometer in the test-tube. After a reading was taken the solution was removed from the test-tube, allowed to cool and diluted to a known concentration with water and the process was repeated until sufficient readings were obtained.

PART III.

RESULTS AND DISCUSSION.

RESULTS.

The light-scattering results are shown in Figures 6, 7, 8. (p. 79a, b, c) as plots of $(c - c_1)/(T - T_1)$ against $(c - c_1)$, where c is the solute concentration in g./ml., and T is the turbidity. It was noted by Balmbra et al¹⁶ that breaks in plots of c against T were obtained for the synthetic detergent hexaoxyethylene glycol monododecyl ether. These breaks had all the appearance of cmc's, but occurred at concentrations much greater than the cmc. The concentration c_1 probably represents a higher association limit than the cmc. Below c_1 the turbidity of the solutions is the same as that of solvent, within experimental error, and values of c_1 were obtained by extrapolating back large scale plots of c against T (using measurements made at low concentrations), to the solvent or to extremely dilute solution turbidity. The values of c_1 are given in Table 3; they increase with temperature, while the cmc's of non-ionic detergents have been found generally to decrease with temperature.

At 25^o, the cmc's of Hn₇ and Hn₉ were found to be 0.957×10^{-6} and 1.33×10^{-6} g./ml. respectively⁹, which are in the region of 10^3 times smaller than the values of

FIGURE 6 LIGHT SCATTERING H_{70}

Plot of $\frac{c-c_1}{T-T_1}$ against c
for Temperatures shown in $^{\circ}\text{C}$.

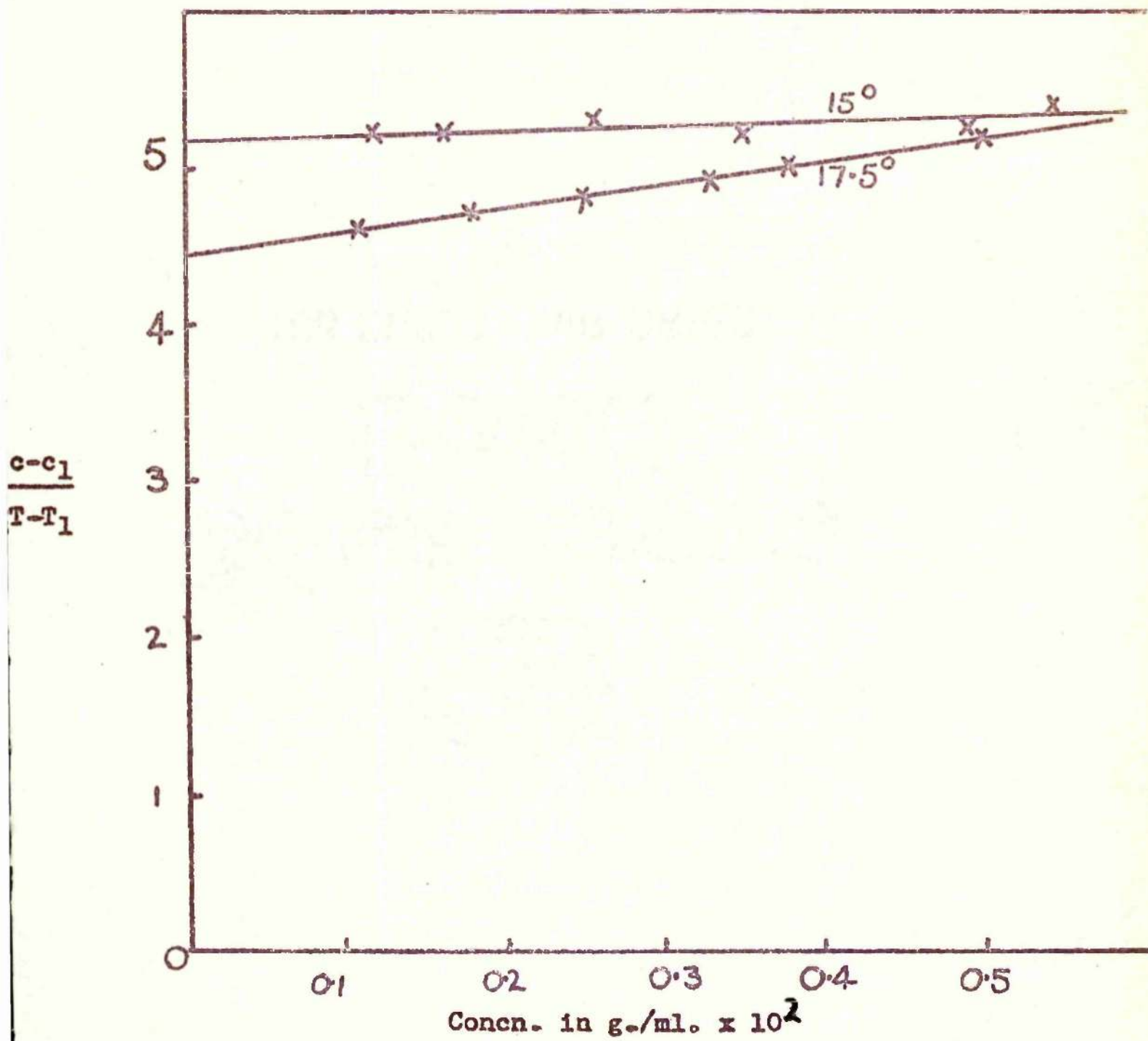


FIGURE 7 LIGHT SCATTERING H_{90}

Plot of $\frac{c-c_1}{T-T_1}$ against c
for temperatures shown

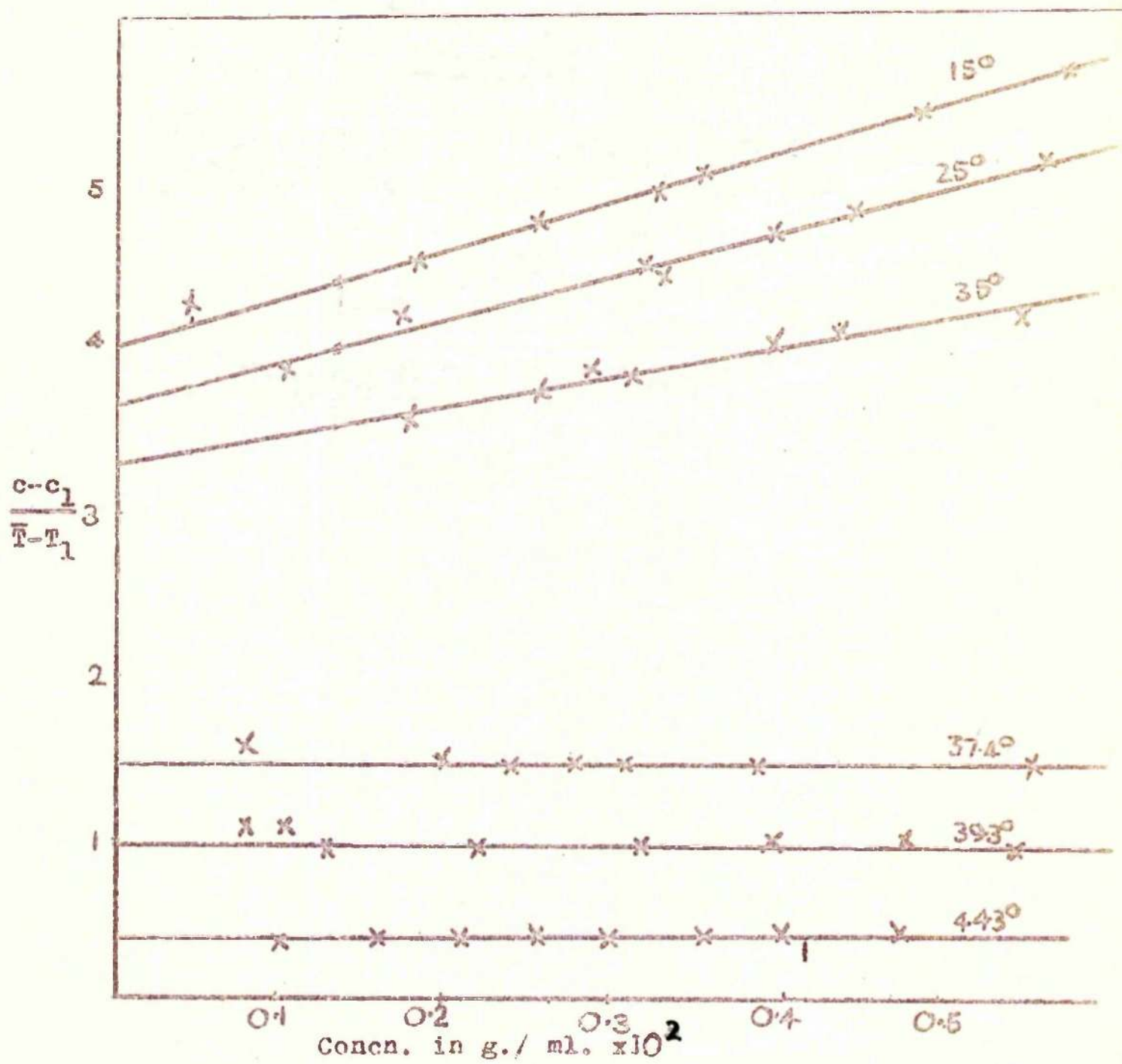
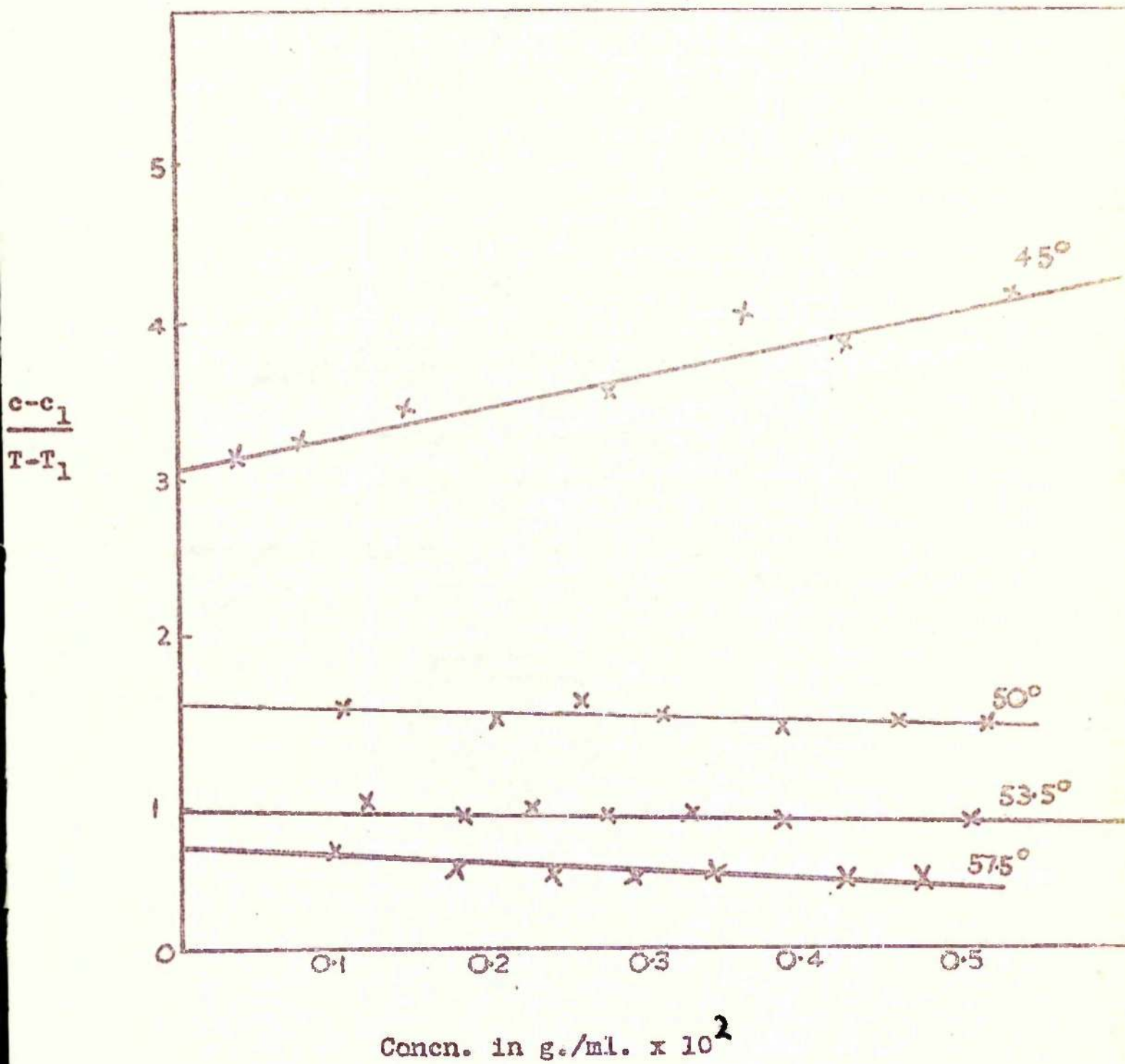


FIGURE 8 LIGHT SCATTERING Hn_9
 Plot of $\frac{c-c_1}{T-T_1}$ against c
 for Temperatures shown in $^{\circ}\text{C}$.



c_1 . The light-scattering results are summarised in Table 3, along with relevant data from Elworthy and Macfarlane.^{8,9}

The micellar weights were calculated from equation (56), using Debye's⁸³ procedure of subtracting the turbidity and concentration at the association concentration, in this case T_1 and c_1 :-

$$H(c - c_1) / (T - T_1) = 1/MP(\theta) + 2Bc \dots \quad (56)$$

The optical constant, H , and the other symbols have been defined on page 54. The micellar weights given in Table 3 have been corrected for depolarisation and dissymmetry. At the lower temperatures, values of Z_{45} close to unity were obtained, indicating that dust had been satisfactorily removed from the solutions, and that stray light was absent. At the higher temperatures, some dimension of the micelles appears to have become greater than $\lambda/20$, and small values for Z_{45} were obtained. As there is very little difference between the values of the particle scattering factors for the various molecular shapes in this range of dissymmetry, the values for monodisperse coils were used.

TABLE 3.

Light-Scattering Results and relevant data for Hn₇, Hn₈ and Hn₉ at various temperatures.

	Temp. °C	M x 10 ⁻⁵	m	Z ₄₅	ρ	dn/dc	B x 10 ⁴	c ₁ (G/ml x 10 ³)
Hn ₇	15	0.90	164	1.03	0.002	0.1361	0.42	0.20
	17.5	1.14	207	1.03	0.002	0.1355	1.46	0.20
	* 20	1.37	249	1.00	0.012	0.1350	0.84	0.36
	* 25	3.27	594	1.02	0.015	0.1350	-	0.30
Hn ₈	15	1.31	220	1.04	0.010	0.1331	2.42	0.20
	25	1.43	240	1.01	0.008	0.1317	2.43	0.20
	35	1.61	271	1.04	0.019	0.1305	1.56	0.25
	37.4	3.98	668	1.11	0.002	0.1304	-0.04	0.40
	39.3	6.02	1010	1.12	0.022	0.1300	-0.09	0.45
	44.3	16.7	2800	1.17	0.007	0.1294	-0.1	0.50
Hn ₉ *	25	1.40	219	1.03	0.016	0.1353	3.28	0.20
	45	1.76	275	1.03	0.0	0.1324	1.95	0.20
	50	3.50	549	1.087	0.010	0.1322	-0.14	0.40
	53.5	5.29	827	1.11	0.008	0.1320	-0.17	0.52
	57.5	8.8	1377	1.14	0.013	0.1310	-0.50	0.60

* Quoted from Macfarlane and Elworthy⁹.

m = number of monomers, Z = dissymmetry, ρ = depolarisation
dn/dc is quoted in ml/g.

For all detergents studied, the micellar weights increased as temperature rose; the increase is gradual at low temperatures, but becomes more rapid at higher temperatures, as is shown by a plot of $\log M$ against temperature, (Figure 9, p. 82a), although the rise in M with temperature for Hn_7 is less gradual than for the other detergents. The second virial coefficients decrease with increasing temperature, and become negative at the highest temperature.

The viscosity results are shown in Figures 10, 11, and 12, (p. 82, b, c, d), as plots of η_{sp}/c against c . Reasonable straight lines were obtained in all cases. The intercept $[\eta]$ increases with temperature, as does the slope. Figure 13, (p. 82 e), shows a plot of $\log [\eta]$ against temperature. Two straight lines are present which intersect at temperatures of 22, 36.3, and 43° for Hn_7 , Hn_3 and Hn_9 respectively. Similar effects are shown in Figure 9, (p. 79 d), for Hn_8 and Hn_9 using micellar weights from light-scattering. There appears to be a threshold temperature (called T_h) above which both micellar weight and intrinsic viscosities rise exponentially with increasing temperature. This rise in the intrinsic viscosities may represent a large increase of micellar asymmetry or hydration, the former appearing to be more likely. As the series of detergents

Log. M v. T°C for Hn₇, Hn₈ and Hn₉.

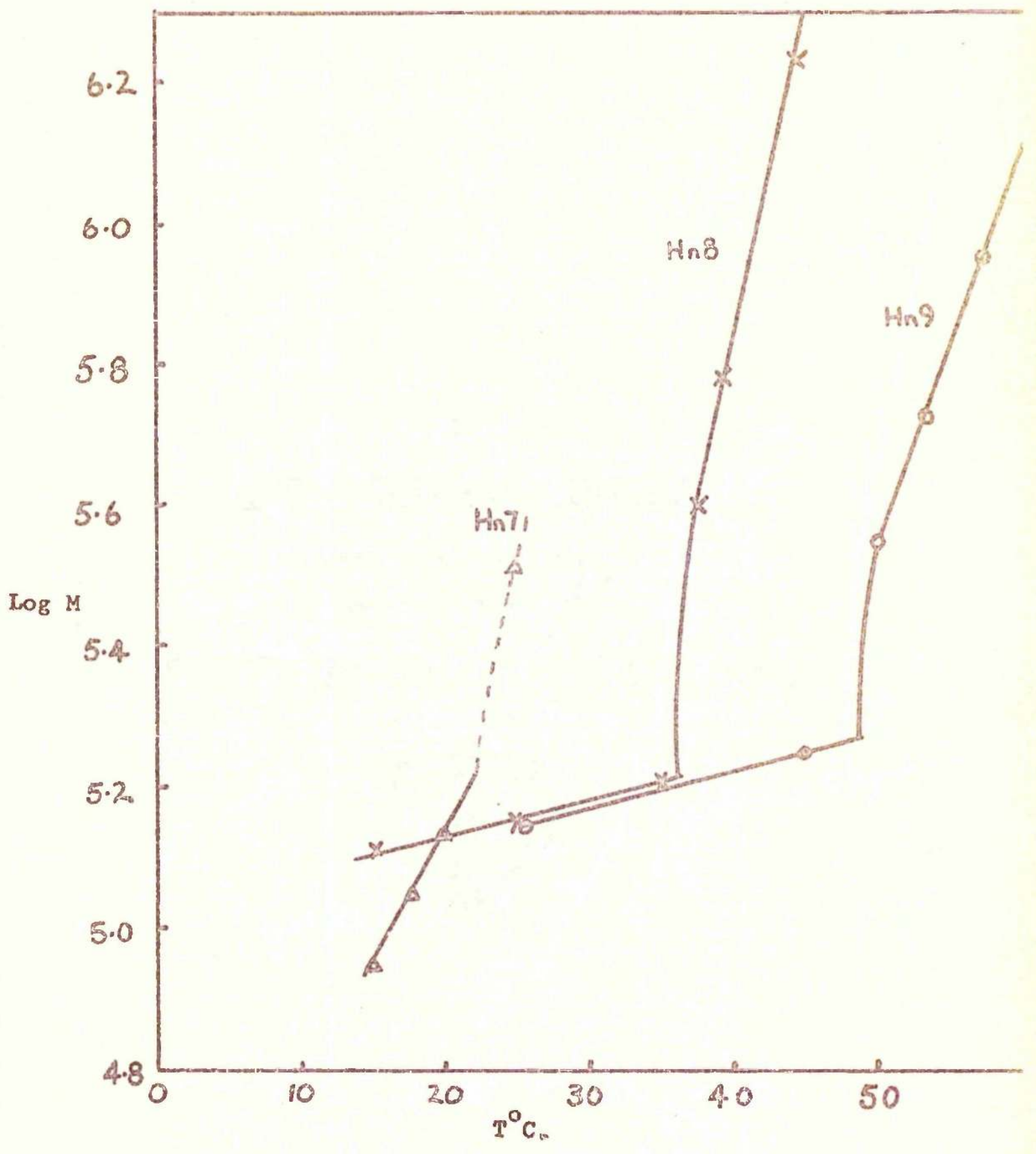
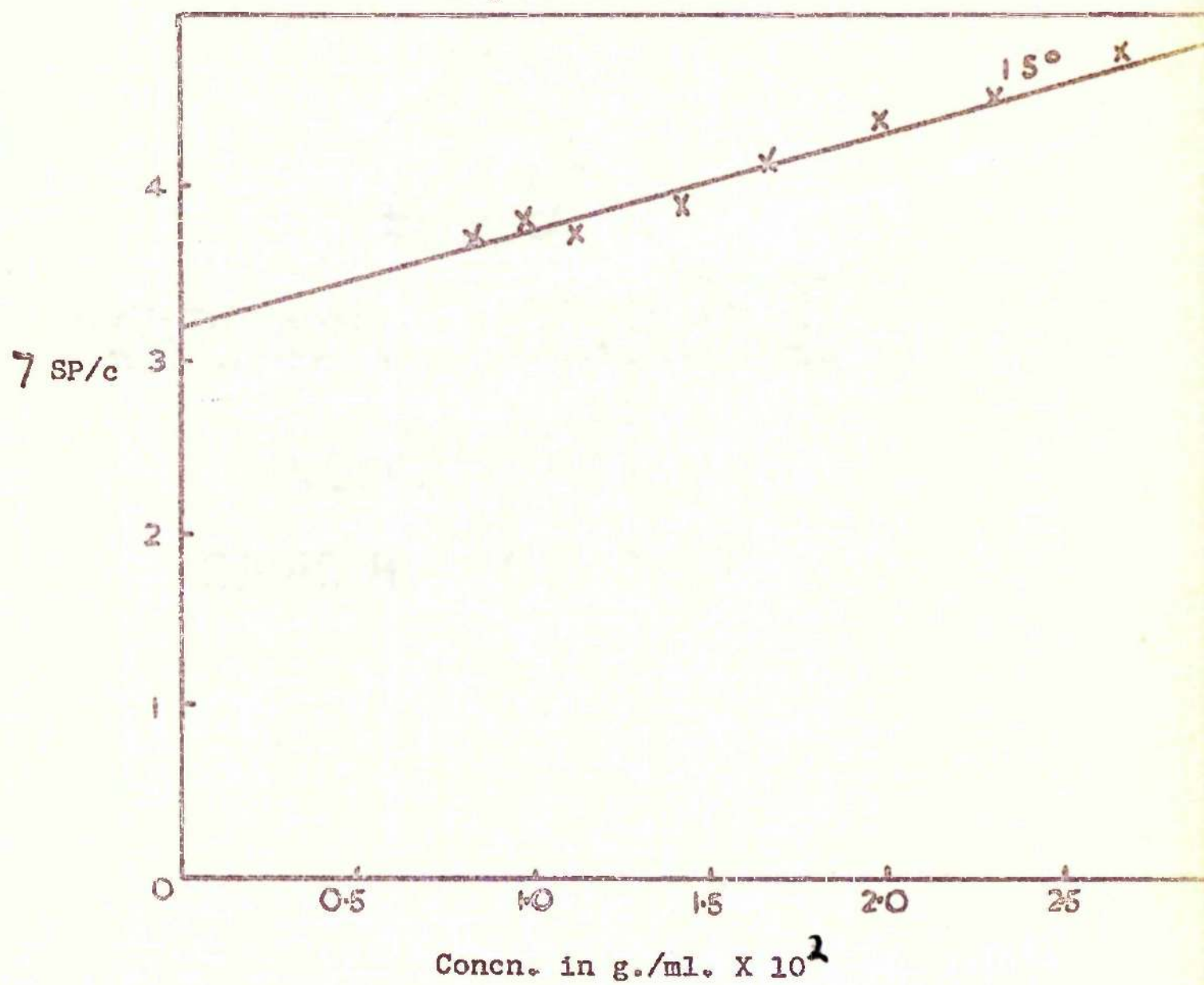


FIGURE 10
VISCOSITY $H_{\eta 7}$
Plot of $(\frac{7_{sp}}{c})$ against concentration
at temperature shown.



Plot of $\left(\frac{\eta_{sp}}{C}\right)$ against concentration at temperatures shown

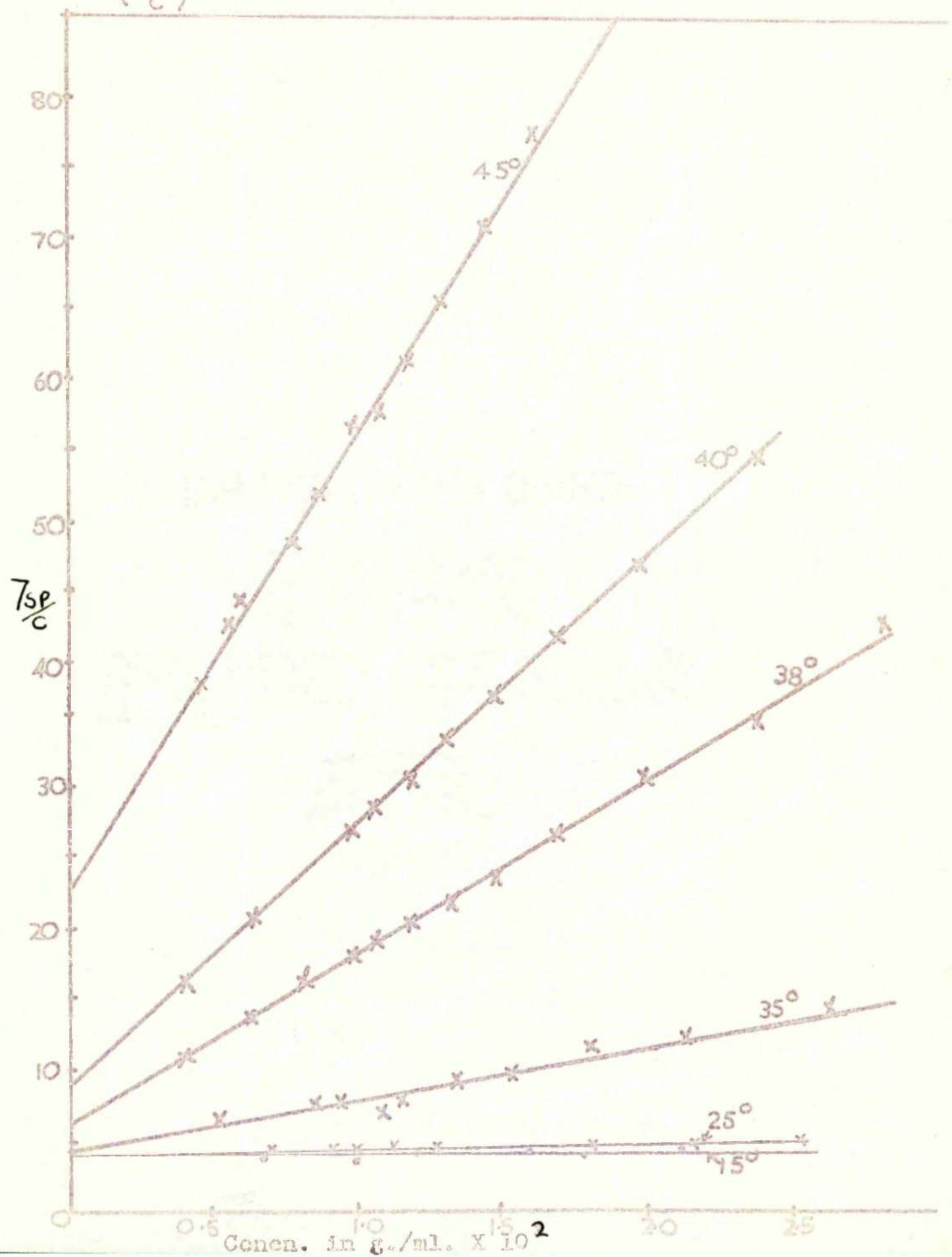


FIGURE 12 VISCOSITY η_{sp}

Plot of $\left(\frac{\eta_{sp}}{c}\right)$ against concentration at temperatures shown.

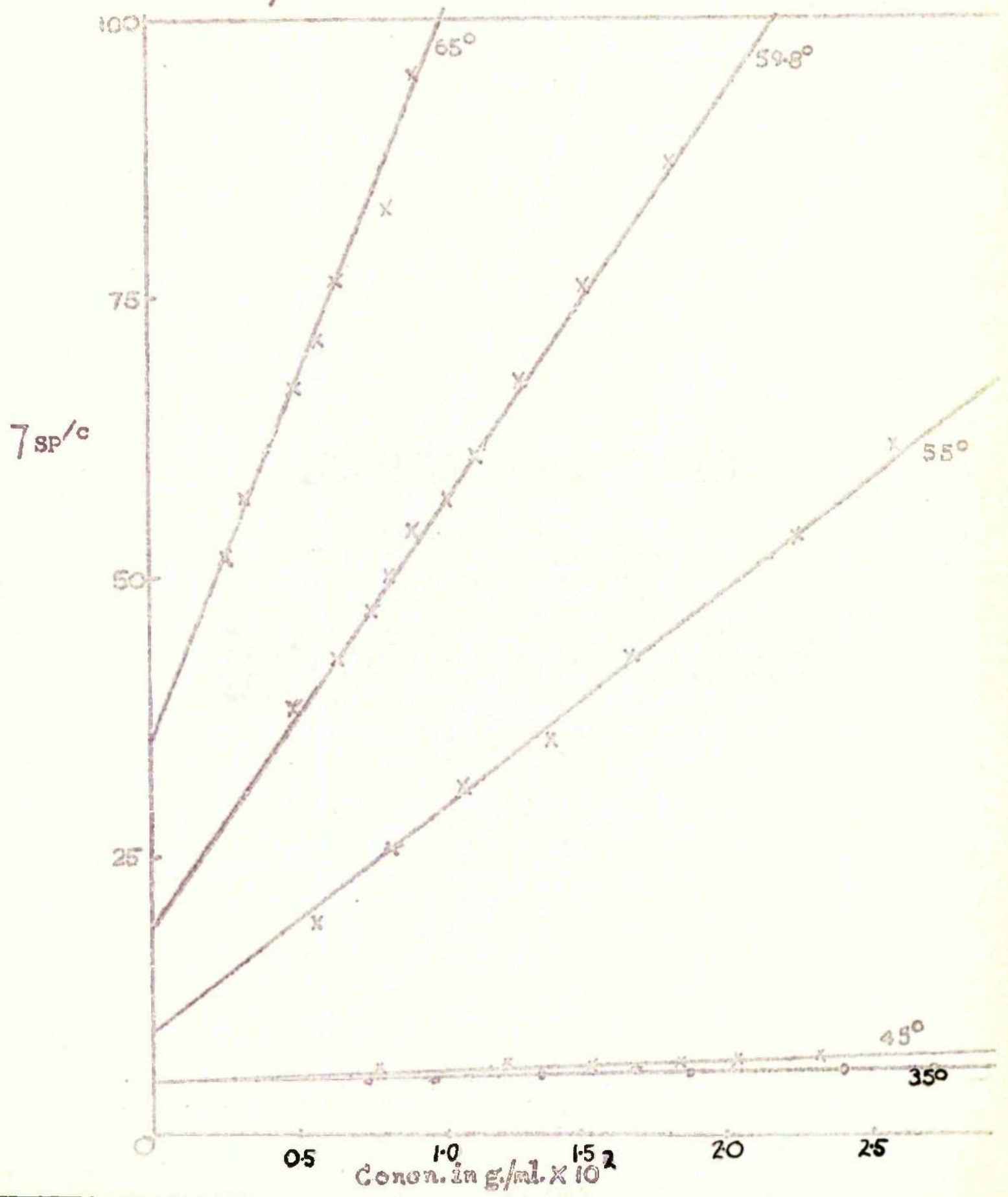
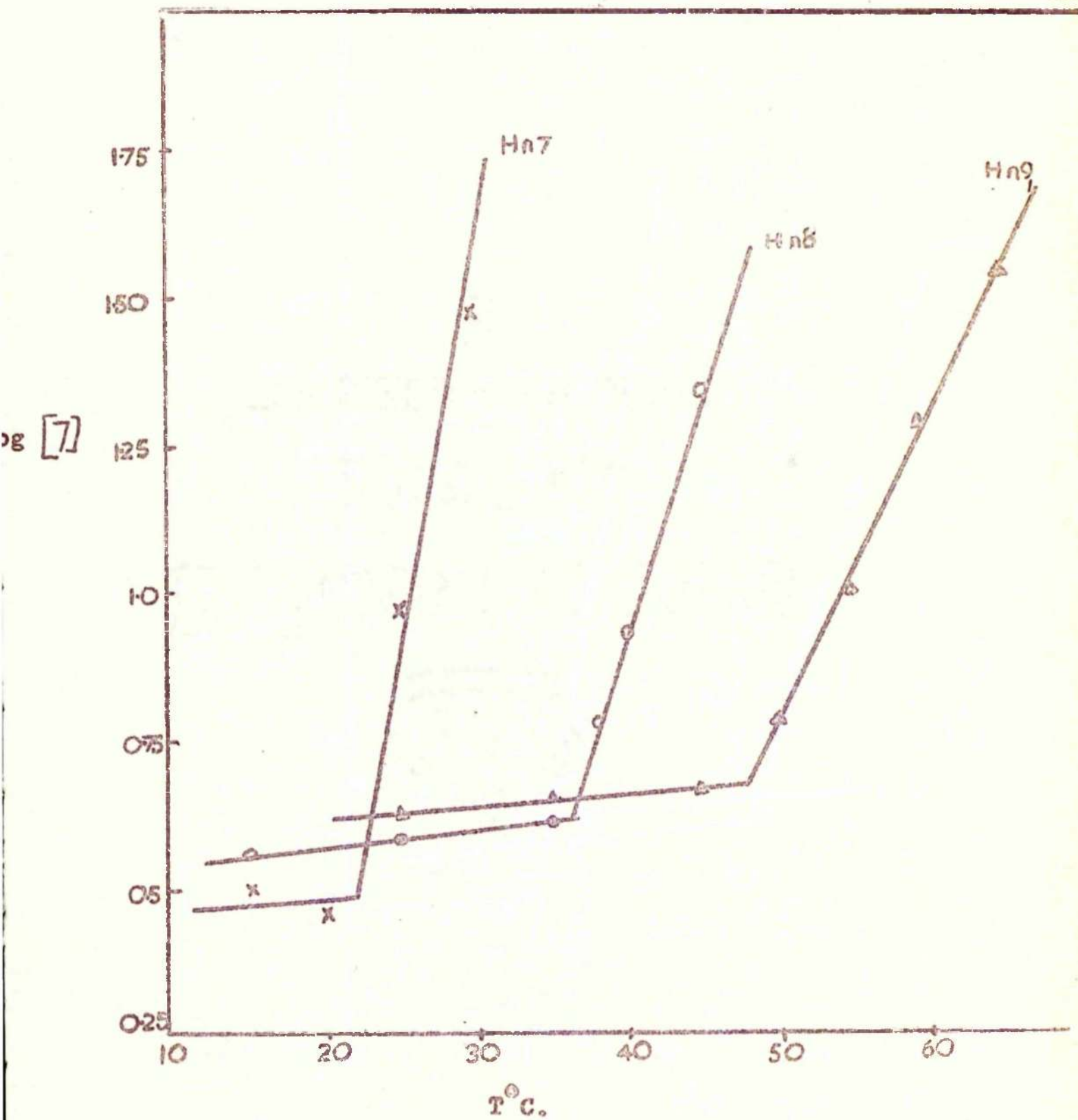


FIGURE 13.

Variation of log of Intrinsic Viscosity, $[\eta]$, with temperature for Hn_7 , Hn_8 and Hn_9 .



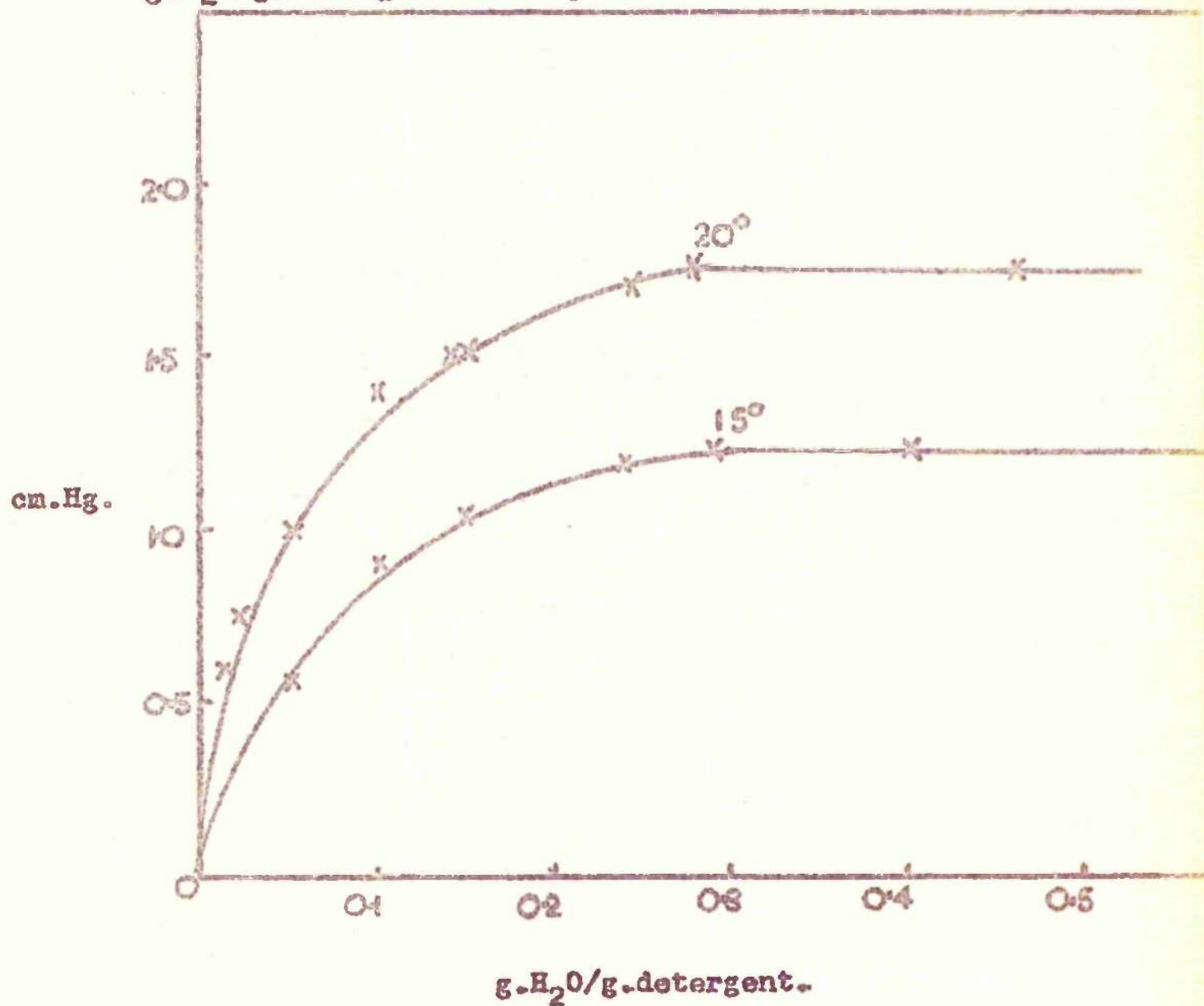
is ascended, the slope of the lines above T_h becomes less.

The vapour pressure results are shown in Figures 14, 15, and 16 (p. 83 a, b, c), as plots of vapour pressure, p , (mm. Hg.) against concentration, a , (g.water/g.detergent). Plots of a/x against x , where x is the relative vapour pressure, were used for extrapolation to $x = 1$, and determination of concentration at this point. Examples of the extrapolation are shown in Figure 15a (p. 83d) for Hn_8 ; the graphs were linear above $x = 0.85$, and the values of a at $x = 1$ are given in Table 4 as $W(\text{v.p.})$. Elworthy and Macfarlane¹⁷ suggested that the value of W obtained in this way could be taken as an estimate of micellar hydration. It was thought that at this concentration, sufficient water was present to solvate the polyoxyethylene chains fully, and give a system of particles, which although concentrated, would have a vapour pressure indistinguishable from that of pure water within experimental error, due to the inherent largeness of the micelles. The extrapolation to $x = 1$ gives a concentration at which the micelles have just become separate from one another. This empirical procedure was tested¹⁷ by calculating W (visc.) from equation (53) in cases where the micelles were spherical; good agreement between this

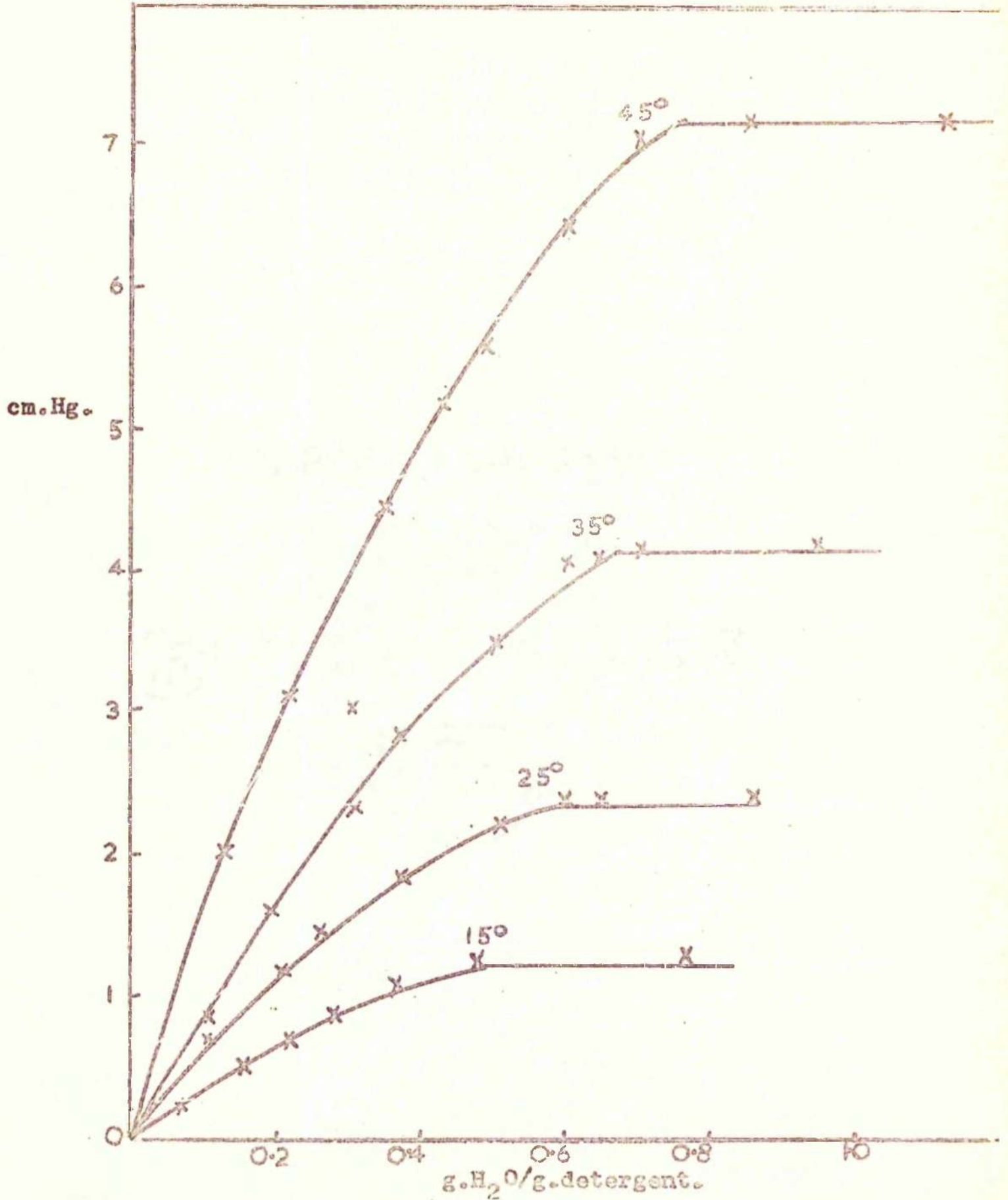
FIGURE 14.

Vapour Pressure Hn_7 .

Plot of Vapour Pressure (V.P.) in cm. Hg. against
g. H_2O /g. detergent at temperature shown



Vapour Pressure H_2O .
 Plot of Vapour Pressure (V.P.) in cm. Hg. against
 $\text{g. H}_2\text{O/g. detergent}$ at temperature shown.



Vapour Pressure Hn_9

Plot of Vapour Pressure (V.P.) in cm.Hg. against
 $\text{g.H}_2\text{O/g.detergent}$ at temperature shown.

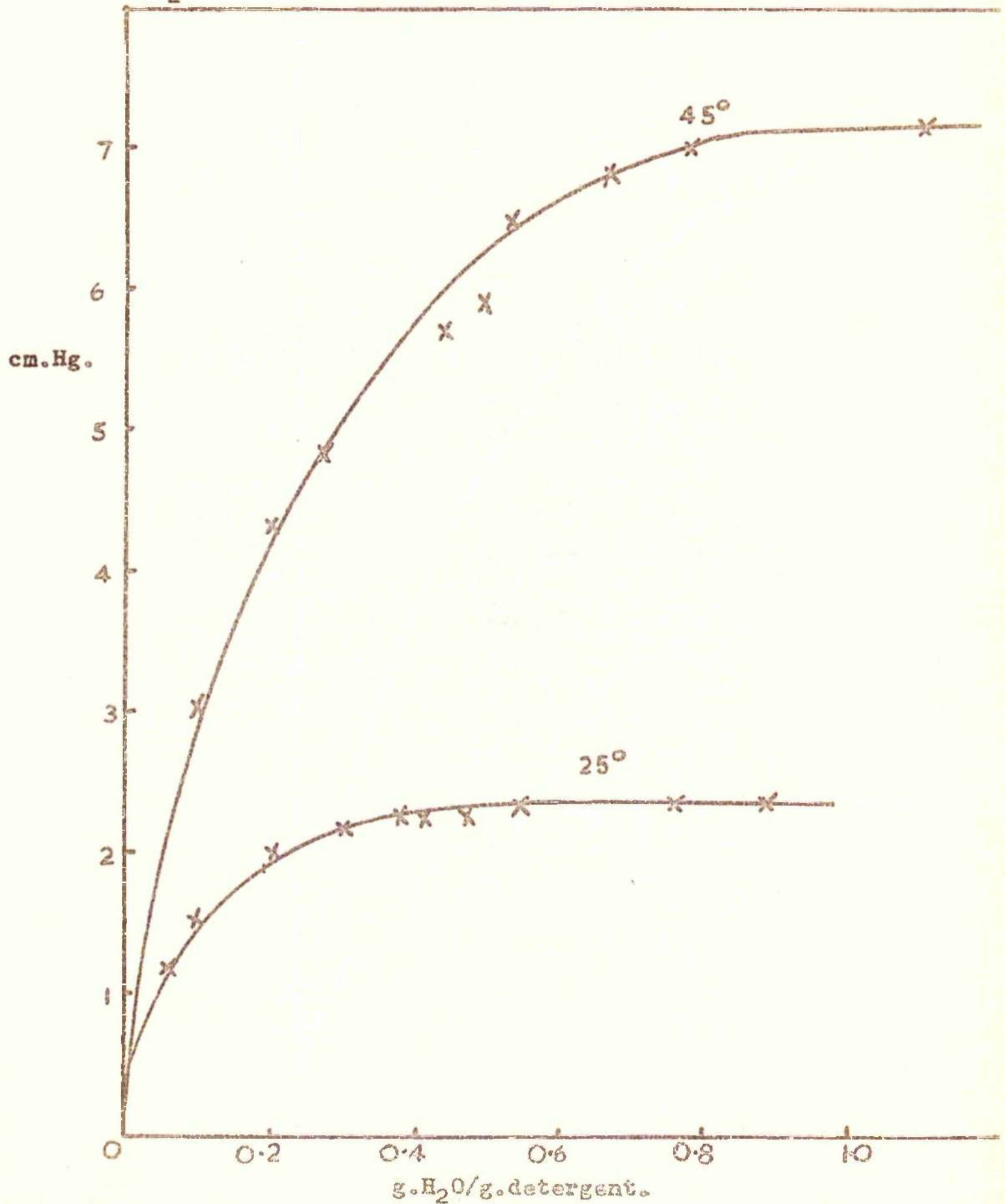
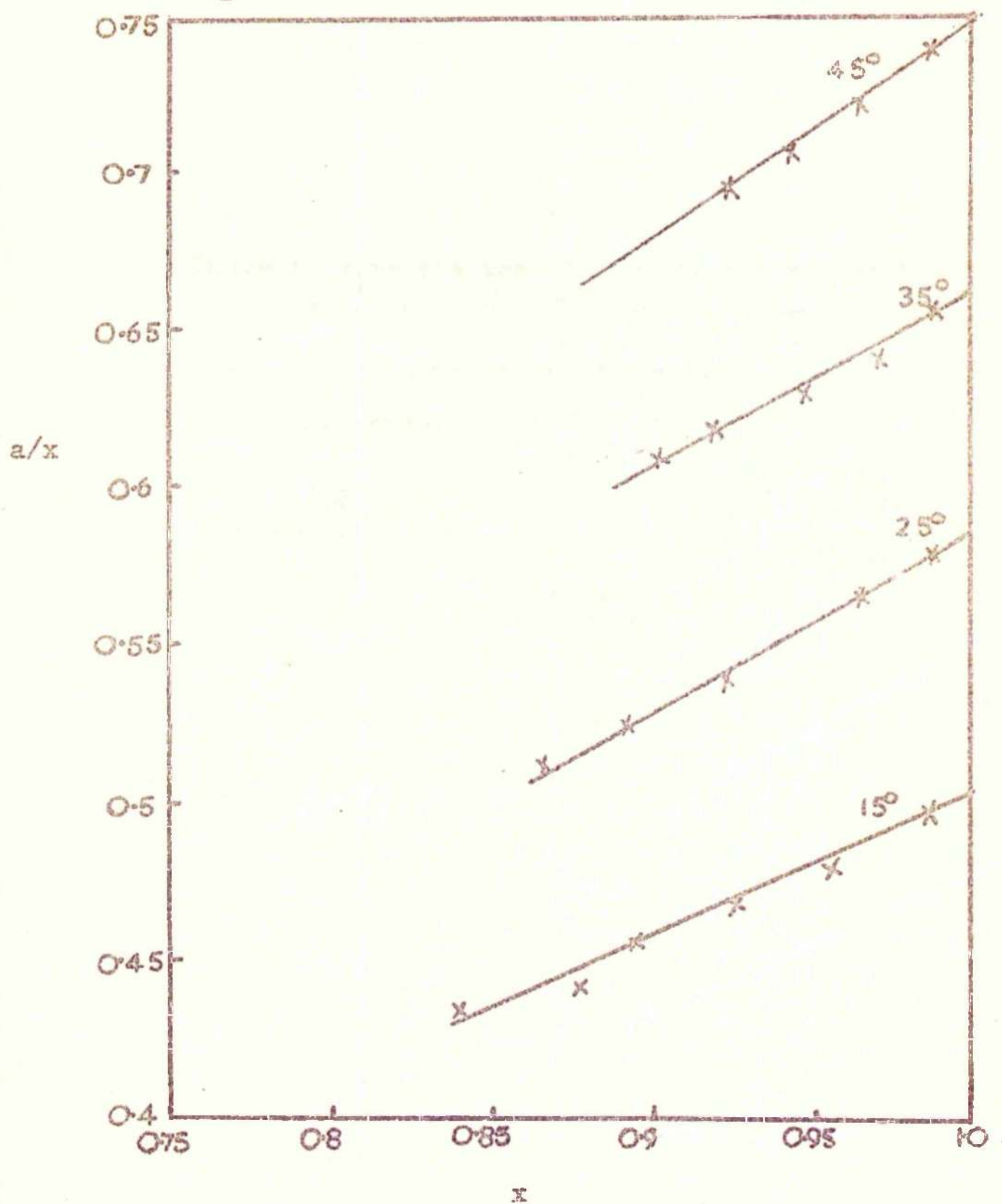


FIGURE 15a.

Plot of a/x against x for Hg_g . Where a is $\text{g. H}_2\text{O/g. detergent}$ and x is relative vapour pressure.



value of hydration and that from vapour pressure was obtained. Below the threshold temperature there is no physical reason why the micelles should be asymmetric, and a comparison of W (visc.) calculated from equation (53) is made with W (v.p.). The agreement is reasonable on the whole, especially as Macfarlane¹⁷ has shown that the limits of error in determining W (visc.) can be 5 - 15%. There is some scatter of results for Hn_7 at the two lowest temperatures, probably due to the difficulties of accurately measuring small intrinsic viscosities and vapour pressures.

TABLE 4_eVariation of $[\eta]$ and hydration with temperature.

	Temp. °C.	15	20*	25*	30*			
Hn ₇	$[\eta]$	3.20	2.91	9.70	29.94			
	W (v.p.)	0.29	0.28	0.44	0.52			
	W (visc.)	0.23	0.13					
Hn ₈	Temp. °C.	15	25	35	38	40	45	
	$[\eta]$	3.60	3.88	4.20	5.96	8.50	22.0	
	W (v.p.)	0.50	0.58	0.66				0.75
	W (visc.)	0.42	0.52	0.64				
Hn ₉	Temp. °C.	25 [†]	35	45	50	55	59.8	65
	$[\eta]$	4.29	4.50	4.69	6.03	10.1	18.7	34.9
	W (v.p.)	0.65		0.83	0.88			
	W (visc.)	0.72	0.77	0.83				

$[\eta]$ is expressed in ml/g.

W is expressed in g.water/ g.detergent.

* From Macfarlane and Elworthy⁹

† From Macfarlane and Elworthy⁸

v.p. = vapour pressure

visc. = viscosity.

Plots of hydration against temperature Figure 17, page 86a, could be represented by

$$\text{Hn}_7 \quad W = 0.100 + 0.014 T$$

$$\text{Hn}_8 \quad W = 0.315 + 0.0097 T$$

$$\text{Hn}_9 \quad W = 0.500 + 0.0075 T$$

where W was the mean hydration in g.water/g.detergent, and T was temperature in $^{\circ}\text{C}$. From these equations it appears that the longer the polyoxyethylene chain becomes, the smaller is the rise of W with temperature.

Although with Hn_8 , there was a large change of $[\eta]$ and M with temperature at 36.3° , no apparent break was found in W (v.p.) against temperature, a good straight line being achieved. Since it was found impossible to measure vapour pressure above 50°C in the case of Hn_9 , it was assumed that W (v.p.) v. T° was a straight line for Hn_9 , and values of W (v.p.) were obtained at higher temperatures by extrapolation.

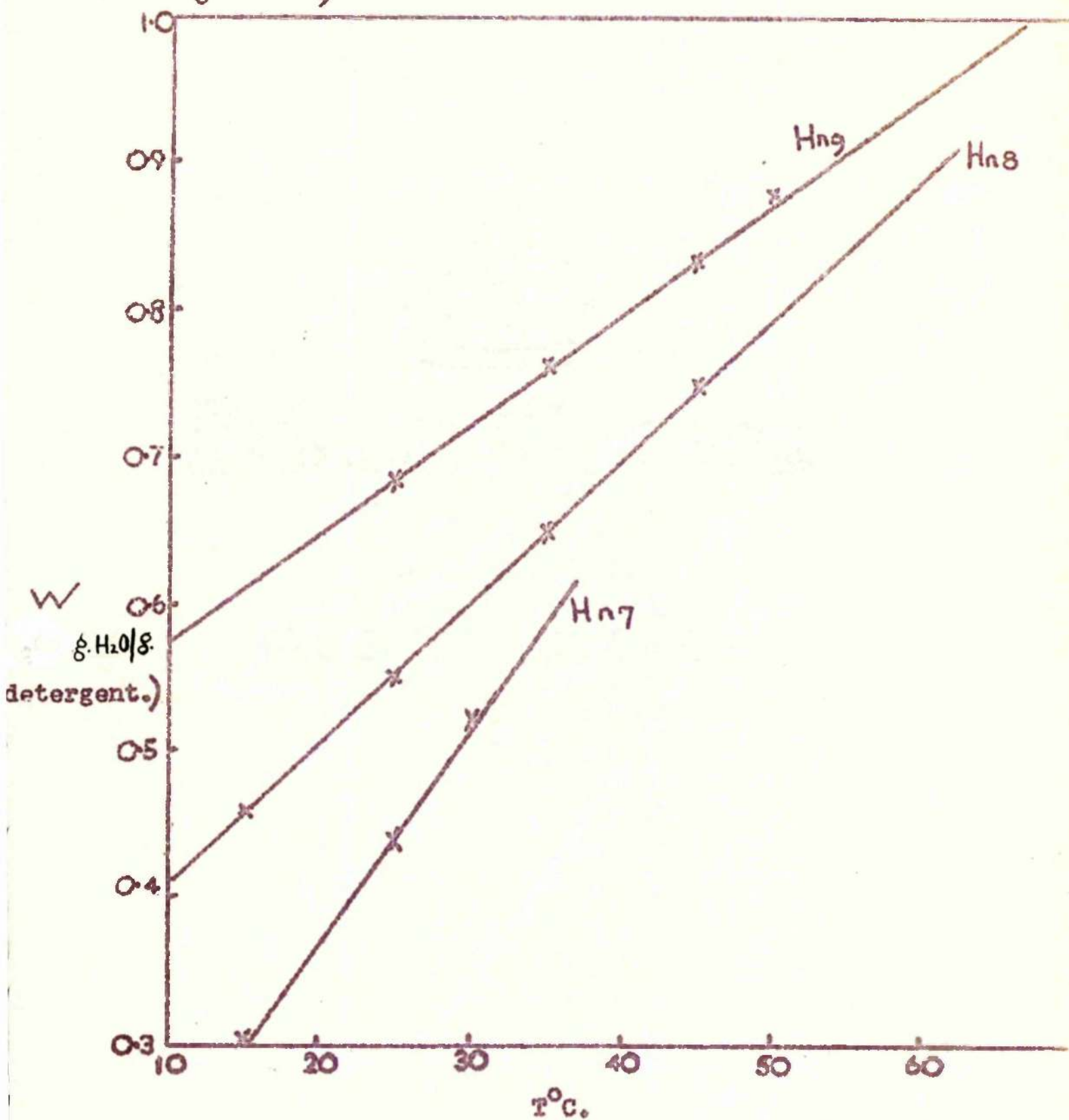
The vapour pressure results for Hn_8 were also used to provide a rough idea of some of the thermodynamic properties of the system. The results were treated as adsorption isotherms, from plots of a against x , using⁷⁸:

$$\Delta \bar{H} = \bar{H}_s - \bar{H}_l = R \left(\frac{\partial \ln(P/P_0)}{\partial (1/T)} \right)_{P, N_1, N_2} \quad (57)$$

FIGURE 17.

HYDRATION.

Variation of hydration with temperature for Hn_7 ,
 Hn_8 and Hn_9 .



and

$$\Delta \bar{S} = \bar{S}_s - \tilde{S}_1 = \frac{1}{T} \left(\Delta H - RT \ln(p/p_0) \right) \quad (58)$$

where \tilde{H}_1 and \tilde{S}_1 are molar enthalpies and entropies of water, \bar{H}_s and \bar{S}_s are partial molar enthalpies and entropies of the sorbate, N_1 and N_2 are the number of moles of sorbate and sorbent respectively, and p/p_0 is the relative vapour pressure.

The differential partial molar enthalpies ($\Delta \bar{H}$) and entropies of hydration were calculated (Table 5). $\Delta \bar{H}$ was calculated for the three temperature intervals ($15^\circ - 25^\circ$, $25^\circ - 35^\circ$, and $35^\circ - 45^\circ$) available from the vapour pressure results. Both $\Delta \bar{H}$ and $\Delta \bar{S}$ are positive in sign, and are of roughly the same size as values determined for Hn_7 by Elworthy and Macfarlane¹⁷. Generally the thermodynamic properties decrease as a increases, and increase as the temperature is raised. Below $a = 0.4$ the scatter of results made the calculations unreliable.

TABLE 5.

Differential partial molar enthalpies and entropies of sorption of Hn_8 .

a	$\Delta \bar{H}_{20}^{\circ} \text{C}$	$\Delta \bar{H}_{30}^{\circ}$	$\Delta \bar{H}_{40}^{\circ}$	$\Delta \bar{S}_{20}^{\circ}$	$\Delta \bar{S}_{40}^{\circ}$
0.4	1.5	1.8	2.3	5.6	10.2
0.45	1.2	1.4	2.3	4.6	7.6
0.50	1.3	1.5	2.3	4.5	7.8

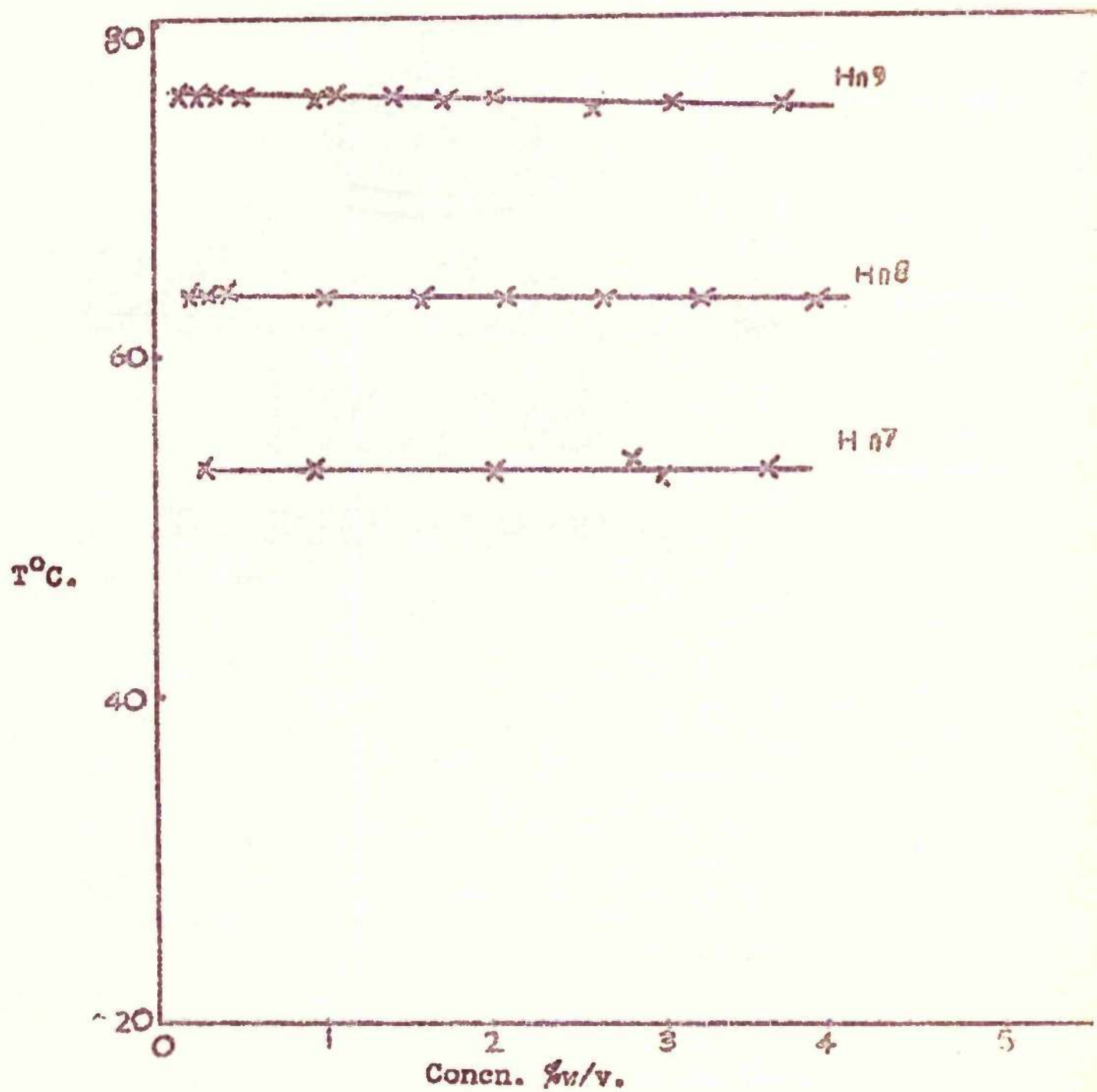
$\Delta \bar{H}$ is expressed in Kcals.mole⁻¹. $\Delta \bar{S}$ in cal.s.mole⁻¹ deg⁻¹.

Cloud points are shown in Figure 18, page 88a. Over the range studied they do not vary much with concentration, but increase as the poloxyethylene chain lengthens, being 54°, 64°, and 76° for Hn_7 , Hn_8 , and Hn_9 respectively.

It was necessary to determine the densities of the detergents.

Because of the difficulty in finding a liquid in which the detergents were insoluble, the densities were calculated from the molar volumes of the glycols and of hexadecane, neglecting the molar volumes of hydrogen. As a check on this method the densities of Hn_8 at 45°C and of Hn_9 at 45°C and 53.5°C were measured directly in a 1ml. pycnometer, giving 0.950 g./ml. for Hn_8 and 0.968 g./ml.

FIGURE 18.

Cloud Points of Hn₇, Hn₈ and Hn₉.

and 0.954 g./ml. for Hn_9 at 45°C and 53.5°C respectively. The densities of hexadecane were obtained from the literature⁷⁹ checks being made at two temperatures. Density values are shown in Table 6, and 6a.

TABLE 6.

Densities of glycols, hexadecane and detergents at the temperatures shown.

Hn_7

$T^\circ\text{C}$	15	20	25	30
$n_7^t d_4^t$ g./ml.	1.130	1.127	1.123	1.119
$d_4^t \text{Hn}_7$ calcul. g./ml.	0.949	0.946	0.942	0.939

Hn_8

$T^\circ\text{C}$	15	25	35	45
$n_8^t d_4^t$ g./ml.	1.170	1.168	1.153	1.137
$d_4^t \text{Hn}_8$ calcul. g./ml.	0.978	0.973	0.963	0.952
$d_4^t \text{Hn}_8$ measured g./ml.				0.950

Hn_9

$T^\circ\text{C}$	45	50	53.5	57.5
$n_9^t d_4^t$ g./ml.	1.148	1.135	1.132	1.131
$d_4^t \text{Hn}_9$ calcul. g./ml.	0.968	0.961	0.957	0.955
$d_4^t \text{Hn}_9$ measured g./ml.	0.968		0.954	

TABLE 6a.

Density of Hexadecane at Temperatures shown.

90.

Hexadecane.

$T^{\circ}C$	d_4^t	d_4^t (experimental)
15	0.7760	
25	0.7699	0.7701
35	0.7639	0.7637
45	0.7570	
50	0.7535	

DISCUSSION.The Structure of the Micelles Below T_h .

In the region below the threshold temperatures, 22° , 36.3° , and 48° C for Hn_7 , Hn_8 , and Hn_9 respectively, both molecular weights and viscosity intercepts increase fairly slowly with increasing temperature. The latter are all fairly close to the Einstein value of 2.5 for unsolvated spheres. Values of micellar hydration calculated from both viscosity intercepts and vapour pressure results show an increase with temperature; this increase will be discussed later. From the values of m , W , and M and the densities of detergent and water, assuming the micelles are spherical, the micellar dimensions were calculated.

The radius of the micelle, r_1 , was calculated from

$$r_1 = \left(\frac{3V}{4\pi} \right)^{1/3} \quad (59)$$

where V is the total micellar volume, including the hydrating water. The micellar interior is likely to be liquid in nature, and the radius of the hexadecane region,

$$r_h = \left[\frac{3 \times \text{molecular volume hexadecane} \times m}{4\pi} \right]^{1/3}$$

The difference between r_1 and r_h is the radial length occupied by the polyoxyethylene chains, and is denoted r_e . The results of the calculations are given in Table 7.

TABLE 7.

Micellar properties of Detergents at various Temperatures below T_h .

Detergent	Temp. °C	$V \times 10^{-5}$ (Å ³)	r_1 Å	r_h Å	r_e Å
Hn ₇	15°	2.03	36.4	26.7	9.7
	17.5°	2.61	39.6	28.9	10.6
	20°	3.25	42.7	30.7	12.0
Hn ₈	15°	3.23	42.6	29.4	13.1
	25°	3.76	44.8	30.4	14.4
	35°	4.52	47.6	31.7	15.9
Hn ₉	25°	3.93	45.4	29.5	15.9
	45°	5.43	50.8	31.9	18.9

As the temperature rises, the radial length of the polyoxyethylene chain increases. It is thought that at normal temperatures this chain may be arranged as an expanding spiral^{9,10}, or, at any rate, in some similar arrangement whereby the length of the chain is less than the fully extended length. From catalin models, the fully

extended monomer lengths are 54.4\AA , 58.9\AA , and 63.5\AA for Hn_7 , Hn_8 , and Hn_9 respectively, and the length of the hexadecane portion is 21.6\AA . It has been pointed out eg. by Tanford⁸⁴ that an increase in temperature decreases intramolecular and intermolecular attractive forces; as a result of this polymer coils expand. A similar process appears to occur with the non-ionic detergent micelles studied here, and due to this the possibility of trapping more water molecules in the mesh of polyoxyethylene chains will be greater at a higher temperature than at a lower one. The positive values of $\Delta \bar{H}$ and $\Delta \bar{S}$ found (Table 5) increase with temperature, indicating that a mixing process is predominating over any specific arrangement of water molecules around the polyoxyethylene chains, and that the mixing is greater at higher than at lower temperatures, which also fits in with the increase of micellar hydration.

Examination of other papers describing micellar hydration of non-ionic detergents revealed no experimental evidence of a decrease in hydration with increasing temperature. The present work indicates that an increase in hydration with temperature occurs, this increase being consistent with the extension of polyoxyethylene chain

in the micelles as temperature is raised.

It seems possible that the increase of molecular weight found up to T_h may be due to geometrical factors. Remembering that the polyoxyethylene part of the molecule is contracted, the monomer has a wedge shape, which means that only a certain number could be placed into a spherical shape. Increase of temperature extends the polyoxyethylene chain, decreases the width of the widest part of the wedge, and may allow more monomers to be placed in the spherical shape. It is unlikely that this is a complete explanation, but it seems a reasonable hypothesis.

The Structure of the Micelles at T_h .

Values of M at T_h were found by extrapolating, the linear parts of Figure (p. 82) below the T_h to the value of T_h . The properties of the micelles at these temperatures were calculated and are shown in Table 8.

TABLE 8.Properties of Micelles at T_h .

	Hn_7	Hn_8	Hn_9	
$M \times 10^{-5}$	1.61	1.63	1.81	
m	292	274	284	
$W \text{ g./g.}$	0.40	0.67	0.86	
$V \times 10^{-5} (\text{\AA})^3$	3.90	4.62	5.74	
A {	r_1	45.3	48.0	51.6
	r_h	32.4	31.8	32.3
	r_e	12.9	16.2	19.3
	$\frac{r_e}{n}$	1.85	2.02	2.14

n = number of ethylene oxide units.

Within the limits of experimental error, it appears that the numbers of monomers in the micelles, at the threshold temperature, are the same for each detergent. As Hn_9 is the most heavily hydrated of the detergents its micellar volume is the largest.

In calculating the dimensions of the hydrocarbon core of the micelles a fluid interior was assumed, thus giving a greater volume at T_h than at lower temperatures. The polyoxyethylene chain is not fully extended at T_h .

The extended lengths are 54.4 Å, 58.9 Å, and 63.5 Å from molecular models. The radial length per ethylene oxide unit is seen to increase with detergent chain length.

It is also possible to calculate ⁸⁰ the end to end length of hydrocarbon chains, L, from

$$L^2 = \sigma^2 y \left(\frac{1 + \cos \theta}{1 - \cos \theta} \right) \left(\frac{1 + a}{1 - a} \right) \quad (60)$$

where σ = C - C bond length, y = number of links in the chain, θ = supplement of the valency angle, and a is the average value of the cosine of the angle of rotation for one rotation.

When there is no hindered rotation $(1 + a)/(1 - a)$ becomes unity. For hexadecane $L = 13.8$ Å. As the ends of the hydrocarbon chains cannot all be in the micelle centre, it is assumed that a space must be present there, its surface being covered by the ends of 283 monomers (mean value), each with a cross-sectional area of approximately 16 Å² (i.e. crystallographic area of hydrocarbon chain ⁸¹). The radius of this space is 19 Å and the radius of the hydrocarbon region is $19 + 13.8$ i.e. 32.8 Å. The results from Table 8 and those calculated from equation (60) give approximately the same value for

the radius of the hydrocarbon part of the micelles.

Because of a lack of knowledge of rotational energy barriers equation (60) cannot be used to calculate the lengths of the polyoxyethylene chains. However, as the ether bond angle is close to the C - C angle, and as the bond length is 1.42 \AA , for a polyoxyethylene chain, with the same number of linkages as a hydrocarbon, the following values of L are obtained.

Temp.	22° Hn_7	$36.3^{\circ} \text{ Hn}_8$	$47.9^{\circ} \text{ Hn}_9$
$\text{\AA} \left\{ \begin{array}{l} L \\ L (a = 0) \end{array} \right.$	17.2	17.8	18.4
r_e (from Table 4)	12.9	16.2	19.3

The lengths of the polyoxyethylene chains are too small when calculated for freely rotating bonds ($a = 0$). It has been stated that the presence of ether linkages in hydrocarbon chains greatly increases the flexibility⁸². For Hn_7 the value for r_e , 12.9 \AA , calculated from micellar volumes lies between the two values obtained from equation (60). The values of r_e for Hn_8 and Hn_9 are close to the value of L calculated for an equivalent hydrocarbon chain in the presence of restricted rotation. It may be that, as the series is ascended, increased hydration

increases the interactions between chain and solvents and so increases the length.

Above T_h micellar growth is very rapid and asymmetry develops. At T_h the number of monomers present in the micelle may be the maximum possible number which can form a spherical shape. If this is so it is possible that the addition of further monomers as the temperature increases would alter the shape of the micelle. It has been shown that the parts of a polyoxyethylene chain close to the surface of the hydrocarbon part are very closely packed at normal temperatures and that they may therefore prevent water from coming into contact with that region. As temperature increases the area of the hydrocarbon region increases (m increases) and there is a lengthening of the polyoxyethylene chains. These effects may decrease the protective shielding by the innermost part of the polyoxyethylene chains of the hydrocarbon region from the effects of water. It may be that water comes into contact with the surface of the hydrocarbon region causing an increase in interfacial tension at some point on the hydrocarbon/chain boundary, which would have a contracting effect and cause the micelle to elongate. Although this cannot be proved it does at

least suggest a basis for understanding the sudden growth of molecular weight at a particular temperature.

Structure of Micelles above T_h .

Figure 9, (p. 82a) shows a sharp increase of M above T_h , followed by a slower rise, for Hn_8 and Hn_9 . $\log. M$ is linear with temperature for Hn_8 and Hn_9 in this second region (37.4 - 44.3°C for Hn_8 , and 50 - 57.5°C for Hn_9).

From a plot of $\log[\eta]$ against $\log M$ Figures 19, 20, (p. 99 a, b), the slopes of the graphs are 0.90 and 1.07 for Hn_8 and Hn_9 respectively. Simha's shape factors may be generalised, in the region of v of interest to

$$\text{Oblate ellipsoids } v = 1.45 + 0.661 b/a \quad (61a)$$

$$\text{Prolate ellipsoids } v = \text{const.} + \text{const.}' a/b^{1.2-1.5} \quad (61b)$$

For flexible coiled molecules Tanford gives

$$[\eta] = \text{const.}'' M^{1/2} \quad (61c)$$

The axial ratio for ellipsoidal molecules is proportional to molecular weight, so for plots of $\log. [\eta]$ v. $\log. M$ a slope of 1 should be obtained for oblate ellipsoids, 1.2 - 1.5 for prolate ellipsoids and 0.5 for flexible coils in poor solvents where $B = 0$ or is negative.

The slopes obtained, (Figures 19 and 20) indicate that the micelles

FIGURE 19.

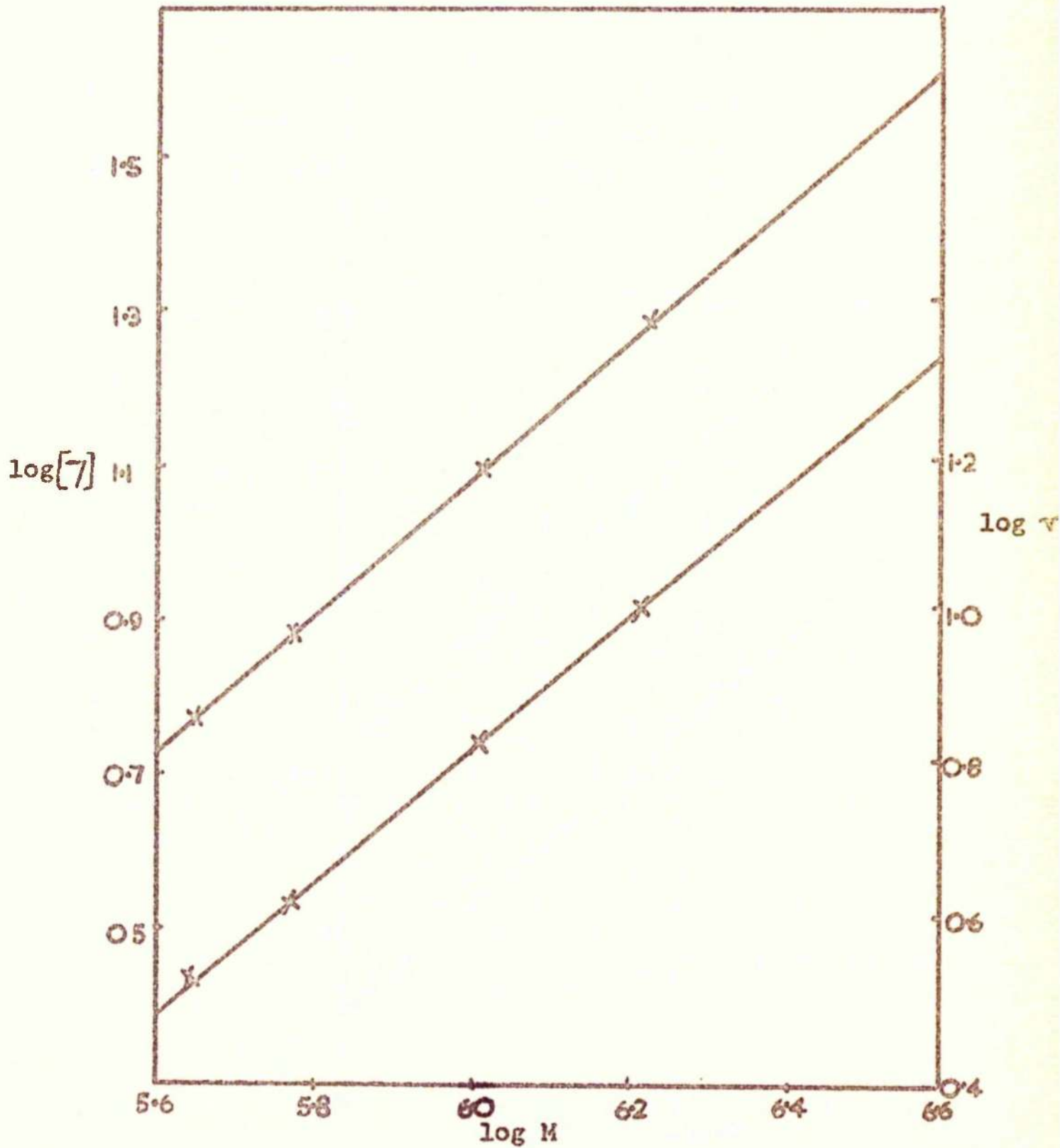
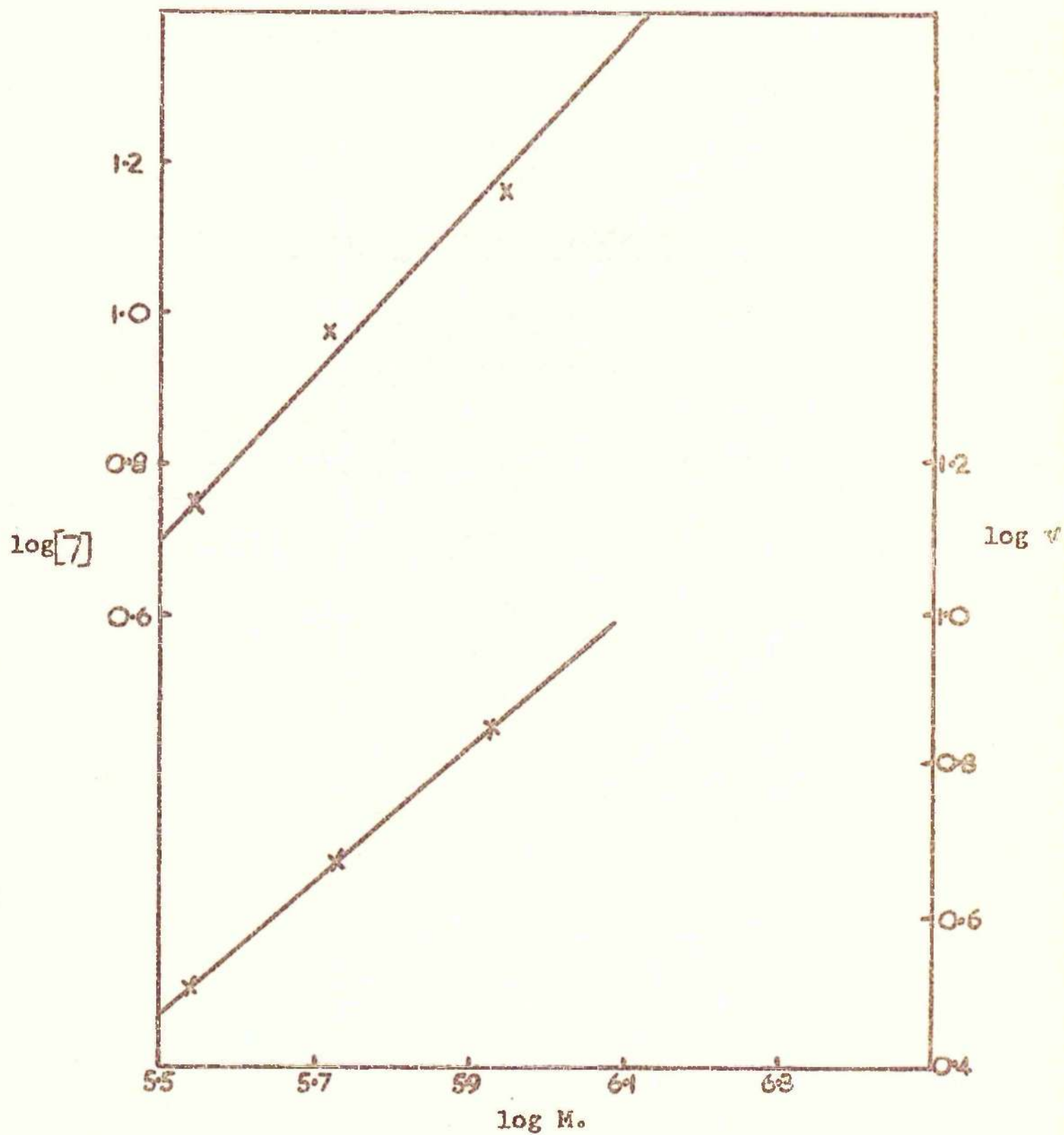
Plots of $\log [\eta]$ and $\log \nu$ against $\log M$ for Hn_8 .

FIGURE 20.

Plots of $\log[7]$ and $\log v$ against $\log M$ for Hn_9 .

resemble oblate ellipsoids more than any other model shape.

It has been assumed that hydration W is constant for the above treatment. However values of v may be calculated using W values from Table 4, and the slopes of $\log v$ against $\log M$ plots are 0.85 and 0.38 for Hn_3 and Hn_9 respectively Figs. 19 and 20 (p. 99a, b), indicating that the oblate model fits the particle best.

Using the oblate model, calculation of micellar dimensions are given in this temperature region in Table 9.

TABLE 9.

Micellar Dimensions of Hn_3 and Hn_9 between 37.4 - 44.3°C and 50 - 57.5°C respectively.

Hn_3	T	v	b/a	$v\bar{A}^3 \times 10^{-6}$	\bar{A}	
					a	b
	37.4	3.12	2.5	1.14	48	120
	39.3	4.37	4.5	1.74	45	203
	44.3	10.9	14.2	4.98	44	620
Hn_9	50	3.13	2.5	1.12	47	118
	53.5	4.62	4.8	1.71	43	209
	57.5	7.22	8.7	3.93	47	414

From Table 9 it can be seen that short semi-axes are reasonably constant, within experimental error, and are reasonably close to the fully extended monomer lengths. It would be seen therefore that above T_h the polyoxyethylene chains extend fairly rapidly. Thus a quick growth of disk-shaped micelles occurs which presumably continued with increasing temperature, until the micelles become so large that they are macroscopically visible. At the cloud point the micelles are of such dimensions that a second phase is formed which could be expected to contain the majority of the detergent⁴⁰.

The steeply rising parts of the graphs in Fig. 9 are worth examination between T_h and 37.4°C for Hn_8 and T_h and 50°C for Hn_9 . From points interpolated from Figs. 9 and 13, (p. 82 a, e), the slope of $\log.[\eta]$ against $\log. M$ graphs were 0.45 for Hn_8 and 0.50 for Hn_9 . Results from this small temperature range where M increases very rapidly with temperature are tentative, but they do suggest that the micelles resemble coils rather than the other models in this region. The micelles have not yet become very asymmetric, and consist of a hydrocarbon core surrounded by reasonably flexible polyoxyethylene chains.

Provided that this type of structure remains spherical it resembles a coiled molecule. An increase in the molecular weight of say, a polystyrene molecule in solution, means that the volume of solution pervaded by the molecule increases spherically about the centre of mass. However, an increase in micellar weight is subject to the condition that all the hydrocarbon chains must remain in the interior of the micelle, and so micellar expansion can only occur in two dimensions. The results show that this appears to be the case, and the micelles take on oblate shape.

Other considerations.

Second virial coefficients for spherical micelles below T_h were calculated on the basis of excluded volume from the equation $B = 4V/M_2^2$, where V is the micellar volume, M_2 is the molecular weight of the micelle and B is the second virial coefficient. The values calculated are shown in Table 10.

TABLE 10.Second Virial Coefficients for Spherical Micelles below T_h

Temperature °C.	B x 10 ⁴				
	15	20	25	35	45
Hn ₇	0.56	0.43			
Hn ₈	0.45		0.44	0.42	
Hn ₉			0.48		0.43

The agreement with values calculated from light-scattering results, Table 3, is not close. It would seem that other factors must introduce non-ideality as well as the excluded volume. A contribution to the chemical potential $\mu_1 - \mu_1^0$, is given by the excluded volume effect, and this contribution remains approximately the same as temperature increases.

At low temperatures B experimental is greater than B calculated, and hence other factors must contribute to the non-ideality. The derivation of the excluded volume assumes that $\Delta \bar{H}_{mix}$ is constant as concentration is changed, making no contribution to $\mu_1 - \mu_1^0$, and this may not be correct. The decrease of B with increasing temperature must also be accounted for; it has been shown

that as the temperature is increased the polyoxyethylene chain straightens. It has been stated⁸⁵ that an extended chain is in a more ordered state than a coiled up one. The process of extension may provide a lowering of the entropy of the system which opposes the effects of excluded volume and $\Delta \bar{H}_{mix}$, and which predominates at higher temperatures to give a negative second virial coefficient. The micellar structure, with its hydrocarbon region, and its regions of mixing between water and polyoxyethylene chains, is a complex one, and it is felt that only a qualitative discussion of the various thermodynamic effects can be attempted at the present time.

The temperature at which $B = 0$, corresponds quite closely to the value of T_h . eg's. For Hn_3 $B = 0$ at approx $37^\circ C$ (T_h is 36.3°). For Hn_9 $B = 0$ at approx $49^\circ C$ (T_h is 48°)

However it is not considered that the solution is truly ideal at this temperature, but that a balance of factors is at work.

It should be noted that the cloud points are roughly 30° above T_h for all detergents, so phase separation does not occur when $B = 0$, but at a considerably higher temperature.

REFERENCES.

1. Macfarlane C.B., Ph.D. Thesis, Univ. of Glasgow, 1963.
2. Perry S.Z. and Hibbert H.H., Canad. J. Res., B., 1936, 14, 77.
3. Fordyce R., Lovell E.H. and Hibbert H.H., J. Amer. Chem. Soc., 1939, 61, 1905.
4. Gingras B.A. and Bayley C.H., Canad. J. Chem., 1957, 35, 599; 1958, 36, 1320.
5. Mulley B.A., J. Chem. Soc., 1958, 2065.
6. Mulley B.A., Proc. 3rd. Int. Cong. Surface Activity, 1960, 1, 31.
7. Corkill J.M., Goodman J.F., and Ottewill R.H., Trans. Faraday Soc., 1961, 57, 1627.
8. Macfarlane C.B. and Elworthy P.H., J. Chem. Soc., 1962, 537.
9. Macfarlane C.B. and Elworthy P.H., J. Chem. Soc., 1963, 907.
10. Schick J.M., Atlas S.M. and Erich F.R., J. Phys. Chem., 1962, 66, 1326.
11. Kushner L.M. and Hubbard W.D., J. Phys. Chem., 1954, 58, 1163.
12. Elworthy P.H., J. Pharm. Pharmacol., 1960, 12, 260T.

13. Becher P., J. Colloid Sci., 1961, 16, 49.
14. Stauff J. and Rasper J., Koll. Z., 1957, 151, 148.
15. Kushner L.M., Hubbard W.D. and Doan A.S.,
J. Phys. Chem., 1957, 61, 371.
16. Balmbra R.R., Clunie J.S., Corkill J.M. and
Goodman J.F., Trans. Faraday Soc., 1962, 58, 1661.
17. Elworthy P.H. and Macfarlane C.B., J. Chem. Soc.,
in the press.
18. Reich I., J. Phys. Chem., 1956, 60, 257.
19. Hoeve C.A.J. and Benson G.C., J. Phys. Chem.,
1957, 61, 1149.
20. Aranow R.H., J. Phys. Chem., 1963, 67, 556.
21. McBain J. in "Colloid Science", Alexander A.E. and
Johnson P., Oxford, 1950, p.31.
22. Gornish E. and McBain J.W., J. Amer. Chem. Soc.,
1947, 69, 334.
23. Hsiao L., Dunning H.N. and Lorenz P.B.,
J. Phys. Chem., 1956, 60, 657.
24. Nakagawa T., Kuriyama K. Inoue H. and Tori K.,
J. Chem. Soc. Japan, 1956, 77, 1563.
25. Bury C.R. and Browning J., Trans. Faraday Soc.,
1953, 49, 209.

26. White P. and Brown G.C., Trans Faraday Soc., 1959, 55, 1025.
27. Nakagawa T., Kuriyama K. and Tori K., J. Chem. Soc. Japan, Pure Chemistry Section, 1957, 78, 1573.
28. Kuriyama K., Inoue H. and Nakagawa T., Koll. Z., 1962, 183, 68.
29. McLay W.N., J. Colloid Sci., 1956, 11, 272.
30. Alexander A.E. and Johnson P., "Colloid Science", Clarendon Press, Oxford, 1950, p. 686.
31. Mulley B.A. and Metcalf A.D., J. Pharm. Pharmacol., 1956, 8, 776.
32. Nakagawa T., Kuriyama K. and Inoue H., J. Colloid Sci., 1960, 15, 268.
33. Greenwald H.L. and Brown G.L., J. Phys. Chem., 1954, 58, 825.
34. Flockhart B.D. and Ubbelohde A., J. Colloid Sci., 1953, 8, 423.
35. Nakagawa T., Inoue H., Tori K. and Kuriyama K., J. Chem. Soc. Japan, Pure Chemistry Section, 1958, 79, 1194.
36. Kuriyama K., Inoue H. and Nakagawa T., Annual Report Shinogi Res. Lab., 1959, 2, 1061.

37. Kuriyama K., Koll. Z., 1962, 180, 55.
38. Livingstone H.K., J. Colloid Sci., 1954, 9, 365.
39. Kuriyama K., Koll. Z., 1962, 181, 144.
40. Nakagawa T. and Tori K., Koll. Z., 1960, 168, 132.
41. Lord Rayleigh, Phil. Mag., 1871, 41, 447.
42. Debye P.J., Applied Phys., 1944, 15, 338.
43. Einstein A., Ann. Phys. Lpz., 1910, 33, 1275.
44. Schmoluchowski M., Bull. Int. Acad. Sci. Crocarice, 1907, 1057.
45. McIntosh D.S. and Elworthy P.H., J. Pharm. Pharmacol., 1961, 13, 663.
46. Ottewill R.H. and Pareira H.C., J. Phys. Chem., 1958, 62, 912.
47. Bauer in "Physical Methods of Organic Chemistry", 3rd. Ed. ed. Weissberger, Vol. 1, Interscience Publ. Inc., New York, 1960, p. 1211.
48. Gibson R.E. and Adams R.H., J. Amer. Chem. Soc., 1933, 55, 2679.
49. Schick M.J., J. Colloid Sci., 1963, 18, 378.
50. Higuchi T. and Lach J.L., J. Amer. Pharm. Assoc., Sci. Ed., 1954, 43, 465.
51. Guttman D. and Higuchi T., J. Amer. Pharm. Assoc., Sci. Ed., 1956, 45, 659.

52. Nakagawa T., J. Pharm. Soc. Japan, 1954, 74, 1116;
1956, 76, 1113.
53. Nakagawa T., Kuriyama K. and Inoue H., Symposium
on Colloid Chemistry (Chem. Soc. Japan), 12th
Symposium, 1959, R32.
54. Aoki M. and Iwayama Y., J. Pharm. Soc. Japan,
1959, 79, 576.
55. Ross R. and Olivier J.P., J. Phys. Chem., 1959, 63, 1671.
56. Becher P., J. Phys. Chem., 1959, 63, 1675.
57. Einstein A. Ann. Physick., 1906, 12, 289; 1911, 34, 591.
58. Simha R., J. Phys. Chem., 1940, 44, 25.
59. Mehl J.W., Oncley J.C. and Simha R., Science,
1940, 92, 132.
60. McMillan W. and Mayer J., J. Chem. Phys., 1945, 13, 276.
61. Moilliet J.L., Collie B., and Black W., "Surface
Activity", Spon., London, 1961, p. 1.
62. Shinoda K., Nakagawa T., Tamamushi B., Isemura T.,
"Colloidal Surfactants", Academic Press, London,
1963, p. 1.
63. Shinoda K., Yamaguchi T. and Hori K., Bull Chem. Soc.
Japan, 1961, 34, 239.
64. Nakagawa T., Kuriyama K., Inoue H., and Oyama T.,
J. Chem. Soc. Japan, Pure Chemistry Section,
1958, 79, 348.

65. Nakagawa T. and Inoue H., J. Chem. Soc. Japan,
Pure Chemistry Section, 1958, 72, 345.
66. Moelwyn Hughes, E., "Physical Chemistry", 2nd. Ed.,
Pergamon Press, 1961, p. 389.
67. Cabannes J., "La diffusion moléculaire de la lumière",
Presses Universitaire de France, 1929, Paris.
68. Zimm B.H., J. Chem. Phys., 1948, 16, 1093, 1099.
69. Debye P.J., J. Phys. Chem., 1947, 51, 18.
70. Lord Rayleigh, Proc. Roy. Soc., 1910, A84, 25.
Gans R., Ann. Phys. Lpz., 1925, 76, 29.
71. Stacey K.A., "Light-Scattering in Physical Chemistry",
Butterworths, London, 1956, p. 60.
72. Stokes R.H. and Robinson R.A., "Electrolyte Solutions",
2nd. Ed., Butterworths, London, 1959, p. 457.
73. Heilbron I.H. and Bunbury H.M., "Dictionary of
Organic Compounds", Eyre and Spottiswoode, 1953, 1, p. 446.
74. Mulley B.A. and Metcalf A.D., J. Colloid Sci.,
1962, 17, 528.
75. Macfarlane C.B. and Elworthy P.H., J. Pharm. Pharmacol.,
1962, 14, 100T - 102T.
76. Schick J.M., J. Colloid Sci., 1962, 17, 801.
77. Tanford C., "Physical Chemistry of Macromolecules",
Wylie, London, 1961, p. 195.

78. Barrer R.M. and Kelsey K.E., Trans. Faraday Soc.,
1961, 57, 452.
79. Int. Crit. Tables, McGraw Hill, London, 1933, 3, p. 30.
80. Taylor W.J., J. Chem. Phys., 1948, 16, 257.
81. Glasstone S., "Textbook of Physical Chemistry",
2nd. Ed., McMillan, London, 1951, p. 399.
82. Bunn C.W. and Holmes D.R., Disc. Faraday Soc.,
1958, 25, 95.
83. Debye P.J., Ann. N.Y. Acad. Sci., 1949, 51, 575.
J. Phys. Chem., 1949, 53, 1.
84. Tanford C., "Physical Chemistry of Macromolecules",
Wiley, London, 1961, p. 201.
85. Longuet-Higgins H.C., Disc. Faraday Soc., 1958, 25, 86.